Russian Original Vol. 36, No. 2, February, 1974

August, 1974

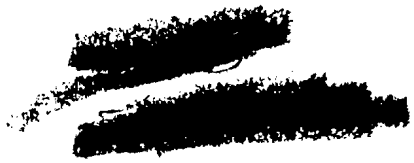

SATEAZ 36(2) 113-206 (1974)

SOVIET ATOMIC ENERGY

АТОМНАЯ ЭНЕРГИЯ
(ATOMNAYA ÉNERGIYA)

TRANSLATED FROM RUSSIAN

CONSULTANTS BUREAU, NEW YORK

SOVIET ATOMIC ENERGY

Soviet Atomic Energy is a cover-to-cover translation of *Atomnaya Énergiya*, a publication of the Academy of Sciences of the USSR.

An agreement with the Copyright Agency of the USSR (VAAP) makes available both advance copies of the Russian journal and original glossy photographs and artwork. This serves to decrease the necessary time lag between publication of the original and publication of the translation and helps to improve the quality of the latter. The translation began with the first issue of the Russian journal.

Consultants Bureau journals appear about six months after the publication of the original Russian issue. For bibliographic accuracy, the English issue published by Consultants Bureau carries the same number and date as the original Russian from which it was translated. For example, a Russian issue published in December will appear in a Consultants Bureau English translation about the following June, but the translation issue will carry the December date. When ordering any volume or particular issue of a Consultants Bureau journal, please specify the date and, where applicable, the volume and issue numbers of the original Russian. The material you will receive will be a translation of that Russian volume or issue.

Subscription
$87.50 per volume (6 Issues)

Single Issue: $50
Single Article: $15

Prices somewhat higher outside the United States.

CONSULTANTS BUREAU, NEW YORK AND LONDON

227 West 17th Street
New York, New York 10011

4a Lower John Street
London W1R 3PD
England

Published monthly. Second-class postage paid at Jamaica, New York 11431.

Soviet Atomic Energy is abstracted or indexed in *Applied Mechanics Reviews, Chemical Abstracts, Engineering Index, INSPEC—Physics Abstracts and Electrical and Electronics Abstracts, Current Contents,* and *Nuclear Science Abstracts.*

SOVIET ATOMIC ENERGY

A translation of *Atomnaya Énergiya*

August, 1974

Volume 36, Number 2 February, 1974

CONTENTS

CONTENTS

(continued)

The Russian press date (podpisano k pechati) of this issue was 1/24/1974. Publication therefore did not occur prior to this date, but must be assumed to have taken place reasonably soon thereafter.

ARTICLES

In July 1973 in the city of Shevchenko the first industrial atomic power station incorporating a fast BN-350 reactor went into power production. After coming up to a nominal power of 1000 MW the BN-350 reactor develops 150 MW of electrical power and 120 m^3/day of fresh water. In this issue of the journal the Editorial Board is publishing four articles setting out the basic results of the starting and tuning (adjusting) operations carried out on the BN-350 reactor, and also certain advances in studying the radiation hazards around the reactor. These articles were presented at the Second Symposium of the Member Countries of the Socialist Economic Union on fast reactors held in Obninsk (USSR) on October 1-5, 1972. A communication summarizing the Symposium is presented on p. 185 of this issue.

EXPERIENCE IN STARTING AND TUNING (ADJUSTING) OPERATIONS WITH THE BN-350 REACTOR AND IN ITS INITIAL POWER PRODUCTION

A. I. Leipunskii, F. M. Mitenkov,
V. V. Orlov, D. S. Yurchenko,
V. I. Shiryaev, V. M. Arkhipov,
Yu. E. Bagdasarov, R. P. Baklushin,
S. M. Blagovolin, K. T. Vasilenko,
Yu. I. Gribanov, A. A. Demin,
A. G. Karabash, A. V. Karpov,
G. V. Kiselev, F. A. Kozlov,
L. A. Kochetkov, I. A. Kuznetsov,
V. V. Pakhomov, V. M. Poplavskii,
A. A. Rineiskii, and A. V. Ushakov

UDC 621.039.526

The BN-350 nuclear power station has been described earlier, together with a discussion of design problems and the experimental testing of the equipment [1-4]. At the end of 1971 most of the constructional and assembly work on the BN-350 had been completed. In May 1972 auxiliary systems were brought into service to facilitate operation of the basic circuits: the sodium–potassium cooling system of the cold traps of the first and second circuits, the cooling system of the freezing zones of the gates of the first circuit, electrical heating systems for the equipment and pipelines and the gas heating of the reactor vessel, the cooling systems for the biological shielding of the reactor and the boxes of the first circuit. At the same time some 700 m^3 of sodium were prepared and purified for filling the first and second circuits. In October 1972 starting and tuning operatings were initiated on the basic circuits, and all the most important components, mechanisms, and equipment as well as the installation as a whole were tested and aligned. In all operations on the BN-350, experience gained in the starting and exploitation of the BR-5 and BOR-60 reactors was effectively used. In this important and extremely responsible period, the execution of which led to the physical initiation of the reactor, the majority of the design and engineering decisions were duly verified, as well as the efficiency of the large sodium circuits and basic reactor equipment.

November 29, 1972 saw the physical initiation of the BN-350 reactor. In the final stage – the initial production of power by the reactor, completed on July 16, 1973, by the starting of the turbine under load – additional important information was gathered as to the efficiency of the basic equipment of the nuclear power station.

Translated from Atomnaya Énergiya, Vol. 36, No. 2, pp. 91-97, February, 1974. Original article submitted October 22, 1973.

In this paper we shall present a description of starting and tuning operations on the BN-350, together with the results of some important stages in the work and initial power production.

Preparation of the Coolant for the First and Second Circuits

The sodium was transported from the factory in special 1 m^3 containers under a layer of argon. The system for manufacturing the coolant had six electric furnaces, so that six portable sodium containers could be employed at the same time.

Although care was taken in the factory to prevent paraffin from falling into the sodium, a certain amount still remained. Subsequent tests showed that this amounted to 0.1-3 kg of paraffin per container. In order to remove the paraffin each container was processed before the sodium was pumped out, the paraffin being distilled off by heating in vacuo. Experience in preparing the coolant for the BOR-60 and also a series of special experiments revealed the best conditions for removing the paraffin: the sodium in the portable vessel was heated to 230-240°C, after which the paraffin was distilled under vacuum into a special air-cooled trap. Every 3 h the trap was inspected, and if the amount of paraffin had not exceeded 1.5 kg the sodium was pumped out of the portable container through a cellular filter into a 50 m^3 storage settling tank. However, if the amount of paraffin in the trap were greater than 1.5 kg, the distillation cycle was extended for another 2 h. Practice showed that this period was sufficient to remove the paraffin. Settling in the storage tank continued for several days in order to allow paraffin inclusions not removed under vacuum to float to the top. From the settling tank the sodium was pumped into a 50 m^3 receiving tank for purification with a cold trap. The pumping was always carried out in such a way as to leave the level of sodium in the settling tank some 500 mm above the cut-off of the intake tube of the tank, in order to prevent any possible paraffin film from passing into the receiving tank.

The sodium was purified by forced circulation through a cold impurity trap. Using an internal (plug) oxide indicator, the amount of impurity in the sodium was measured periodically; before the onset of purification this corresponded to an indicator clogging temperature of 210-220 and after purification to 120-150°C. The manufacturing system incorporated a universal distillation sampler which enabled samples to be taken for the chemical determination of metallic and nonmetallic (carbon, oxygen, nitrogen, etc.) impurities in the sodium. Samples could be taken both while pumping the sodium from the portable containers into the storage tank and while purifying the sodium in the receiving tank. After purification the sodium was passed under pressure into the overflow tanks of the first and second circuits. Since the coolant was always prepared in advance, the sodium in the overflow tanks of the first and second circuits had already settled for several months. The proportions of the main impurities in the sodium prepared for filling the first and second circuits (in parts per million) were: 50 K, 25 Ca, 20 C, 7 O, 5 H, and 4 N [5]. The same system was used to prepare the coolant for cooling the trap filters and the drum for the expended packs (Na–K eutectic).

Starting and Tuning Operations in the First Circuit

The starting and tuning operations in the first circuit involved the following main processes:

verification of the vacuum-tightness of the circuit;

drying of the circuit by vacuum treatment and heating;

verification of all the mechanisms, equipment, and measuring and testing instruments;

filling the circuit with sodium;

development of the procedures for starting the circulation and the combined operation of the pumps;

purification of the sodium in the circuit and running-in of the pumps;

study of the hydraulic characteristics of the circuit.

The vacuum-tightness of the first circuit was verified by evacuating the circuit and testing with a helium leak detector. The limiting vacuum achieved in the first circuit was $5 \cdot 10^{-2}$ mm Hg with a leakage of $4 \cdot 10^{-3}$ mm Hg/h. The circuit was prepared by electrically heating the fittings and pipelines and gas heating the main body, gas being simultaneously circulated through the circuit by regular pumps. The temperature was raised at 5-6°C/h in steps of 20°C with a 10-15 h rest at each step.

During the heating of the circuit the readings of strain gages and the displacement of reference points on the main body of the apparatus, the fittings, and the pipelines were carefully checked. The maximum temperature of the vessel and the internal fittings of the reactor was reached after 10 days and equalled 200-250°C.

The first circuit was filled with sodium previously heated in the overflow tanks to about 250°K. To provide additional purification, before passing into the circuit the sodium was pumped through the standard trap filter of the first circuit, which played the part of a mechanical filter. The circuit was filled gently, without any serious thermal stresses in the fittings. The volume of the sodium in the first circuit was about 500 m^3.

The first circuit of the BN-350 reactor was a complex hydraulic system with a large number of free sodium levels (in the reactor, six pump tanks, and six filter overflow tanks). The circulation through the first circuit was therefore arranged successively, individual pumps being started at 250 and 1000 rpm and pumps being set in parallel operation at 250 rpm. The stability of operation of the pumps was checked in various combinations, so was the behavior of the sodium levels and the reverse valves as the pumps were started and stopped. During the running-in of the first circuit the heat was taken off by a single steam generator.

Investigations showed that the hydraulic characteristics of the first circuit agreed closely with design values. Deviations in individual loops were insignificant. For any combination of pumps working in parallel, normal operation was assured at both 250 and 1000 rpm. The stability of the sodium levels in all the vessels of the circuit was also assured. The vibration of the equipment and pipelines was insignificant. The cavitation margins of the pumps corresponded to the design data; connecting and disconnecting the pumps produced a smooth change in sodium level.

On the basis of the foregoing tests, the following order was decided for starting circulation in the first circuit:

1) the head pressure gates of the three loops chosen for connection are opened to the starting position (those of the other three loops being closed);

2) the three selected pumps are started at 1000 rpm one after the other at intervals of 1-3 min;

3) the head gates of the fourth and fifth pumps are opened in the same way and the pumps are started at intervals of 1-3 min;

4) the head gates of all the working pumps are opened fully at the same time.

The sodium in the first circuit was purified continuously as adjustment of the circuit proceeded, using cellular filters placed in the tail sections of all the simulation packs in the reactor, as well as cold traps. An attempt to set the cold traps in operation while the pumps were turning at 250 rpm was unsuccessful owing to the inadequate flow of sodium through the traps. Hence the initial purification of the sodium in the circuit was effected by circulating it through the traps using the electromagnetic pumps of the tank equipment. The main purification was carried out with the pumps operating at 1000 rpm and the sodium circulating through three of four cold traps.

The first measurement of oxide content in the first circuit was carried out after circulating the sodium through the traps for 100 h. The clogging temperature of the plug indicator was 185°C. After passing the whole volume of the sodium through the cold traps 30 times, the clogging temperature of the indicator fell to 120°C. The results of a chemical analysis of coolant samples periodically taken from the first circuit by means of a distillation sampler indicated an appreciable reduction in the impurity content of the sodium by virtue of its purification in the cold traps: the carbon content fell from 25 to 10, and the oxygen from 22 to 2.5 parts per million.

After the running-in of the first circuit had been completed the 10 simulation packs were extracted. On inspecting the cellular filters of these no mechanical inclusions were found. This indicated that the measures taken to preserve the purity of the circuit during assembly and starting and tuning operations were reasonably effective.

Starting and Tuning Operations in the Second and Third Circuits

The starting and tuning operations in the second and third circuits were carried out in accordance with the foregoing stages characterizing the physical initiation of the system and its initial production of

power. At the stage of the running-in of the first circuit and during the physical initiation of the system, one loop had been made and set in operation in each of the second and third circuits; at the stage of first power production three loops were operative in each case.

The sequence of the starting and tuning operations in the second circuit was:

1) the achievement of general vacuum tightness in the circuit;

2) verification of the close locking of the equipment;

3) plotting of the zero readings of the strain-gage system and reference points;

4) passage of nitrogen through the circuit and its components;

5) evacuation and drying;

6) heating of the liquid metal circuit (during the heating the readings of the strain-gage system were taken and the position of the reference points was established);

7) filling of the loop with sodium (without the indication and filtration system);

8) bringing the auxiliary systems into the working mode;

9) starting the circulation with the pumps working at 250 rpm;

10) measurement of pipeline vibrations;

11) filling the indication and filtration system with sodium;

12) determination of the oxide content of the sodium;

13) starting the cold trap and preliminary purification of the sodium;

14) starting the pumps at 1000 rpm and running the circuit in at nominal revolutions;

15) measurement of pipeline vibrations;

16) final purification of the sodium with the pumps working at 1000 rpm;

17) chemical analysis of the sodium;

18) determination of the characteristics of the second circuit systems.

The starting and tuning operations in the second circuit were carried out with a sodium temperature of 150-250°C.

The difficulties encountered in hermetizing the second circuit were associated with the large volume of the vacuum spaces (80-100 m^3), the branched nature of the tracts, and the large number of welds separating the inside of the second circuit from the surrounding medium. The greatest difficulties were encountered in connection with the absence of vacuum tightness in the tube assemblies of the steam generators and in one of the heat exchangers. Nevertheless, an extremely high vacuum tightness was eventually achieved, the limiting vacuum being 10^{-2} mm Hg. The contour was regarded as hermetic if the leakage (fall in vacuum) was no greater than 10 μ/h. During the vacuum treatment the hermetic state of the water-filled steam generator was also subjected to a preliminary (cdd) test. From the limiting degree of vacuum, and from the appearance of traces of moisture in gas samples of the second circuit, the hermetic state of the steam generator after assembly operations could readily be judged.

As criteria we used the following approximate computing characteristics of the circuit parameters during vacuum treatment, expressed as functions of the water leakage in the joints of the steam generator:

Leak, g/h	$0.7 \cdot 10^{-6}$;	10;	1220
Rate of leakage, μ/sec	0;	$0.6 \cdot 10^{-2}$;	0.7
Limiting vacuum, mm Hg	10^{-2};	0.15;	1.5
Amount of moisture at a pressure of 10 mm Hg, wt. %	0;	0.02;	2.2

Preliminary analysis of the stressed state of the elements of the second circuit showed that during the heating of the sodium-free second circuit conditions were most severe at the nodes of the intermediate heat exchanger. It was precisely this factor that determined the rate of heating of the whole circuit. In order to verify and develop the heating process, we carried out special experiments with strain gages in

the structure of the heat exchanger; these showed that heating in steps of 20°C at 5°C/h and with a rest of 10 h at each stage was quite acceptable. The heating of the circuit filled with sodium at this rate was in no way dangerous.

The filling of the pipelines and fittings of the second circuit with coolant using the design system of drains and air lines caused no difficulties. However, a change of 1 atm in the pressure of the gas spaces led to a change in the sodium levels in the system, and this affected the gas pockets remaining in individual parts of the circuit. The use of sodium circulation with the pumps working at 250 rpm for 5-10 h usually led to the complete removal of the gas spaces in the circuit.

The vibration characteristics of the main sodium pipelines of the circuit were satisfactory with the pumps working at both 250 and 1000 rpm, subject to a sufficient level of sodium in the evaporators. On reducing the level of sodium in the evaporators to 300 mm above the axis of the suction tube many large gas bubbles passed into the overflow tube of the evaporators; large fluctuations of the main circulation pipelines developed, with amplitudes up to 50-60 mm.

After the filling of the second circuit with sodium, the impurity content of the coolant usually corresponded to a blocking temperature of 150 ± 180°C according to the plug indicator. The incorporation of the cold traps with the pumps operating at 1000 rpm reduced the clogging temperature of the indicator to 120-130°C in 10-15 h.

In order to reduce the corrosion damage of 1Kh2M steel during the prestarting hydraulic tests on the third circuit, hydrazine hydrate (500-1000 mg/liter, referred to hydrazine) was added to the distillate, this being directly introduced into the steam generators.

In order to ensure the required quality of the supply water (with respect to oxygen) during the starting and tuning operations, hydrazine hydrate was introduced into the supply tract of the distillate at the actual stage of preparation, which also greatly reduced the passage of iron into the water from the supply-water pipelines.

Filling of the steam generator with water at 150-160°C was carried out with the sodium in the second circuit at a temperature of 170-180°C In the course of the starting and tuning operations, special attention was paid to testing the emergency systems of the steam generator and the circuits designed to prevent dangerous consequences if the sodium accidentally came into contact with water when a heat-exchanger tube broke. The test program was set up so as to determine the efficiency of the protective systems of the second and third circuits (PS-II and PS-III) before the simultaneous filling of the steam generator with sodium and water.

During the testing of PS-II the second and third circuits were filled with an inert gas. The emergency signal for the operation of the system was simulated by raising the pressure in the second circuit by 0.5 atm. The inertia of the system of drives used for the forced rupture of the membrane-rupture device, the tripping pressure of the preventative devices in the separator tank of the second stage, the permeability of the system for the ejection and separation of the reaction products, and the tightness of the safety valves in the separator tank, were all determined.

Testing of the PS-III at the first stage was carried out when the second circuit was filled with an inert gas, the steam generator heated to 250-270°C, its water-steam space filled with water, and the pressure in the latter held at 30-50 atm by virtue of electric heating.

In the electric circuit the emergency signal for a rise in pressure in the gas space of the second circuit (due to a severe leak) was also simulated. During the tests the inertia of the high-speed equipment in the water-supply line and the line corresponding to the emergency drying of the steam generator was determined, so were the conditions for disconnecting the pumps of the second circuit and the time required for the ejection of water and steam from the steam generator, i.e., the period of possible danger if water leaked into the sodium.

At the second stage the PS-III was tested with the second circuit full of sodium, the pumps working at 1000 rpm, and with steam being generated in the steam generator.

In general, the parameters of the first and second circuits and the characteristics of the emergency systems and protective devices of the steam generator were in accordance with design.

Experimental Studies of the Dynamic Characteristics and Parameters

During the starting and tuning operations, a series of experiments was carried out on the dynamics, testing, and adjustment of the protective systems, as well as the signalling and automatic-control systems. The experiments were started during the running-in of the main circulation pumps and the purification of the circuits, when the transient hydraulic processes were being studied and the cavitation characteristics of the circuits measured. Instead of the full-scale fuel packs, steel simulation packs were installed in the reactor. At this time the running down of the pumps was measured at 1000 and 250 rpm, and transient processes were studied when one pump was shut down out of four or five working. When the pumps were running at 1000 rpm the disconnection of one pump was accompanied by the sharp closing of the reverse valve. The flow of sodium in the disconnected loop fell to zero in 3–4 sec. The valve closing process lasted about 2 sec.

The cavitation characteristics of the first circuit were measured under the severest conditions – three pumps running at 1000 rpm. The pressure of the gas in the apparatus was reduced, the flow of sodium in the loops was measured, and the pumps were tested by ear at the same time. The measurements confirmed earlier values of the cavitation reserves.

After physical initiation, the hydraulics of the circuits were again studied, but on a wider scale than when the pumps were being run in. Certain experiments were repeated in order to estimate the influence of the hydraulic resistance of the reactor. Measurements of the running down of the first-circuit pumps showed that the resistance had only a weak influence on these processes. The rate of rotation of the pumps was measured, so were the flows of sodium in the loops when the power supply of individual pumps was shut off for 1, 2, and 3 sec. The results were needed in connection with the calculation of various emergency situations in the power supply system which could not be simulated experimentally.

The reduction in the flow of a failed loop with the pumps working at 1000 rpm took place slightly more quickly with increasing hydraulic resistance of the reactor. The experiments involving the shutting down of one pump out of five working were repeated several times. The flows of coolant in the loops, the rates of revolution of the pumps, and the displacements of the pipelines were measured. In individual experiments the hydrodynamic effects of the reactivity were also determined.

At the same time as studying the transient hydraulic processes, tests were also made on the emergency protective systems based on changes in sodium flow in the first circuit of the installation, and these systems were adjusted accordingly. In the most dangerous emergency situation, the protective system should operate no more than 1-1.5 sec after the flow has started becoming weaker. In view of this, the requirements as to the precision with which the emergency signalling and protective devices should be made are very high. The experiments involved determining the dynamic characteristics of the protective devices and the secondary instruments, in simultaing emergency situations, and establishing all the delay components of the emergency signals.

Special experiments were conducted to calibrate the main flow meters, the signals from which operated the safely devices.

In view of safety requirements relating to emergencies arising from disruptions in the energy supply of the installation, in addition to the signal based on changes in the sodium flow in the first circuit, a signal based on the fall in voltage in particular sections of the distributor system from which the electric motors of the pumps were fed was also introduced into the emergency system. The signal indicating a fall in voltage in the most severe situations should arrive at the same time as the signal indicating a fall in sodium flow. Such situations were simulated in the experiments. The operation of the emergency protective devices was accordingly verified. Simulation was also enacted for such breakdowns in the energy supply system as were not required to trip the emergency devices, since they were capable of being removed by switching to reserve supply sources.

With the reactor operating at the minimum controllable power level the hydrodynamic effects of the reactivity were then measured – effects associated with the displacement of the fuel packs of the reactor when the flow of coolant through the latter altered. The effects were determined for the simultaneous disconnection of five, four, or three pumps of the first circuit, and also when one out of the five working pumps was shut down. The maximum extent of the effect on changing the flow of coolant from the nominal value to zero was 5-6%. For a low flow of coolant the effect had a positive sign (the fuel packs moved

toward the center of the active zone). The dependence of the effect on the flow of coolant agreed closely with theoretical predictions as to its mechanism. More precise information regarding the displacement of the fuel packs of the reactor under the influence of changing pressure of the coolant in the gaps between them will be obtained after making a detailed mathematical analysis of the experimental results.

The barometric reactivity effects associated with a change of pressure in the reactor due to the evolution of gas from the sodium and a change in the volume of the gas bubbles already present in the coolant were also studied at the lowest controllable power level. The effects were determined while changing the excess pressure in the apparatus from zero to the working value (0.9 atm). In this range of pressures no reactivity effects were observed. This further confirmed that the effects measured on disconnecting the pumps of the first circuit were associated with the displacement of the fuel packs themselves.

The temperature coefficient of reactivity was measured by heating the reactor with circulation pumps at the minimum level of reactor power. The effect was determined on a base of 70°C and amounted to $\sim 3.77 \cdot 10^{-5} {}^{\circ}C^{-1}$.

An extensive series of experiments was directed at elucidating the details of reactivity feedback. The asymptotic power effect was determined for a slow rise in power, with a steady flow (consumption) of coolant, by reference to the position of the absorbing rods. The effect was measured under various pump working conditions: with two pumps working at 250 rpm, three at 1000 rpm, and four at 1000 rpm.

The reactivity feedback mechanism was studied by rapidly perturbing the reactor with respect to reactivity and then recording the transient process. The perturbations were effected by ejecting one emergency (safety) rod with an efficiency of ~1%, rapidly displacing an automatic control rod by 100-150 mm (the perturbation here reaching 0.05%) in the self-regulating mode, and by rapidly changing the setting of the power control in the automatic-control mode. The natural noise of all the main reactor parameters was also recorded. Experiments were carried out using slight artificial perturbations obeying periodic and pseudo-random laws. The accuracy of measuring all the effects was ensured by initially stabilizing the reactor to a state in which the rate of change of the reactivity was no greater than 0.01%/h. The pressure in the steam generators was meanwhile held to an accuracy of ±0.5 abs. atm.

The manner in which the slow and fast safety (emergency) devices operated was studied in order to determine the factors chiefly affecting the magnitude of the thermal stresses arising in the construction elements under these conditions. The experimental curve giving the fall in power after the operation of the slow safety device agreed closely with the theoretical curve. This indicated that the relationship between the linear efficiency of the control and safety rods and the depth of their immersion in the reactor provided for in the design had indeed been accurately defined. The efficiency of the mixing (agitation) of the sodium in the reactor tank was studied under conditions corresponding to the operation of the slow safety device for various rates of flow of the coolant, which determined the magnitude of the thermal stresses in the outlet pipelines and the vessels of the intermediate heat exchangers.

In all operating modes associated with a change in the sodium temperature the transient processes in the intermediate heat exchangers and steam generators were also studied. Specially to be noted were the transient processes in the steam generators when the pumps of the second circuit were started and a rapid change occurred in the steam production and the steam pressure in the generators. The aim of the experiments in this case was that of determining the conditions under which the safety of the process could be guaranteed.

Special experiments were undertaken in order to study the processes associated with the change in sodium temperature at the entrance into the reactor. In these experiments the dynamic characteristics of the expansion of the head (pressure) collector of the reactor and the influence of this expansion on the reactivity were studied. These experiments will prove useful when constructing a complete model of the reactivity feedback.

Experiments to determine the effective heat capacity of the circuits and the thermal losses to the surrounding medium were carried out by heating the installation with the principal circulation pumps and then cooling it. Experiments were furthermore carried out for different numbers of loops; the loops of the second circuit were heated and cooled in one of the experiments in isolation from the first circuit.

Experimental investigations into the dynamics of the installation will be continued at higher levels of power.

Initial Power Production of the Installation

From the very outset of the starting and tuning operations on the BN-350, in all design procedures and preliminary processing the term "initial power production" was taken to mean, not some specific instant of reaching the originally specified parameters, but a whole complex of operations and investigations. This incorporated a stage-by-stage, gradual lifting of the power and parameters, while at each stage planned experiments were undertaken and their results analyzed, together with the results obtained in the actual use of the installation.

On July 16, 1973 one of the turbogenerators connected to the power system was set in action by the steam of the BN-350; the remaining heat was used to freshen sea water for the city of Shevchenko.

LITERATURE CITED

1. A. I. Leipunskii et al., "The BN-350 nuclear power station," in: Transactions of the Symposium of Member Countries of the Socialist Economic Union and Prospects of Work on the Creation of Nuclear Power Stations with Fast Neutron Reactors [in Russian], Vol. 1 ONTI FÉI (United Technical Publishers, Physical Power Institute), Obninsk (1968), p. 123.
2. A. I. Leipunskii et al., "Sodium technology and equipment of the BN-350 reactor," At. Énerg., 22, 13 (1967).
3. A. I. Leipunskii et al., "Erection of a nuclear power station with a BN-350 reactor," At. Énerg., 23, 409 (1967).
4. A. I. Leipunskii et al., "Experience in the design and use of fast reactors in the USSR," At. Énerg., 31, 344 (1971).
5. R. P. Baklushin et al., "Starting and tuning operations in the main circuits of the BN-350 reactor," Communication to the Conference of the Coordinated Scientific-Technical Council on Fast Reactors [in Russian], Prague (March, 1973).

STUDY OF THE PHYSICAL CHARACTERISTICS OF THE BN-350 REACTOR ON STARTING

V. V. Orlov, G. B. Pomerantsev, D. S. Yurchenko, K. T. Vasilenko, B. G. Dubovskii, Yu. A. Kazanskii, G. V. Kiselev, I. M. Kisil', M. Ya. Kulakovskii, V. I. Matveev, N. V. Skorikov, M. F. Troyanov, G. B. Usynin, V. I. Golubev, A. A. Vaimugin, A. I. Voropaev, P. G. Dushin, V. P. Zinov'ev, V. F. Lyubchenko, V. F. Mamontov, and P. L. Tyutyunnikov

UDC 621.039.526:621.039.52.034.6: 621.039.519

The BN-350 reactor constructed in the city of Shevchenko is the first industrial fast reactor in operation. The starting of this reactor is a most important stage in the adoption of fast power reactors as part of the program of development of nuclear power technology in the USSR.

The designed thermal power of the reactor is 1 GW. The reactor is cooled with sodium. The fuel is enriched uranium dioxide. The construction of the reaction was described in [1-3].

In 1972 tuning operations were initiated in respect of individual sections of the reactor, followed by comprehensive starting operations. On November 29, 1972 the reactor went critical. A program of investigations into the static physical characteristics was then carried out in the reactor, including measurements of the efficiency of the control rods, the efficiency of the fuel packs, the sodium void reactivity effect, the temperature coefficient of reactivity, the distribution of various reactions over the volume of the active zone and the screen, and the hydrodynamic and barometric reactivity effects.

After execution of this program in the reactor, preparations for passing into the power operating mode commenced.

Calculated and Experimental Bases of the Physical Characteristics of the Reactor

During the design of the BN-350 reactor a great number of theoretical-calculation, methodical, and experimental investigations were carried out in order to establish the basis of its physical characteristics.

As a result of the development of a system of constants allowing for the resonance blocking of the cross sections, the well-known 26-group system of constants was created in 1963 [4]. As time progressed this system of constants was improved and developed, mainly in connection with the appearance of new information regarding the neutron interaction cross sections. As the constants were corrected, the physical characteristics of the reactor were reconsidered and refined as well.

In calculating the reactor the diffusion approximation was generally employed. The validity of this approximation was verified by comparing with higher approximations. A considerable proportion of the calculations was carried out in one-dimensional geometry, using simple and effective programs [5]. The

Translated from Atomnaya Énergiya, Vol. 36, No. 2, pp. 97-103, February, 1974. Original article submitted October 22, 1973.

TABLE 1. Efficiency of the Boron Rods % Δk/k

Rods	Measurements	Design
AR-2F	0,128±0,003	—
AR-1F	0,256±0,006	0,21
AR-1	0,238±0,007	0,21
AR-2	0,232±0,007	0,21
TK	0,80±0,03	0,90
AZ-1	1,08±0,05	1,06
AZ-2	1,03±0,05	1,06
AZ-3	1,07±0,05	1,11

TABLE 2. Efficiency of the Compensating Packs, % Δk/k

Packs	Measurements	Design
KP_1	0,190±0,005	0,208
KP_2	0,189±0,005	0,199
KP_3	0,190±0,005	0,199
KP_4	0,194±0,005	0,208
KP_5	0,178±0,005	0,193
KP_6	0,174±0,005	0,199

TABLE 3. Effect of the Complete Removal of Sodium From One Pack of the Active Zone and the Screen at a Temperature of 220-230°C ($\times 10^{-5}$ Δk/k)

Place of measurement	Distance from the center of the active zone, cm	Experiment	Calculated
Zone of slight enrichment	9,85	—6,7±1,5	—3,0
	19,7	—4,6±1,5	—3,4
	39,4	—6,5±1,5	—5,5
	54,6	—10,1±1,5	—8,1
Zone of great enrichment	59	—7,4±1,0	—9,6
	69	—9,8±1,0	—13,1
	78,7	—8,8±1,0	—7,1
Screen	98,5	—1,8±1,5	—0,2

values of the Laplacians required in order allow for the transverse leakage of neutrons were determined from programs based on synthetic methods [6, 7] which were also used in order to calculate the changes taking place in the isotopic composition of the fuel and the reactor characteristics for various degrees of burn-up. In the decisive stages of the calculation computing programs in two-dimensional geometry were used in order to refine the results and establish the details of the neutron fields [5].

In order to determine the reactivity effects and calculate the efficiency of the control rods, perturbation theory was also widely employed. In the latter case the methods of perturbation theory were combined with direct calculations of centrally-positioned rods [8].

During the development of the reactor, an extensive program of experimental investigations into physical models of the reactor was carried out on the BFS-1 testbed. The program embraced a study (in various states of the reactor) of the critical parameters, the efficiency of samples of various materials and models of the control and safety rods, the spectral characteristics, the distribution of reaction velocities, the sodium reactivity coefficient, and so on. The results of these investigations were presented and analyzed in [9-12].

The results of the simulation of the reactor on the BFS tested were used in two ways. Firstly, a direct calculation of all the experimental results was carried out by the same methods and with the same constants as those used in calculating the reactor itself. Secondly, the characteristics of the critical assembly were "transferred" by perturbation theory to the reactor characteristics, allowing for differences between the composition and geometry of the assembly and the reactor. These two methods of comparison gave very similar results.

However, neither the calculations nor the simulation could embrace all details of the reactor construction, the real composition and geometry. The disposition of various materials in the assembly and reactor, respectively, differed considerably. Such characteristics as the temperature and power effects of reactivity could not be studied at all in the critical assembly.

For this reason measurements of the physical characteristics of the BN-350 directly in the reactor constituted the first serious means of examining the whole conception of theoretical-computing and experimental investigations aimed at establishing the physical characteristics of the fast power reactor.

Achievement of the Critical State. The Critical Mass

Before charging the fuel packs of the active zone, the first circuit and the reactor tank were filled with sodium, the packs of the lateral screen and all the rods of the control and protection (safety) system were charged, while steel simulation packs were placed in the active zone. The temperature of the sodium was maintained at a level of 220-230°C by electric heating. Circulation of the sodium was achieved by using two pumps at a low rate of revolution (25% of nominal).

In assembling the critical mass and carrying out the physical measurements, the reactor was equipped with a special starting device ensuring reliable control (monitoring) after charging the first packs of the active zone, using an initiating neutron source of relatively low intensity ($5 \cdot 10^8$ neutrons/sec). Charging of the active zone of the reactor was carried out from the center, by replacing the simulator packs with fuel packs. After the charging of each batch of packs the boron rods were "weighed" by the inverse

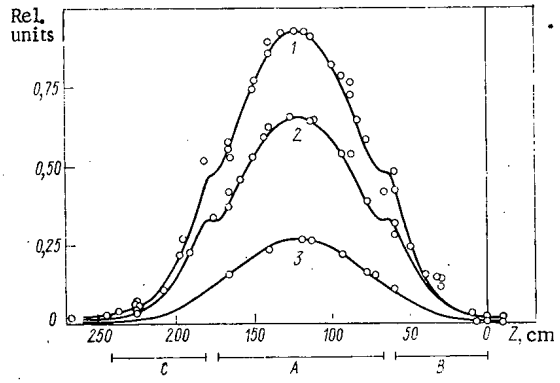

Fig. 1. Distribution of ^{235}U fissions with respect to the height of the reactor at various distances R from the vertical axis: A) active zone; B) upper reflector; C) lower reflector; 1) R = 0 and 29.5 cm; 2) R = 59 cm; 3) R = 88.5 cm.

multiplication method. The fuel rods – burn-up compensators – were not moved during the charging of the active zone and remained in the lower position. In plotting the extrapolation curve, allowance was made for the change in the efficiency of the neutron flux detectors, associated with the change in the dimensions of the active zone. This facilitated a substantial linearization of the inverse multiplication curve, and a refinement of the extrapolations used in the course of assembling the critical mass.

The critical mass of the reactor, with the boron rods completely extracted from the active zone, allowing for the replacement of the initiating source by the fuel pack, amounted to 201 packs. The computed value was ~200 packs.

Efficiency of the Control and Safety Rods

The control and safety system of the reactor contains 12 rods [1]: two boron automatic-control rods (AR), three boron emergency protection (safety) rods (AZ), one boron rod for compensating the temperature and power effects of reactivity (TK), and six compensating packs (KP) for compensating the loss of reactivity during burn-up.

In the boron rods, 60% enriched boron carbide is used. The compensating packs consist of two parts: absorbing packs made from impoverished uranium oxide, and fuel packs comprising fuel elements of the active zone.

The efficiency of the rods is measured in several ways. The relative efficiency is determined by the inverse multiplication method in the subcritical state, and by the method of overcompensation in the critical state. The absolute calibration is carried out by reference to the warming-up period of the reactor, using a precision period meter, and also by measuring the positive and negative changes in reactivity (during the warming-up period and after introducing an absorbing rod into the active zone respectively) by means of an analog reactivity meter adjusted for the calculated parameters of the delayed neutrons of the reactor.

In measurements by the method of overcompensation, the reactivity meter enabled compensation of the reactivity to be achieved with an accuracy of $7 \cdot 10^{-6}$ $\Delta k/k$. The various methods of measurement gave results agreeing with one another to within the corresponding experimental errors.

Automatic Control, Temperature Compensation, and Safety Rods

The efficiency of four automatic control rods was measured. After the physical measurements, the rods of the AR-1F and AR-2F types were replaced by standard rods, for which the efficiency measurements were repeated (AR-1 and AR-2).

The efficiency of the temperature compensator was obtained by the method of overcompensation from the measured efficiency of the compensating packs.

In determining the efficiency of the AZ (safety) rods two methods were employed: measurements based on inverse multiplication and those based on the throwing (dropping) of rods, the reactivity so introduced being measured with a reactivity meter. Measurements of this kind were carried out repeatedly. The results of the measurements, and also the design values of the efficiency, are presented in Table 1.

Compensating Packs (KP)

The efficiency of one compensating pack was measured by reference to the reactor warm-up period, using a period meter. The efficiency of the remaining compensating packs was determined by the overcompensation method. In addition to this, the efficiency of each compensating pack was measured with a reactivity meter during immersion of the rod. All these methods gave results agreeing with each other,

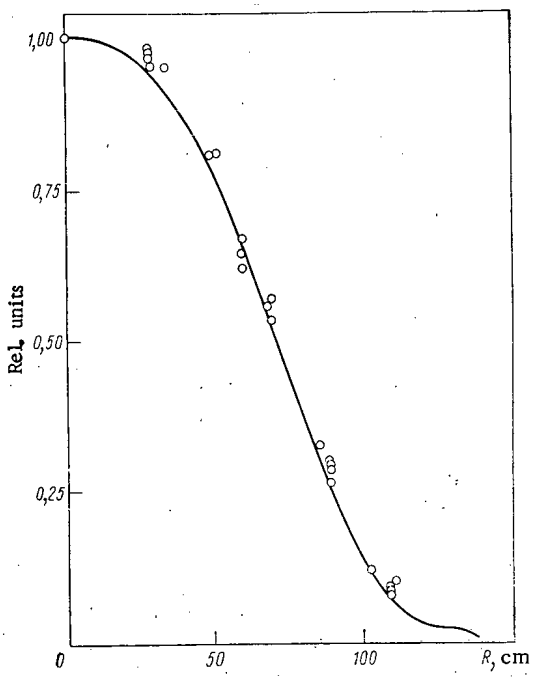

Fig. 2. Radial distribution of ^{235}U fissions.

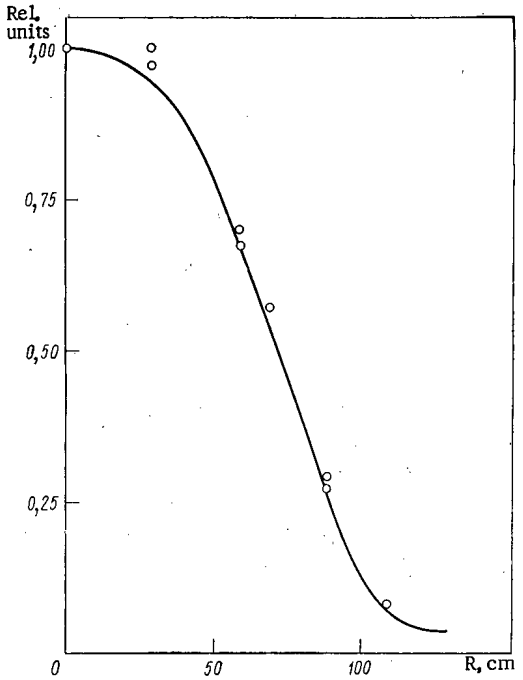

Fig. 3. Radial distribution of ^{239}Pu fissions.

within the limits of experimental error. The results of the measurements are presented and compared with design data in Table 2.

Interference of the Control Rods

The measurements showed that interference between the automatic control rods never exceeded the limits of measuring error. A similar conclusion was drawn for the temperature-compensation and automatic control, and also for the temperature-compensation and emergency (safety) rods. The efficiency of the compensating-pack rods situated close to the immersed temperature-compensation rods is ~15% lower than that corresponding to the raised temperature-compensator.

In analyzing the interference of the emergency (safety) rods, a certain tendency was observed toward a reduction in the efficiency (as determined by the throw method) of two and three rods by comparison with the inverse multiplication method. One possible explanation for this is the fact that no allowance is made for the neutron source in the kinetic equations solved by the reactivity meter.

The results of these measurements of the efficiency of the control rods showed that the maximum difference between the actual efficiency of the rods and the design value equalled ~10%. Control and safety were in fact in accordance with design. The adequacy of the compensation system will be determined after the reactor has been working under full power.

Efficiency of the Fuel Packs

The efficiency of the fuel packs was determined by the overcompensation method, by reference to a calibrating compensating pack. The overcompensation was effected in such a way that, after the substitution of the packs under consideration and the displacement of the compensating pack, the reactor had a positive reactivity of 0.01-0.07% $\Delta k/k$.

The measured efficiencies of the packs in the active zone after replacing a pack with sodium equalled 0.145-0.203% $\Delta k/k$. The measuring error was 0.007% $\Delta k/k$. The calculated values determined from perturbation theory lay close to the experimental values, allowing for the measuring errors. The sign and magnitude of the slight differences between the measured and calculated efficiencies depend on the location of the pack.

Measurements were also made of the reactivity effects which occurred on replacing the packs of the lateral screen with packs of the active zone. These effects were equal to 0.11-0.13% $\Delta k/k$ and agreed fairly well with calculation.

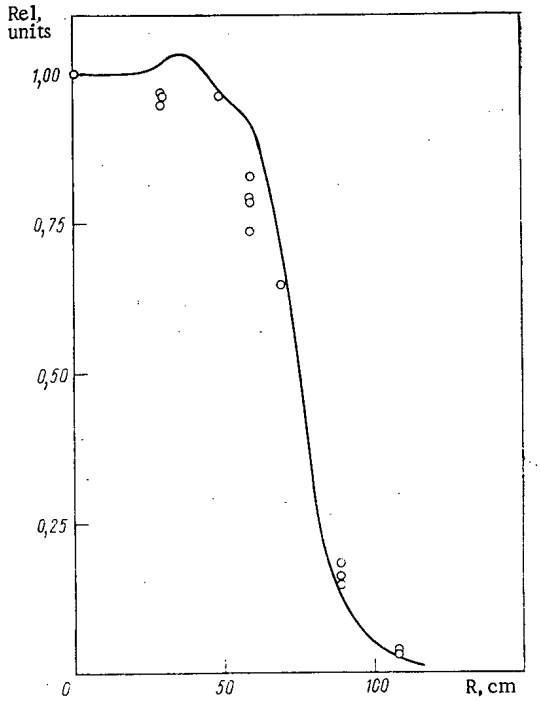

Fig. 4. Radial distribution of the fissions of natural uranium.

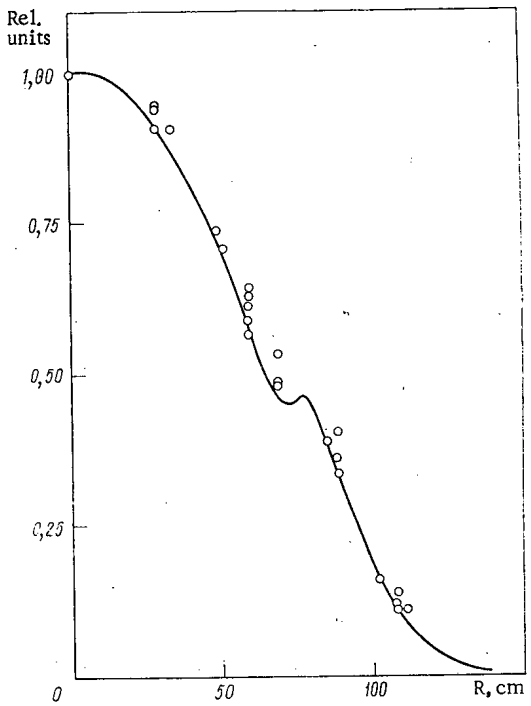

Fig. 5. Radial distribution of ^{23}Na capture.

The Sodium Void Reactivity Effect

The effect was measured by means of special "dead" packs without any sodium placed in the reactor in place of the fuel packs. After each installation of "dead" packs at various points of the reactor, all the boron rods were raised to the top end position and the warm-up period was determined. Then the packs were extracted from the reactor, dehermetized, and replaced in the same positions, after which the warm-up period was measured once again.

The difference between the periods enabled the desired effect to be determined. Since the effect to be measured was small, two or three packs were placed symmetrically with respect to the center at the same time.

The principal error in these measurements was associated with the temperature correction for the difference between states measured at different instants of time, and with the inaccuracy involved in reproducing exactly the same state of the reactor several times. Before each measurement of the state of the reactor, it was verified that the reactor had the same basic state for the same charging of the active zone. The use of data relating to the reproducibility of the basic state ensured a reasonably small value of the error in the effect. In these measurements special attention was given to the careful monitoring of the reactor temperature.

The results of the measurements made on the sodium void reactivity effect, presented in Table 3 together with computed data based on perturbation theory, showed that the effect of the complete removal of sodium from one pack was negative for all cells of the active zone and the screen. It should be noted that calculations based on perturbation theory give a fairly good idea of the magnitude of the effect of removing sodium from one pack.

The second method of measuring the sodium effect lay in the following. Instead of a fuel pack, cans containing hermetic gas spaces of different heights without any fuel were installed. Measurements with four types of cans enabled us to determine the effect of the displacement of the gas space with respect to the height of the can and demonstrated the necessity of introducing complex corrections in order to allow for the leakage of neutrons along the can, heterogeneity, unlocking, and slowing down, which greatly impedes the interpretation of the experimental results.

Temperature Coefficient of Reactivity

At the stage of the physical experiments approximate measurements of the temperature coefficient of reactivity were made. The temperature was varied by electric heating and by the circulation of sodium through the cold oxide traps, with only a slight flow of sodium through the reactor (two pumps working at low revolutions). The measurements were made at 150-240°C. The asymptotic temperature coefficient of reactivity was exactly the same in the ranges 200-240 and 160-180°C, or more precisely $(3.4 \pm 0.2) \cdot 10^{-5}$ and $(3.9 \pm 0.2) \cdot 10^{-5}$ $\Delta k/k/°C$ respectively.

The experiments revealed a certain nonlinearity of the temperature effect, which could not be explained by the nonlinearity of the Doppler effect by itself. The most likely reason for this nonlinearity lay in the inadequate temperature stabilization, due to the low rate of sodium circulation.

The calculated value of the temperature coefficient of reactivity at 250°C is $\sim 2.8 \cdot 10^{-5}$ $\Delta k/k/°C$.

Barometric and Hydrodynamic Reactivity Effects

Repeated changes in the pressure of the inert gas in the reactor for various sodium flow rates produced no changes in reactivity. This indicates that no gas accumulation takes place in the active zone.

Measurements of the reactivity effects on connecting and disconnecting the pumps of the first circuit showed that disconnection led to a slight positive reactivity effect, equal to $4.2 \cdot 10^{-4}$ and $3.2 \cdot 10^{-4}$ $\Delta k/k$ for four and three pumps respectively.

These effects are much smaller than the maximum hypothetical effects, equal to $\sim 3 \cdot 10^{-3}$ $\Delta k/k$.

Density Distribution of Various Reactions

The relative density distributions of various reactions over the volume of the reactor were measured by the activation method, using special measuring packs with a construction analogous to the fuel packs (the central fuel elements being removed). In the channel so formed we placed a steel ampoule with a set of various indicators all along it.

The measuring packs were placed in the reactor in place of the corresponding fuel packs and irradiated for several hours. Then the packs were extracted, the ampoule was withdrawn and opened, and the indicators were subjected to analysis. Seven packs were irradiated in one exposure. We measured the distributions of the following reactions: the fission of ^{235}U, natural uranium, plutonium; the capture of ^{238}U, sodium, gold, copper, manganese, nickel, and aluminum.

Figures 1-5 show the main results of the measurements in comparison with calculated data obtained from two-dimensional diffusion calculations.

The distribution of ^{235}U fissions with respect to the height of the active zone agrees closely with calculation. We find slightly higher values of the measured fission rates in the middle of the top end screen. At the same time, in the lower end screen the agreement between calculation and experiment was considerably better. In view of the fact that the fission of ^{235}U in the end screens makes only a slight contribution to the total power, these deviations have no practical significance. The radial distributions of ^{235}U fissions agree fairly closely with calculation; the possible measuring error is 5-10%. The same conclusion follows for the distribution of ^{239}Pu fissions and ^{23}Na captures.

The fission distribution of natural uranium agrees satisfactorily with calculation.

CONCLUSIONS

1. Analyses of the static physical characteristics revealed during the starting of the BN-350 reactor have for the first time enabled the methods of predicting these characteristics to be verified under the true-service condition of a fast power reactor.

2. These measurements show that, during the development and establishment of the reactor, the physical characteristics were determined to a reasonable accuracy. This facilitated the entry of the reactor into initial power production. When the reactor is being used at full power it will be possible to determine the power reactivity effect and the effect of fuel burn-up, to evaluate the adequacy of the reactivity compensation system, and to determine the period of continuous operation.

3. The set of computing data thus obtained, together with the results of measurements carried out on model critical assemblies and the reactor itself, offer new prospects for analyzing the accuracy of the predicted physical characteristics of fast power reactors and for perfecting the methods of calculation.

LITERATURE CITED

1. A. I. Leipunskii et al., "The BN-350 nuclear power station," Amer. Nucl. Soc., Suppl. to ANS-100 (1965), p. 15.
2. A. I. Leipunskii et al., "Erection of a nuclear power station with a BN-350 reactor," At. Énerg., 23, No. 5, 409 (1967).
3. Yu. E. Bagdasarov et al., Technical Problems of Fast Neutron Reactors [in Russian], Atomizdat, Moscow (1969).
4. L. P. Abagyan et al., Group Constants for Calculation of Nuclear Reactors [in Russian], Atomizdat, Moscow (1964).
5. Sh. S. Nikolaishvili et al., "Methods and programs for computing fast-neutron reactors," in: Transactions of the Trilateral Soviet–Belgian–Dutch Symposium on Problems of Fast Reactor Physics, Vol. 1 [in Russian], Izd. TsNIIatominform (Central Scientific-Research Institute of Atomic Information), Moscow (1970).
6. V. V. Khromov et al., in: Certain Problems of the Physics and Technology of Nuclear Reactors [in Russian], Atomizdat, Moscow (1965), p. 51.
7. A. M. Kuz'min and V. V. Khromov, in: Physical Engineering Problems of Nuclear Reactors [in Russian], Atomizdat, Moscow (1966), p. 33.
8. V. V. Orlov et al., "Fundamental principles in the choice of control organs for fast power reactors and the temperature and power effects of fast reactors," Kernenergie, 12, No. 4, 112 (1969).
9. A. I. Leipunskii et al., "Review of papers on the physics of fast reactors based on the BR-1, IBR, and BFS reactors," in: Transactions of a Symposium of the Member Countries of the Socialist Economic Union on the Present State and Future Prospects of Work in Creating Nuclear Power Stations with Fast-Neutron Reactors, Vol. 2 [in Russian], ONTI FÉI (United Technological Publishers, Physical Power Institute), Obninsk (1968), p. 177.
10. V. V. Orlov et al., "Experimental-computing studies of the physics of the control organs of the BN-350 reactor on the BFS-22 test bed," Preprint FÉI-306 [in Russian], Obninsk (1972).
11. A. M. Sirotkin et al., "Computing studies of heterogeneous effects in critical assemblies," in: Physics of Nuclear Reactors [in Russian], Atomizdat, Moscow (1968), No. 1, p. 106.
12. V. V. Bondarenko et al., Proc. Symp. Fast Reactor Physics, Vol. II, IAEA, Vienna (1968), p. 305.

APPARATUS FOR MONITORING THE BN-350 REACTOR AND ENSURING SAFETY DURING ITS PHYSICAL INITIATION

B. G. Dubovskii, V. V. Bondarenko,
A. A. Vaimugin, A. S. Vodolazhskii,
I. G. Gaidurov, A. N. Efeshin,
P. G. Dushin, V. I. Kozlov,
I. M. Kisil', V. A. Krasilov,
V. F. Lyubchenko, V. F. Mamontov,
A. E. Merkulov, G. B. Pomerantsev,
N. V. Skorikov, Yu. F. Taskaev,
and I. M. Shvedenko

UDC 621.039.519:621.039.58:
621.039.526

During the first charging of a nuclear reactor with fuel, as well as in experiments at the physical power level and during the initial use of the reactor at full power, safety is largely determined by the incorporation of reasonably sensitive and reliable measuring instruments in the neutron-power monitoring system. The sensitivity of the standard starting equipment of power reactors is insufficient for a number of reasons (the difficulty of creating a powerful starting source, the high level and broad spectrum of industrial noise). The laboratory adjustment of the standard apparatus is ineffective, since under laboratory conditions it is hard to reproduce all forms of interference. The creation of screened rooms for the standard measuring apparatus, which involves extra laying of cables, the use of independent supply sources, and so on, are not justified because of the "one-off" nature of the experiment, since in the subsequent power mode of operation the noise contribution is insignificant.

One alternative is the development of additional channels in the starting apparatus, the sensors being disposed in nonstandard places. The reactor shaft might provide such a place in the case of the BN-350 reactor [1, 2].

The purpose of the additional channels was to monitor the power of the reactor during all manipulations involving the active zone. Special attention was paid to the creation of highly-stabilized current instruments, which have a number of advantages under the condition of low γ-fields encountered in the physical initiation of the system.

In developing a reactivity meter, allowance was also made for the various requirements of engineering psychology; the principal such requirement as regards "man-machine" systems is to present the information in such a way that the operator may correct any deviation from the norm quickly and easily. To this end a small number of basic instruments have been created such as to present the information in a simple, sometimes mnemonic, form. More and more use is now being made of command instruments, an obligatory condition of which is simplicity of representation of the operating mode monitored, usually in analog form. A correct solution of the problem is one in which the operator holds the process within specified limits by acting upon one executive device and using information from one command instrument.

In constructing a command instrument, the main difficulty lies in finding a parameter, to be measured or calculated, which will, on the one hand, depend on many variables of the process, and on the other provide an unambiguous representation of the state of the system and the process being monitored. As regards nuclear reactors, a convenient quantity for use in the command instrument is the reactivity $\rho = (k_{eff}-1)/k_{eff}$, which depends on many variables describing the behavior of the reactor, and at the same time may easily be calculated from the character of the time change in the neutron flux, using specialized

Translated from Atomnaya Énergiya, Vol. 36, No. 2, pp. 104-107, February, 1974. Original article submitted October 22, 1973.

computing devices (reactivity meters) or standard computers connected to an information-processing circuit. In reactivity meters the slightly worse computing accuracy is compensated by the possibility of calculating in a real time scale. When the reactor is working in a steady power mode, the role of the reactivity meter is to process information regarding the true state of the reactor and to provide early warning of the onset of any transient processes. The reactivity meter operates stably with a sensitivity of $\sim 5 \cdot 10^{-2}$ cent and allows reactivity effects to be followed when the temperature of the active zone changes by about 0.1°C.

Monitoring Apparatus for the State of the Reactor during Physical Initiation

A ^{238}Pu–Be starting source with an intensity of $5.3 \cdot 10^8$ neutrons/sec created a neutron flux two orders of magnitude lower than that required for the reliable monitoring of standard starting apparatus. In order to bridge this gap, the sensors of supplementary pulse and current instruments were placed in the reactor shaft, while in the standard blocks (units) of ionization chambers (BIC) more sensitive than usual chambers and counters were placed. These measures were sufficient for the reliable monitoring of power during ordinary changes in the composition of the active and breeding zones.

Three linear pulse channels with SNM-18 counters and three similar channels with KNT-54 chambers were set in the reactor shaft. All the channels were connected to scaling devices through discriminator amplifiers. One of the channels of each type had an output to a logarithmic intensity meter and from this to an automatic recording potentiometer. Provision was made for connecting an acoustic reactor-power monitoring device to the system.

In the reactor shaft we also placed four KNK-56 chambers connected to a dc amplifier, with a galvanometer on the operator's desk, to a multirange automatic-recording electronic potentiometer with contacts in the emergency protection (safety) system, to a PAMIR-M reactivity meter with automatic recording, and to a TIM-2k current power meter, with automatic recording and a pointer device at the output. The sensors were placed in a polyethylene moderator 50 mm thick and arranged on the outer side of the support ring of the reactor at the height of the center of the active zone at an angle of 120° to each other.

During the physical initiation period, the equipment of the ionization chamber units included:

1) three linear pulse channels with SNM-18 counters (instead of the designed KNT-54 chambers) with standard recording equipment and additional scalers for recording the neutron flux over the range $0.1\text{-}10^2$ neutrons/cm^2 · sec, ensuring emergency cover on the "two out of three" principle;

2) three logarithmic pulse channels with KNT-54 fission chambers and with outputs to supplementary scalers for recording the neutron flux from 5 to 10^5 neutrons/cm^2 · sec and for emergency cover over the period of the reactor on the "two out of three" principle;

3) two linear current channels with KNK-56 chambers (instead of the designed KNK-53) with outputs to multirange automatic-recording potentiometers for measuring the neutron flux over the range $5\text{-}5 \cdot 10^8$ neutrons/cm^2 · sec (current $5 \cdot 10^{-12}\text{-}5 \cdot 10^{-4}$ A) and for emergency cover with respect to excessive power;

4) one current channel with a KNK-56 chamber and an output to an M-135 galvanometer, the current measuring range being $2 \cdot 10^{-13}\text{-}3 \cdot 10^{-4}$ A;

5) three logarithmic channels with KNK-53 chambers to ensure emergency cover over the period of the reactor on the "two out of three" principle at power levels of $10\text{-}10^6$ kW.

The sensitivity of the channels with the SNM-18 counters, determined from the activity of gold foil in the presence of a ^{238}Pu–Be source, was 22 pulses/neutron/cm^2; the sensitivity of the channels with the KNT-54 detectors was about 0.25 pulse/neutron/cm^2.

The foregoing apparatus ensured reliable monitoring of the state of the reactor.

The TIM-2k Current Channel

The equipment of the TIM-2k channel has its own reading instrument and an output to an automatic electronic recorder. For the convenience of the operator, a standard galvanometer on the operator's desk is connected to the TIM-2k output.

The maximum sensitivity of the instrument is $2 \cdot 10^{-13}$ A per scale division, the error in current measurement within the measuring range is ±2%. The instrument reliably recorded the change in the neutron flux during the first charging of the reactor, from a state with $k_{eff} \approx 0.97$ (a KNK-56 chamber in the reactor shaft being connected to the input of the instrument). The instrument reacted to the movement of all the control and safety rods, starting from the raising of the first emergency protection rod.

The TIM-2k was used for monitoring the subcriticality of the reactor and any change in the neutron flux in the subcritical reactor when assembling the critical load, for monitoring the engagement of the control and safety rods with the executive mechanisms, for monitoring the power of the reactor when operating in the power mode or in the steady and transient states.

The reliable operation of the TIM-2k greatly increased safety in the use of the reactor.

The PAMIR-M Reactivity Meter

The instrument was developed specially for the BN-350 reactor. The dynamic range of variation of the neutron flux when calculating the reactivity is two decades, a device being incorporated for decade-by-decade selection of the measuring range. The range of input currents is 10^{-10}-10^{-3} A per scale, the sensitivity of the power meter is 10^{-12} A. The range of measurable reactivities is 1 cent.–5 doll. per scale, the reactivity sensitivity is $5 \cdot 10^{-2}$ cent.

The pass band of the instrument is not worse than 12 Hz for an input current of over 10^{-7} A and falls with diminishing input current. With the reactor operating in the automatic power-maintenance mode, the reactivity meter allows the recording of changes in reactivity which lie outside the limits of sensitivity of the automatic regulator. The reactivity meter has two reading galvanometers (power and reactivity) and two outputs to automatic recorders. The current of the ionization chamber is passed to the input of the power-meter amplifier.

Using the reactivity meter, the following operations may be stably and reliably effected:

1) monitoring changes in ρ under transient conditions at the physical and power levels of production, including the monitoring of fluctuations in ρ during the steady-state operation of the reactor;
2) monitoring the maintenance of ρ during overcompensations;
3) monitoring the maintenance of a specified rate of change of power or temperature during the manual regulation of the reactor;
4) monitoring the efficiency of the automatic control system;
5) studying the temperature, power, barometric, and hydrodynamic reactivity effects;
6) studying the efficiency and calibration characteristics of the control and safety rods and packs;
7) passing signals relating to the power and reactivity to the parameter-recording system when studying the dynamic characteristics and the transient modes of the reactor;
8) parallel monitoring of changes in power and reactivity, in order to improve the safe exploitation of the reactor.

The reactivity meter enables us to derive the calibration characteristics of the control and safety rod organs rapidly and directly from the automatic recorder strip, as the rods are continuously inserted into the reactor.

It is also interesting to use the reactivity meter in order to estimate various reactivity effects, for example, the asymptotic temperature effect (ATER), the void effect, and others, when the effect is estimated from the difference in the positions of the control and safety organs, the efficiency of which is being determined by the reactivity meter. In this way we obtained the temperature coefficients of reactivity in the ranges (160-180)°C $-3.9 \cdot 10^{-5}$ 1/°C and (200-240)°C $-3.4 \cdot 10^{-5}$ 1/°C, estimated (together with measurements made over the warming-up period) the reactivity effects on removing the sodium from the active zone and the end screens (from the central part of the active zone, from the whole active zone, or from the upper third of the active zone and their end screens). The reactivity meter records the effect associated with the simulation of an ejection of sodium from one fuel pack (scale effect 0.0063%). The hydrodynamic effect of reactivity due to the stopping of one principal circulation pump of the first circuit is about 1 cent. We found that there was no barometric effect associated with the change in the amount of gas dissolved in the coolant with changing pressure [3].

Under the conditions of the BN-350 reactor, the reactivity meter proved to be an extremely useful technological instrument, by means of which the operators could readily monitor the reactor in the steady state and during transient processes. The character of the information obtained from the reactivity meter outstrips that of other power or temperature measuring devices and greatly improves safety in the use of the reactor. The unambiguous nature of the algorithm for the control of the reactor by reference to information derived from the reactivity meter, and the rapidity of processing of the input information confirm that the reactivity meter may be classified as a genuine technological command instrument.

During the study of the BN-350 reactor with the PAMIR-M instrument, several hundred measurements of reactivity were made. It was found that the error in determining ρ was no greater than 5%, while the rate of obtaining information was incomparably higher than that of the traditional means of calculating the reactivity from the reactor warm-up period. In addition to this, the reactivity meter enables us to determine negative reactivities under conditions in which the traditional methods, such as those based on the "dropping" of an absorber, are inapplicable for constructional or other reasons.

Apparatus for Measuring the Period

For determining reactivity effects by the method of the asymptotic period during the physical initiation of the BN-350 reactor we used the apparatus described in [4]. The period-measuring method was based on the use of a current integrator as an analog-digital device converting the continuous information into discrete data suitable for subsequent analysis. The apparatus in question was used for estimating the supercriticality of the reactor, for the calibration of the control and safety devices, measurements of the temperature and sodium void reactivity effects, and the determination of the efficiency of the fuel and screen packs.

The authors wish to thank the service personnel and the directorate of the BN-350 reactor and also all those who took part in developing the apparatus, in the measurements, and in the interpretation of the experimental results.

LITERATURE CITED

1. A. I. Leipunskii et al., "The BN-350 nuclear power station," Amer. Nucl. Soc., Suppl. to ANS-100 (1965), p. 15.
2. Yu. E. Bagdasarov et al., Technical Problems of Fast Neutron Reactors [in Russian], Atomizdat, Moscow (1969).
3. V. V. Orlov et al., "Study of the physical characteristics of the BN-350 reactor on starting" (this issue, p. 121).
4. V. F. Mamontov, "Apparatus for measuring the period of a reactor," Preprint FÉI-289 [in Russian] (1971).

STUDY OF THE RADIATION CONDITIONS DURING THE STARTING OF THE BN-350 REACTOR

D. S. Yurchenko, N. D. Tverdovskii,
M. Ya. Kulakovskii, Yu. P. Tsurukin,
B. G. Romashkin, V. A. Sergeev,
G. M. Sergin, O. D. Bakumenko,
and N. V. Skorikov

UDC 621.039.538

As the BN-350 reactor was being started, the radiation conditions were measured stage-by-stage as the reactor power increased. This enabled us to predict the radiation conditions on passing from one power level to another, to estimate the levels of radiation while carrying out technological operations with experimental packs, samples, equipment of the first circuit, and so on.

The program of measurements included: 1) a study of the efficiency of the counteractivation and biological shielding of the reactor; 2) a study of the efficiency of the biological shielding at the site of the first circuit; 3) a determination of the fluxes of radiation to the main constructional units of the reactor; 4) at the stage of physical initiation, a measurement of the levels of radiation in places which would be inacessible after the reactor had reached nominal power; 5) measurement of the activity of the coolant and the gas system of the first circuit.

The radiation measurements ensured the safe conduct of operations when carrying out physical investigations in the active zone of the reactor (operations with experimental packs, the extraction of the ampoules containing the indicators, the preparations of the ampoules, and so on).

In this paper we shall present the results of some investigations into the radiation conditions in the following stages: tests and investigations before starting the reactor; measurements at powers up to 1 kW, up to 150 kW, and up to 50 kW.

These investigations enabled us to predict the radiation conditions at the nominal power of the reactor and to ensure radiation safety when carrying out power initiation.

TABLE 1. Distribution of the γ-Radiation Dose Rate in the Boxes of the First Circuit

Points of measurement	Dose rate of γ-radiation, R/sec
On the heat-insulation surface of a 500 mm diameter pipe	4.5
On the heat-insulation surface of a 600 mm diameter pipe	4.9
Pipe section without heat insulation	6.5
On the heat-insulation surface of the heat exchanger	2.3
On the wall close to the heat exchanger	1.6
At the entrance into the box	0.6

Construction of the Shielding for the BN-350 Reactor

The construction of the shielding for the BN-350 reactor is shown in Fig. 1 [1, 2]. The active zone of the reactor, 160 cm in diameter and 106 cm high, is made up of hexagonal packs. The thickness of the top and bottom end screens is 60 cm each. The lateral breeding zone, 210 cm high and 45.2 cm thick, is made up of packs of the same dimensions. Beyond the lateral breeding zone is a store for worked-out packs 12 cm thick. Further out in the radial direction follow the neutron steel shield 20 cm thick, a layer of sodium 67.5 cm thick, the shield of the reactor vessel, made of stainless

Translated from Atomnaya Énergiya, Vol. 36, No. 2, pp. 107-112, February, 1974. Original article submitted October 22, 1973.

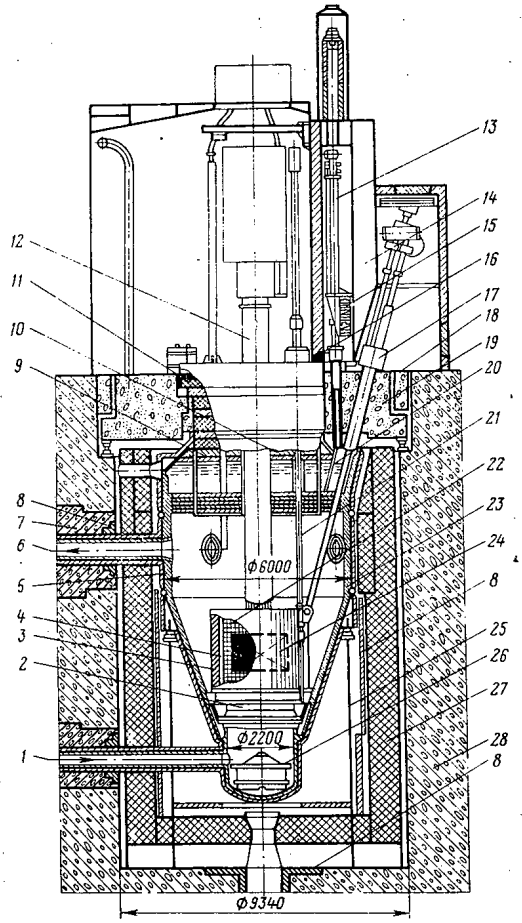

Fig. 1. Longitudinal section of the BN-350 reactor with its component mechanisms: 1) sodium entry; 2) pressure collector; 3) steel blocks; 4) store for worked-out packs; 5) reactor vessel; 6) sodium outlet; 7) boron-containing concrete; 8) steel shield; 9) large rotating stopper; 10) small rotating stopper; 11) steel and graphite shield; 12) central column with control and safety mechanisms; 13) mechanism for transferring the packs; 14) recharging box; 15) cast-iron shot; 16) uranium; 17) elevator; 18) shielding stopper; 19) upper stationary shield (concrete); 20) sodium level; 21) recharging mechanisms; 22) breeding zone; 23) thermal shield; 24) active zone; 25) reactor support; 26) protective coat; 27) lateral shield (iron-ore concentrate); 28) concrete shield.

steel sheets with a total thickness of 7.5 cm, then the reactor vessel, the protective jacket, and the reactor support. The total thickness of these structures is 6 cm. The support (base) of the reactor is a carbon steel shield 16 cm thick. An iron-ore concentrate is poured into an annular tank some 100 cm in size. Beyond the layer of iron-ore concentrate is a layer of ordinary concrete 300 cm thick.

The sodium pipes penetrate the side shield. At the points at which the pipes enter the concrete shield there is a steel shield and boron-containing concrete to prevent the ordinary concrete from overheating and to reduce the neutron flux to the concrete. Beyond the concrete shield, all the pipelines of the first circuit (incoming and outgoing) are bent round in a special box ("neutron trap") to reduce the neutron field at the point at which the pipelines pass out into the box of the first circuit.

The lower shield of the reactor consists of a pressure collector containing the tails of the packs 90 cm thick, a layer of sodium (~250 cm), the reactor vessel and jacket, a layer of carbon steel (~8 cm), and an iron-ore concentrate (~100 cm); below this follows the concrete base. The lower shield is penetrated by the gas pipe for cooling the reactor shaft. At the entrance of the gas pipe into the shield the concrete base is protected by an extra layer of steel.

The part of upper shield is played by the heads of the packs in the active zone and lateral screen (~37 cm), a layer of sodium (~320 cm), a steel plate made up of stainless-steel sheets (~70 cm), a layer of sodium (~100 cm), and also (in the rotating stoppers) a set of carbon steel and graphite layers with a total thickness of ~180 cm. All the gaps penetrating the upper shield are of the two-stage type. The upper stationary shield is made of concrete

Instruments and Methods of Studying the Radiation Conditions

The system for monitoring the radiation conditions in the BN-350 reactor operates when the reactor is working on power, during repair work, technological operations and processes (testing the state of the radioactive systems and sources), and also in emergency situations.

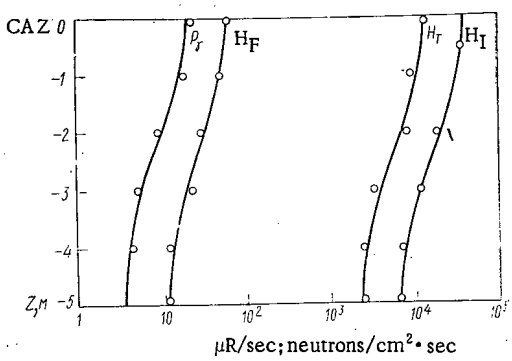

Fig. 2. Flux distribution (neutrons/cm² · sec) of the thermal, intermediate, and fast neutrons (H_T, H_I, and H_F) and dose rate of the γ radiation P_γ (μR/sec) on the surface of the reactor vessel below the center of the active zone (CAZ), measured at a reactor power of ~200 W (Z = distance from the center of the active zone).

The monitoring of the radiation conditions and the technological monitoring of the radioactive parameters are effected continuously by means of stationary remote-control instruments, local instruments (in certain places), and portable instruments, and also by the analysis of samples in laboratory equipment. The operative information is concentrated in the central radiation-monitoring panel. The dose rate of γ radiation and the neutron fluxes are monitored in the servicing, semi-servicing, and service-repair rooms; so are the content of radioactive gases and aerosols in the air of the working rooms and the ejection pipe, radioactive contaminants, and so forth [3, 4]. The following radiation-technological parameters are monitored in the BN-350 reactor: the hermetic state of the fuel-element cans, by reference to the delayed neutrons in the coolant of the first circuit and the ^{88}Kr isotope in the gas cushion of the apparatus; the hermetic state of the radioactive systems and equipment by reference to the appearance of γ activity, radioactive gases, and aerosols in the cooling systems; the efficiency of operation of the purification systems and the accumulation of activity in the filters, and also the activity of the gas effluents [4, 5].

In addition to this, any γ activity in the packs discharged from the system and passing along the technological transportation tract is duly detected.

Measurement with highly-sensitive γ radiometers is carried out in respect of the radiation behind the shield for reactor powers of a few megawatts; this enables us to predict the state of the shielding when the reactor is brought up to nominal power.

Measurement of the neutron radiation in the boxes of the first circuit had to be carried out immediately after the reactor had been brought up to power, while the level of γ radiation from the ^{24}Na was fairly low.

In the prestarting period, in accordance with the general program of investigations, the following preparatory operations and measurements were carried out: charts were set up for the monitoring points in the various rooms and in the equipment; the background characteristics were measured; the state of the shielding in the technological transportation tract was evaluated with the aid of a radiation source; the monitoring apparatus was prepared and calibrated; additional local instruments were set up; the soundness of the movable shielding was verified (stoppers, openings, protective doors, etc.).

Radiation Measurements for a Power of up to 1 kW

The neutron and γ radiation fluxes falling on the reactor vessel and adjacent parts were measured. In order to ensure access to the reactor vessel, a temporarily-open assembly aperture in the shaft of the reactor was employed. The measurements in the shaft were carried out from the instant at which a neutron source of intensity $\sim 5 \cdot 10^8$ neutrons/sec had been installed and during the assembly of the critical mass; this enabled us to assess the weakening of the neutron flux in simulators situated in the cells of the active zone and the screen. In the first brief raising of the reactor to a power of ~1 kW the dose rate of γ radiation on the surface of the pipelines of the first circuit reached ~0.8 μR/sec, which enabled us to estimate the activity of the sodium coolant even on the first occasion of power production and to predict the radiation conditions in the boxes of the first circuit in any subsequent raising of the reactor power. At a power of ~200 W we measured the neutron and γ radiation fluxes in the shaft of the reactor (Fig. 2). The neutron flux (referred to nominal power) on the surface of the reactor vessel was estimated as $\sim 2 \cdot 10^{11}$ neutrons /cm² · sec at the level of the center of the active zone for a specific loading of the reactor (the inner store of the apparatus being filled with steel simulators), and at the level of the inlet pipelines $\sim 7 \cdot 10^{20}$ neutrons /cm² · sec. It should be noted that, on charging the inner store with worked-out packs of the active zone, the neutron fluxes behind the reactor vessel may rise to $\sim 1.5 \cdot 10^{12}$ neutrons/cm² · sec.

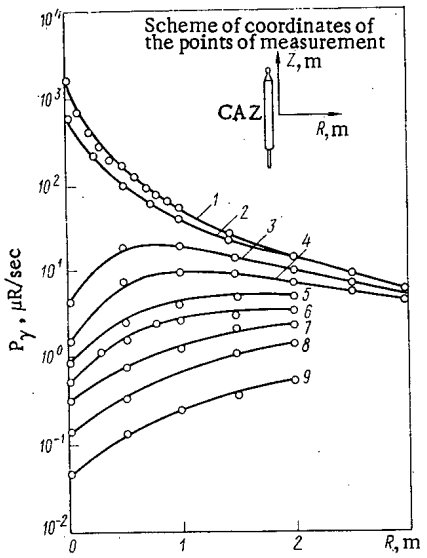

Fig. 3

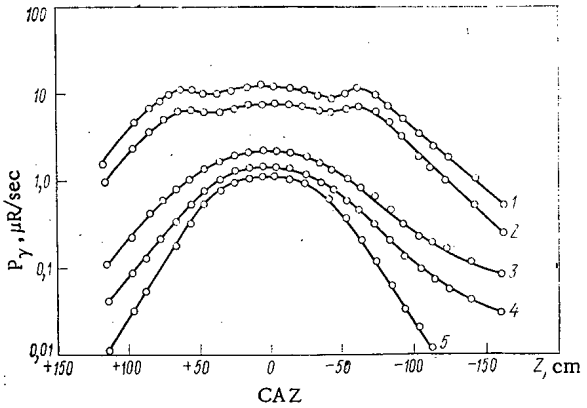

Fig. 4

Fig. 3. Distribution of the dose rate of γ radiation from the measuring pack after irradiation at a power of ~150 kW in the radial (R) and vertical (Z) directions (see scheme of coordinates of the points of measurement): 1) Z = 0; 2) Z = 0.53; 3) Z = 1.25; 4) Z = 1.75; 5) Z = 2.25; 6) Z = 2.65; 7) Z = 3.25; 8) Z = 4.25; 9) Z = 5.75.

Fig. 4. Distribution of the dose rate of the γ radiation along the surface of the stainless steel ampoule after irradiation at a power of ~150 kW for various holding times (Z is the distance from the center of the active zone): 1) 13 h; 2) 16 h; 3) 36 h; 4) 63 h; 5) 320 h.

Radiation Conditions While Carrying Out Physical Investigations

During the physical investigations in the BN-350 reactor (based on activation detectors) the energy-evolution and neutron flux distributions were measured. The principal operations in which special measures had to be taken to ensure normal radiation conditions were those associated with the extraction of the detectors from the measuring packs. Operations relating to the disengagement of the indicator ampoules and measuring pack were carried out manually.

In order to ensure normal radiation conditions above the shield, only the head of the pack was raised; the maximum dose rate of γ radiation then reached ~5 μR/sec at a distance of 0.5 m from the head of the measuring pack of the active zone after the reactor had operated at a power of ~150 kW, and the induced ^{56}Mn activity was then determined. During the preparation of the indicator ampoule, also situated in the shield, the dose rate of γ radiation was determined by the activation of the aluminum linings, and equalled ~5 μR/sec on the surface of the linings situated in the center of the active zone (on irradiation at a power of ~150 kW).

The results of long-distance measurements of the dose rate of γ radiation from the measuring pack and stainless-steel ampoule are presented in Figs. 3 and 4. The fall in the dose rates of γ radiation in the vertical direction is associated with the presence of the end screen and the increase in self-absorption. The rise in the dose rates of γ radiation at the boundary separating the active zone and the end screens from the stainless steel ampoule is due to an increase of the capture cross section in the ^{56}Mn.

Activity of the Coolant of the First Circuit and the Gas Blanket of the Reactor

In order to determine the activity of the coolant of the first circuit at a power of ~150 kW, sodium samples were taken and subjected to γ spectral analysis in a laboratory installation with a semiconducting detector, and the dose rates of the γ radiation from the samples were also measured with a γ radiometer. The activity of the coolant, referred to the nominal power of the reactor, is ~16 Ci/liter, in good agreement with calculated data (~15 Ci/liter). In order to monitor the hermetic state of the fuel elements, samples were taken from the gas blanket of the reactor, passing through the standard gas-sampling system into a DZ-20 gas chamber. The measurements were carried out at a reactor power of up to 50 MW.

When the reactor was operating at a power of ~150 MW (coolant temperature ~350°C, main circulation pumps of the two loops of the first circuit working at 250 rpm), the activity of the ^{23}Ne and ^{41}Ar was respectively $\sim 10^{-4}$ and $\sim 1.5 \cdot 10^{-7}$ Ci/liter.

With the apparatus working at a power of ~50 MW, in the gas blanket of the reactor we found an activity of 10^{-6}–10^{-7} Ci/liter in long-living isotopes, due to surface contamination of the fuel elements. The activity of the gas depends on the operating conditions of the main circulation pumps and the temperature of the coolant.

Radiation Conditions in the Boxes of the First Circuit and behind the Biological Shielding

In order to predict the radiation conditions in the boxes of the first circuit and compare the design data with the actual results, we measured the γ radiation dose rates on the surfaces of the equipment, the pipelines of the first circuit, the walls and box coverings, and also the neutron fluxes around the pipelines at the entrance into the neutron-trap room, with a reactor power of up to 150 kW.

The results of the measurements, extrapolated to nominal power, are presented in Table 1.

After bringing the reactor up to power, the γ radiation dose rate due to the ^{23}Ne was measured almost immediately (< 5 min) on the surface of the pipe coming out of the reactor. The γ radiation dose rate, referred to 1000 MW, was $\sim 3 \cdot 10^4$ μR/sec (with the loops operating in the nominal mode).

The neutron flux measured at a power of ~150 kW at the entrance into the neutron trap (referred to nominal power) equalled $\sim 2 \cdot 10^5$ neutrons/cm^2 · sec around the incoming pipes. The neutron flux around the incoming pipes at the reactor vessel amounted to $\sim 7 \cdot 10^{10}$ neutrons/cm^2 · sec. Thus on the straight part of the pipe ~4 m long the weakening of the total neutron flux was $\sim 3.5 \cdot 10^5$. At the outlet from the neutron trap (inlet into the box of the first circuit), according to estimates based on measurements at a power of ~1 MW, the neutron flux is 10^2 neutrons/cm^2 · sec. For complete charging of the inner store, the neutron flux may increase by roughly a factor of six. The efficiency of the biological shielding of the apparatus and the boxes of the first circuit was checked at each reactor power level. In individual places, local gaps in the shielding were detected, and additional shielding was accordingly installed. On measuring the γ and neutron radiations behind the shielding of the boxes and the apparatus at power levels up to 50 MW, no fields of radiation with an intensity above the threshold of sensitivity of the instruments were observed; hence, when the reactor passes to nominal power, it is not expected that the limiting permissible levels of penetrating radiations [6, 3] will be exceeded behind the biological shielding of the boxes and apparatus.

In measuring the activity of the gas and the aerosols and the dose rates in the cooling systems (boxes of the first circuit, coolant of the second circuit, and so on) no fluxes of radiation or activity above the sensitivity threshold of the apparatus were found; this indicated a hermetic state of the radioactive systems of the equipment.

CONCLUSIONS

1. The results of the radiation measurements confirmed the main design values of the levels of radiation.

2. Estimates of the activity of the sodium based on direct measurements and measurements of the dose rates of γ radiation on the surface of the pipelines were in satisfactory agreement with calculated data; the value of the activity extrapolated to the nominal reactor power equals ~16 Ci/liter.

3. The efficiency of the shielding around the passages of the pipelines in the first circuit was quite satisfactory; it is expected that the neutron flux in the boxes at nominal power will be considerably below the design value.

4. The results of our measurements of neutron and γ radiation fluxes at a power of ~150 kW on the outer surfaces of the reactor and the boxes of the first circuit show that no defects occur in the shielding, apart from individual local defects associated with the assembly of the system.

5. The level of irradiation endured by personnel when working on the extraction of the measuring packs and the preparation of the ampoules containing the indicators was no greater than the permitted daily dose.

6. The foregoing measurements are only part of a general program of investigations into the radiation conditions of the BN-350 reactor.

The next stages will be enacted after the reactor has passed into power production and been used for a considerable period.

LITERATURE CITED

1. Yu. E. Bagdasarov et al., Technical Problems of Fast-Neutron Reactors [in Russian], Atomizdat, Moscow (1969).
2. M. Ya. Kulakovskii et al., "Characteristics of the design of biological and counter-activation shielding in fast reactors," in: Transactions of the Symposium of the Member Countries of the Socialist Economic Union – Present State and Future Prospects of Work on the Creation of Nuclear Power Stations with Fast Neutron Reactors [in Russian], Vol. 2, ONTINFÉI (United Technological Publishers, Physical Power Institute), Obninsk (1968), p. 294.
3. Basic Sanitary Rules for Working with Radioactive Substances and Other Sources of Ionizing Radiations (OSP-72) [in Russian], Atomizdat, Moscow (1973).
4. B. P. Golubev, Dosimetry and Shielding from Ionizing Radiations [in Russian], Atomizdat, Moscow (1971).
5. I. A. Efimov et al., "Principles of monitoring the failure of fuel elements in fast-neutron power reactors by reference to the activity of the sodium and the gas," in: Transactions of the International Conference on Engineering Problems Regarding the Safety of Fast Reactions, Vol. 1 (Karlsruhe, Federal German Republic, 1972), Gesellschaft fur Kernforschung M.B.H. (1973), p. 399.
6. Norms of Radiation Safety (NRB-69) [in Russian], Atomizdat, Moscow (1972).

THE A-1 STATION, CZECHOSLOVAKIA'S FIRST ATOMIC POWER STATION, WITH THE KS-150 HEAVY-WATER REACTOR (DEVELOPMENT AND CONSTRUCTION)

V. M. Abramov, B. B. Baturov,
N. V. Bogdanov, V. F. Zelenskii,
V. E. Ivanov, B. L. Ioffe,
G. N. Karavaev, V. A. Mitropolevskii,
M. M. Pchelin, P. I. Puchkov,
Yu. N. Remzhin, G. N. Ushakov,
P. I. Khristenko, J. Keger,
J. Kelner, M. Kozák,
A. Komárek, K. Kostovský,
V. Patrovský, Č. Skleničká,
L. Tomík, A. Ševčík,
and V. Špet'ko

UDC 621.039.524 46.034.3

The A-1 station, the first atomic power station in Czechoslovakia, with a power of 150 MW (Figs. 1 and 2) was put into operation at the end of December, 1972, at Jaslovské Bohunice.

The purpose of this atomic power station, built through the efforts of Czechoslovakian and Soviet specialists, is not only to produce electrical energy but also to obtain and accumulate the experience necessary for the further development of the nuclear power industry.

The Reactor

The A-1 station houses the KS-150 vessel-type heavy-water reactor, which is gas-cooled and operates at a gas pressure of 65 abs. atm [1-4]. The fuel used is natural metallic uranium.

The use of heavy water, together with the high thermal loads (60 kW/kg) and the high burnup values (more than 1.0%) attained in the fuel elements developed for this reactor, makes it possible, thanks to a

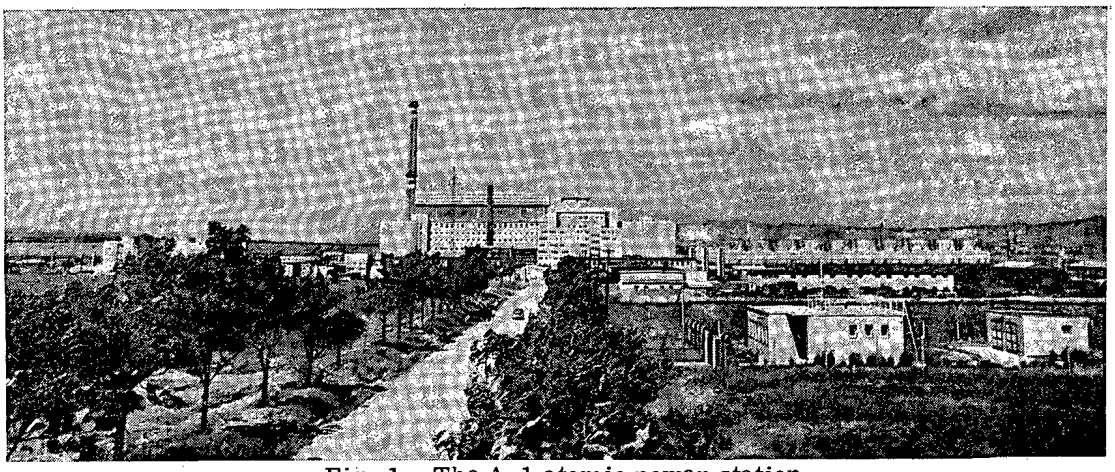

Fig. 1. The A-1 atomic power station.

Translated from Atomnaya Énergiya, Vol. 36, No. 2, pp. 113-124, February, 1974. Original article submitted October 4, 1973.

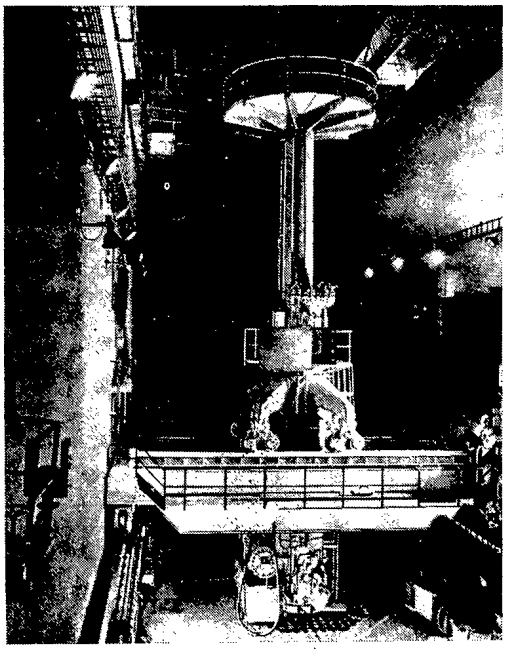

Fig. 2. General view of the reactor room of the power station, showing the recharging apparatus.

good neutron balance, to reduce the amount of uranium required for the initial fuel charge (23 tons of natural uranium) and ensure low uranium consumption per kilowatt of electrical energy generated. At the same time, the investment cost of the power station is increased by the need to purchase heavy water and by the more complicated flow diagram of the station.

The construction of the atomic power station was a joint endeavor by Soviet and Czechoslovakian industry. It was the Soviet Union that developed the technology of producing metallic-uranium fuel elements designed for high burnup, thermal stress, and temperature under conditions of high dynamic heads in the gaseous coolant; the production of aluminum and zirconium alloys and thin-walled tubes made of these alloys; the manufacture of large aluminum tanks to hold the heavy water and of the metal billets for these tanks; the manufacture of leak-proof heavy-water pumps operating at a pressure of more than 60 abs. atm; and the development of jacket leak monitoring systems (JLMS) and control and protection system (CPS).

It was the Czechoslovakian Socialist Republic that mastered the extremely complicated production of steel vessels more than 5 m in diameter and about 20 m high and operating under a pressure of 65 abs. atm, the manufacture of the discharging and charging apparatus (DCA), which made it possible to recharge the reactor while in operation, and the manufacture of turbocompressors of high capacity and power (up to 5 MW and a pressure of 65 abs. atm), steam generators, the piping and fittings, and the special measuring instruments.

The construction of the KS-150 reactor is a great achievement of Soviet and Czechoslovakian technical ingenuity and production capacity.

The technical design of the reactor, the fuel elements, and the station as a whole (Table 1) was worked out by the Experimental Design Office of the Leningrad Metal Works, the Khar'kov Physics and Technology Institute, and the Leningrad division of Teploélektroproekt. The scientific guidance for the project and the development of its physical part were handled by the Institute of Experimental and Theoretical Physics. A large group of Czechoslovakian specialists from the Skoda Works and the Prague Energy Design Office took part in the preparation of the project.

A second type of scheme, using not a vessel reactor but a tube reactor, was also considered in the preparation of the project. However, development of the tube reactor was later discontinued because its design had been found unreliable: there was a possibility of bursting of the active zone if one of the fuel channels immersed in water and kept at a coolant-gas pressure of 44 abs. atm was ruptured under water by the gas (Fig. 3).

Physical Characteristics of the Reactor

Moderator	Heavy water (H_2O up to 0.36%)*
Volume of heavy water (not including communicating pipes)	54 m^3
Weight of natural uranium	23 tons
Radius of active zone	178 cm
Height of active zone	390 cm
Thickness of side reflector	42 cm
Pitch of square lattice	26 cm

* Actually, from October 1972 through June 1973 the concentration of heavy water decreased from 99.9% to 99.4% owing to the entry of water and hydrogen. It is expected that in 1974 a regeneration unit will be installed to increase the heavy-water concentration.

TABLE 1. Power and Structural Characteristics of the Reactor (Design Values)

Characteristic	Nominal operation, temperature at surface of fuel element 500°C	Initial period, temperature at surface of fuel element 450°C
Gross electrical power, MW	143.3	112
Power required by turbocompressors, MW	22.6	20.2
Thermal power of reactor (on the basis of gas), MW	558.7	463
Thermal power of reactor on assumption of 8.2%* heat release in the heavy water, MW	610	505
Energy density, kW/kg		
average	23.3	19.3
maximum	51.3	42.6
Rate of coolant flow through reactor channels, kg/sec	1526	1474
Pressure of coolant in pressure chamber of reactor, abs. atm	65	65
Pressure of coolant in hot plenum of reactor, abs. atm	55.5	56.7
Pressure loss between pressure chamber and hot plenum atm	9.5	8.32
Pressure loss of entire first loop, atm	11.4	–
Temperature of coolant in pressure chamber of reactor, °C	112	114
Coolant temperature in hot plenum, °C	427	384
Dynamic heat of coolant in central channel, kg/m^2	7500	–
Rate of flow of moderator through reactor, tons/h	930	–
Moderator temperature at reactor inlet, °C	40	–
Moderator temperature at reactor outlet, °C	90	–
Maximum diameter of vessel cover, mm	5450	–
Height of vessel (from base to top of fuel channels), mm	22,450	–
Total weight of reactor, tons	1400	–
Number of fuel channels with thermocouple rods	38	–

*Actually the heat release in the heavy water, including heat transfer from the gas, is approximately 6% (as determined from operating experience).

The reactor contains a central zone and a peripheral zone of fuel channels, differing in channel diameter, in the amount of uranium, and in the density to which the channel cross sections are filled with uranium (Fig. 4).

The use of two zones makes possible the physical and thermal balancing of energy release, increasing the power of the reactor.

	Central Zone	Peripheral Zone
Number of channels	44	104
Outer diameter of caisson tube, cm	12.8	11.5
Thickness of caisson tube wall, cm	0.395	0.355
Inner diameter of shield tube, cm	11.2	10.0
Thickness of shield tube, cm	0.1	0.1
Number of fuel rods in assembly	75	63
Coefficient of filling of assembly cross section with uranium	0.24	0.252

Fig. 3

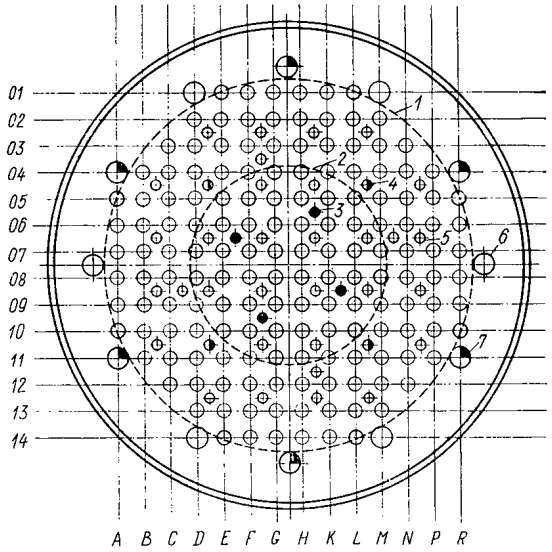

Fig. 4

Fig. 3. Destruction of underwater tubes kept at a gas pressure of 44 abs. atm after rupture of one tube (the photograph shows the tubes and the lower positioning grid).

Fig. 4. Schematic diagram of the active-zone lattice of the KS-150 reactor: 1) outer boundary of peripheral zone: 104 DU100 channels; 2) outer boundary of central zone: 44 DU112 channels; 3) 4 channels for emergency rods; 4) 4 channels for regulating rods; 5) 32 channels for shutdown rods; 6) 6 outlet tubes; 7) 6 inlet tubes.

The diameter of the uranium core of a fuel rod is 6.3 mm. The jacket of a fuel rod is 0.045 cm thick, finned, and made of magnesium containing 2% beryllium.

The characteristic feature of the active zone of the KS-150 reactor from the viewpoint of design is the large diameter of the fuel assembly, a result of which is a substantial difference between the distribution of the thermal-neutron density in the cell and the distribution calculated by the diffusion theory (the distribution of fast-neutron density in the cell is also nonuniform).

The results obtained in the calculation of the critical dimensions by the method of [5] were collected on the basis of experimental data obtained on a critical test stand [6], where the values of the critical Laplacians at various pitch values were determined for fuel-element lattices closely resembling those used in the KS-150 reactor. In addition, the distributions of thermal-neutron density over the fuel assembly and moderator were measured in individual experiments [7, 8].

The main physical characteristics of the active zone of the hot KS-150 reactor, poisoned and slagged with samarium and rhodium, are shown in Table 2. The average moderator temperature was taken to be 70°C, the average uranium temperature 400°C, the H_2O content of the D_2O 0.36% by weight, and the CO_2 pressure 55 abs. atm.

Thus, according to the calculations, the reactor, in a state where it is hot, poisoned, and slagged with samarium and rhodium has a reactivity excess of $\rho = 0.035$.

As shown by the results of a critical experiment [9, 10], for the physical startup of the reactor the true reactivity excess must be somewhat higher (by 0.001-0.003).

If we assume that for startup of the reactor after a brief shutdown without falling into the iodine pit we must have a reactivity excess of $\rho = 0.016$ (which corresponds to a 30-minute shutdown at zero power), then the reactivity excess* at burnup is 0.021, which corresponds to an average burnup value of 3700 MW·days/ton in the discharged fuel in continuous-recharging operation. The concentrations of ^{235}U, ^{239}Pu, ^{240}Pu, and ^{241}Pu in the discharged fuel will be 3800, 2000, 360, and 70 g/ton of natural uranium, respectively.

* In operation with no reactivity excess for shutdown the average burnup value is 5500 MW·days/ton.

TABLE 2. Main Physical Characteristics of the Reactor Active Zone

Parameter	Central zone	Peripheral zone
Probability of avoiding resonance absorption in the ^{238}U	0.886	0.906
Probability of avoiding resonance absorption in the zirconium	0.9974	0.9980
Fast-neutron multiplication factor	1.039	1.035
Absorption of thermal neutrons:		
in the magnesium	$0.4 \cdot 10^{-2}$	$0.4 \cdot 10^{-2}$
in the aluminum	$3.5 \cdot 10^{-2}$	$3.3 \cdot 10^{-2}$
in the zirconium	$0.8 \cdot 10^{-2}$	$0.8 \cdot 10^{-2}$
in the moderator	$1.6 \cdot 10^{-2}$	$2.0 \cdot 10^{-2}$
Poisoning	$3.2 \cdot 10^{-2}$	$3.2 \cdot 10^{-2}$
Slagging with Sm and Rh	$0.8 \cdot 10^{-2}$	$0.8 \cdot 10^{-2}$
Multiplication factor, K_∞	1.085	1.106
Critical multiplication factor, K_{cr}	1.050	1.070
Mean-square migration length $M^2 = L^2 + r$, cm^2	345	360

Note. The thermal-neutron absorption values are taken in relation to thermal-neutron absorption in natural uranium.

Because of the present uncertainty in the constants for uranium and plutonium, the burnup values may be in error by ±25%.

The system of regulating rods and shutdown rods of the reactor (RR and SR) forms a rectangular lattice with a pitch equal to twice the pitch of the fuel-element lattice. In addition, four emergency protection rods (EPR) and four additional shortened rods are arranged outside the lattice. The SR system must ensure reliable "shutdown" of the cold reactor with fresh fuel which has a reactivity excess of $\rho = 0.08$.

In calculating the effectiveness of the individual shutdown rods and regulating rods [11], allowance was made for their interference with one another, which, for the geometry used in the reactor, was found to be positive and fairly large (about 20%). Calculations showed [12] that a cold reactor with the SR lattice inserted has a negative reactivity ($\rho = -0.065$), i.e., that the SR lattice shuts down the reactor when it has 1.8 times the normal excess. The reactivity values of individual emergency protection rods and regulating rods for full insertion were found to be $5.9 \cdot 10^{-3}$ and $2.9 \cdot 10^{-3}$, respectively.

For calculating the strength and service life of the reactor vessel, it is necessary to know the flux of fast neutrons with energies greater than, or of the order of, 1 MeV. In the KS-150 reactor the vessel is separated from the active zone by a thick heavy-water reflector (approximately 40 cm thick) and a steel shield 10 cm thick. Fast neutrons undergo 5-10 collisons as they pass through the heavy-water reflector; therefore, for a sufficiently accurate calculation of the fast-neutron flux hitting the reactor vessel we cannot confine ourselves to the age-theory approximation (or to taking account of direct streaming alone) but must solve the kinetic equation. Calculation for a flux of fast neutrons with energies higher than 1 MeV hitting the inner surface of the vessel at the point where the flux was maximum yielded a value of $\Phi = 4.5 \cdot 10^9$ $cm^{-2} \cdot sec^{-1}$. The energy spectrum of the fast neutrons in the vessel was calculated.

If a value of $\Phi t = 3 \cdot 10^{18}$ cm^{-2} is taken [13] as the permissible value of the integral flux of neutrons with energies over 1 MeV in the reactor vessel, then the service life of the vessel will be 26 years (assuming a load factor of 0.7 for the station). Another method of determining the permissible service life of the vessel is based on the assumption that the amount of change in the elastic properties of the steel is proportional to $\int \Phi(E)EdE$. The calculated service life of the vessel, based on this assumption, on the known neutron spectrum, and on a maximum integral effective neutron flux of $\int \Phi(E)E(dE/\bar{E})t = 5.6 \cdot 10^{18}$ cm, where $\bar{E} = 2$ MeV, will be 21 years.

Overall views of the reactor and a fuel channel are shown in Figs. 5 and 6. An aluminum tank containing heavy water is situated inside the steel vessel. Through the tank run caisson tubes containing the fuel-element assemblies. Above the heavy-water tank is a zone intended for shutdown cooling of the fuel-element assemblies after they have been withdrawn from the active zone and before they have been placed in the discharging and charging apparatus (DCA).

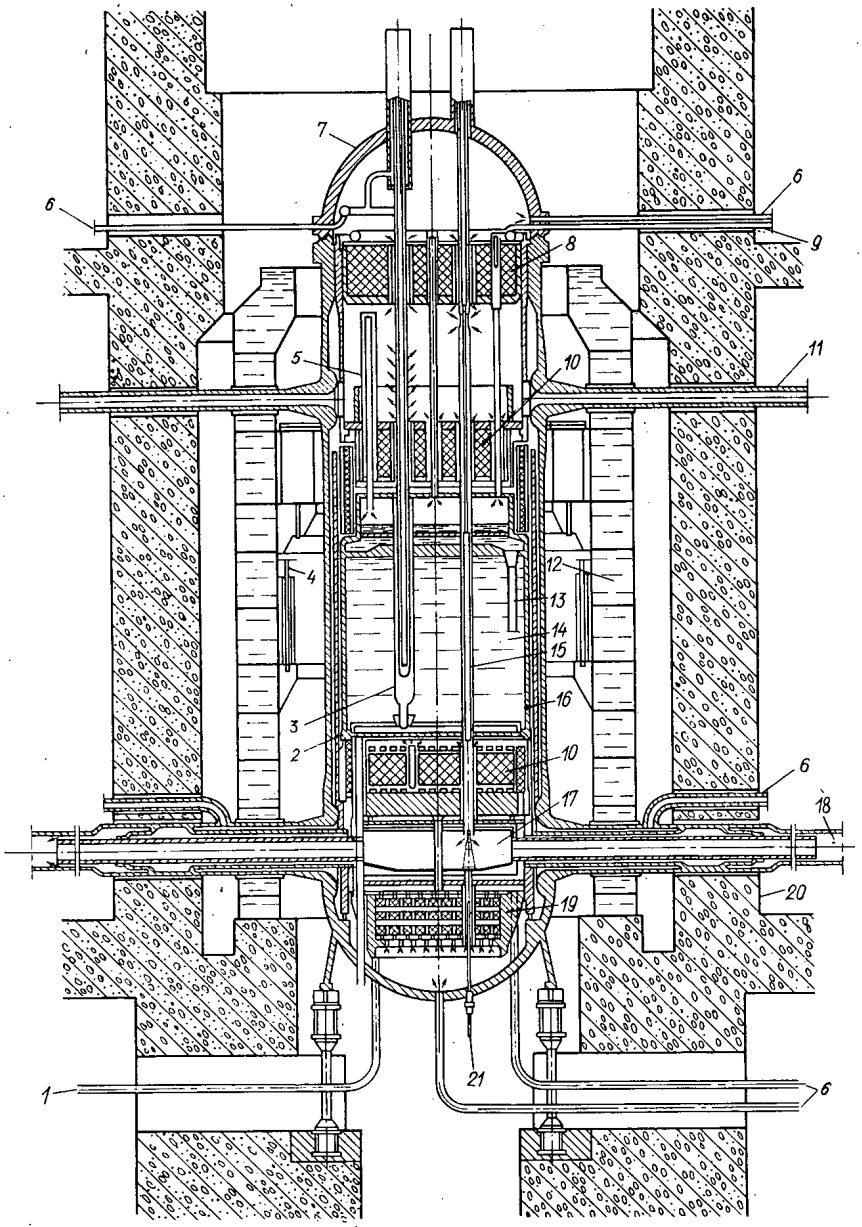

Fig. 5. Longitudinal cross section of the reactor: 1) heavy-water inlet; 2) steel shield; 3) CPS; 4) ionization chamber; 5) shutdown cooling zone; 6) coolant inlet for cooling the parts of the reactor; 7) reactor vessel; 8) external protection; 9) outlet for explosive mixture; 10) graphite shield; 11) coolant inlet; 12) water shield; 13) heavy-water outlet; 14) heavy water; 15) fuel channels; 16) heavy-water tank; 17) hot plenum; 18) coolant outlet; 19) lower shield; 20) concrete shield; 21) outlet of JLMS tubes.

The high-temperature gas cooling of the reactor is carried out by means of a narrow annular interlayer of insulating gas between the shield of the fuel assembly (see Fig. 6) and the caisson tube of the fuel channel, separating the descending hot gaseous coolant from the cold heavy water.

The fuel-element assemblies are held by movable shafts passing through the plug of a biological shield with a closing plug. Thus, the DCA extracts the assemblies from the reactor together with the plugs and the shaft; a single operation with the DCA is sufficient to remove the depleted assembly and replace it with a new one.

The gaseous coolant entering the channels is regulated by means of a slide and the movable part of the plug of the biological shielding, whose actuator is connected to the outside through a packing gland in

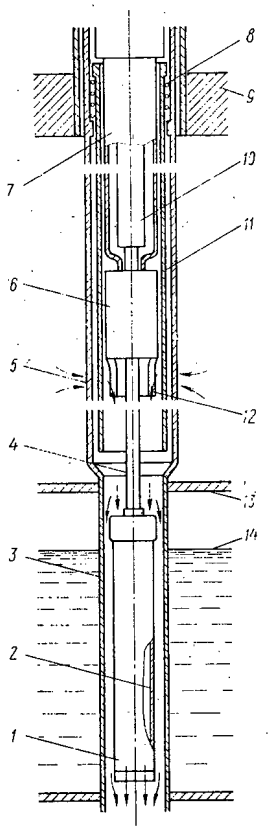

Fig. 6

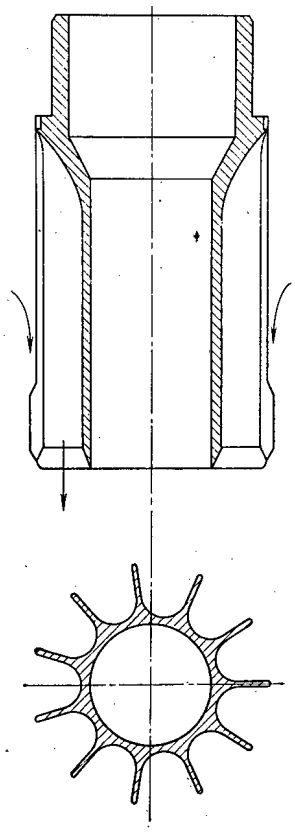

Fig. 7

Fig. 6. Diagram of fuel channel: 1) assembly of fuel elements; 2) shield tube; 3) caisson tube; 4) thin movable shaft; 5) slide; 6) biological-shielding plug; 7) closing plug; 8) spring; 9) cover of reactor vessel; 10) thick shaft; 11) cutoff tube; 12) inlet damping grid; 13) cover of heavy-water tank; 14) level of heavy water.

Fig. 7. Damping fins at coolant-gas inlet to fuel channel.

the closing plug of the fuel channel. When a fuel-element assembly, together with the plugs, is taken out by the DCA, the slide is covered by means of a spring which raises the cutoff tube, and the flow of gas through the channels for cooling the fuel elements takes place through the DCA, which is connected to the gas in the high-pressure part of the reactor. When the assembly is lifted into the shutdown cooling zone, the gas flow rate through it may be sharply reduced by the slide arrangement. The DCA loads the assembly only into the shutdown cooling zone. The fuel-element assembly is lowered into (and raised out of) the active zone by supplementing the thin shaft with a thick one, using a special crane with a lifting capacity of 5 tons. The plugs are packed with special fluoroplastic gaskets and are kept in place by stops and nuts. All of these operations are carried out by remote control. The thin shaft and the shaft for controlling the slide are fitted with cup packings, also made of fluoroplastic.

In an experimental test of the fuel-channel design on the test stand of the Leningrad Metal Works, it was found that catastrophic vibrations of the thin shaft with the fuel-element assembly took place when the shaft was in the shutdown cooling zone, as a result of movements of the coolant gas. A simple and reliable solution was found for avoiding such vibrations: a special array of fins was installed at the gas inlet to the fuel channel, damping the flow by splitting it up into parallel streams (Fig. 7 and designation 12 of Fig. 6).

The maximum temperatures of the gas and of the fuel-element cores are measured by means of thermocouples whose connections are led out of the reactor along the thin and thick shafts. Special cable thermocouples were designed for this purpose.

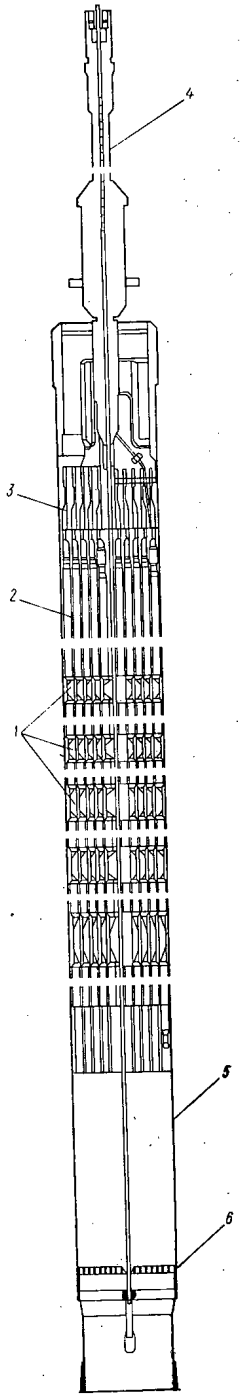

Fig. 8. Assembly of fuel elements with spacing sleeves: 1) spacing sleeves; 2) fuel rods; 3) head; 4) thin shaft; 5) shield; 6) trap.

The fission-fragment activity of the gas at the outlet from the channels is measured by drawing off part of the gas from each channel through a settling tank to special filters and determining their cesium and rubidium activity in a special apparatus of the JLMS.

The temperature-measurement and JLM systems give a complete picture of the status of fuel-element charging in the reactor. However, during the initial period of operation a number of difficulties arose: contamination of the surface of the fuel rods by uranium was found to be higher than the design value, thus reducing the sensitivity of the JLM system, and the distorted variation of the reactor field as a function of height when the excess reactivity was suppressed by means of compensating rods during the initial period of operation introduced some uncertainty into the readings of the fuel-rod thermocouples.

The reactor vessel, which has a removable cover, contains not only the active zone but also the shielding, the baseplate of the tank, and other parts. The minimum thickness of the vessel wall is 150 mm, and the maximum thickness (in the zone of the lower pipes) is 375 mm. The vessel was made from a special low-alloy steel developed in the Czechoslovakian Socialist Republic. It is a complex engineering structure. The development of its metallurgiacl and technological parts and the investigation of its brittle strength, which is a matter of exceptional importance, were carried out with the participation of Soviet specialists.

The heavy-water tank is also a complex structure. The outer diameter of the tank is 449 cm, the height is 572.5 cm, and the thicknesses of the side walls and bottom are 40 mm and 100 mm, respectively. The top and bottom parts of the tank contain aluminum plates to ensure that the water circulating in the tank is uniformly distributed over its cross section.

The space above the surface of the heavy water is designed for degassing it in the event of a gas-pressure drop in the first loop, which is connected to the degassing space through slits in the cover of the tank,* and to collect the explosive mixture formed during reactor operation.

The tank is made of Avial, a special SAV-1 aluminum alloy. Some parts were manufactured in USSR factories. The final welding of the tank was done at the station. The tank and a number of parts were subjected to "plasticizing heat treatment" (developed by the Polzunov Central Boiler and Turbine-Research Institute of Leningrad, to prevent embrittlement of the alloy when it was heated for long periods.

The control and protection systems of the reactor consist of four emergency rods, 32 shutdown rods, and four regulating rods. The rods are placed between the fuel channels and are directly immersed in the water. They are raised and lowered by means of vertical motors built into the CPS channels and a "steel-bolt-and-graphite-nut" mechanism.

An absorbing rod operates at a surface pressure of 65 atm and a temperature of up to 250°C. The rod consists of an inner Avial tube (SAV-6) 57 mm in diameter and with a wall thickness of 3.5 mm, having annular recesses which hold cadmium inserts 1.5 mm thick; the thick tube is covered with a thin tube of SAV-1, after which the entire assembly is drawn out and welded together.

The construction of the reactor's biological shield and the fast-neutron shield of the support structure of the active zone (the steel plate under the Avial tank) was made more difficult by the fact that they had to be made of nonhydrogenous materials (to avert the danger of isotope exchange with the heavy water). The

* Heavy water is saturated with carbon dioxide at an operating pressure of 65 abs. atm and a temperature of 90°C.

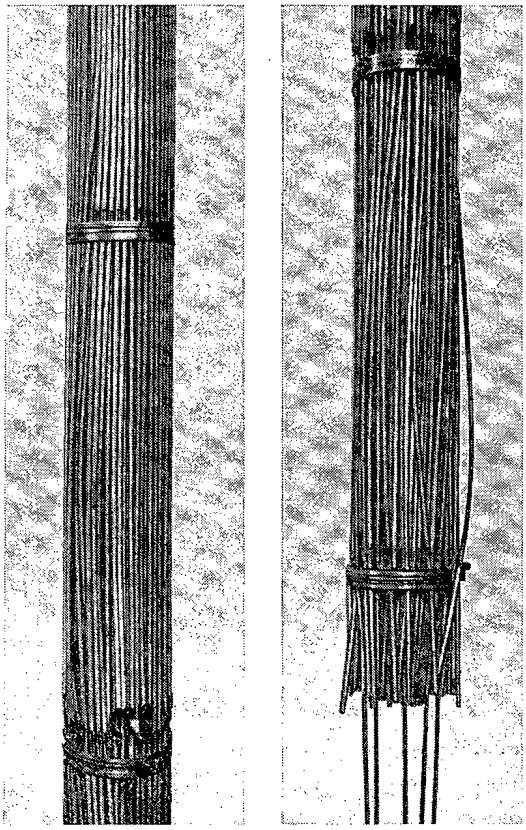

Fig. 9. View of assembly, with spacing grids rigidly attached to the shield tube, after testing.

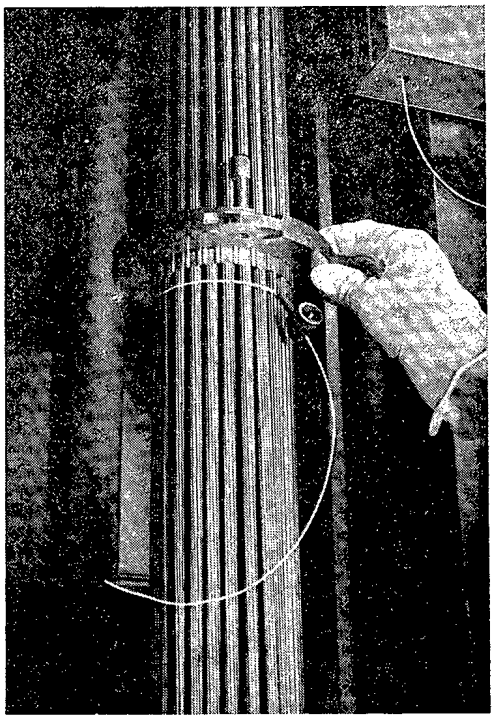

Fig. 10. Putting together an assembly in the shop.

end-of-cylinder shielding was constructed in the form of alternating layers of graphite and steel. The fast-neutron shielding of the side walls of the vessel consists of the heavy-water side reflector and a shield of steel plates, and the shielding for the steel plate under the tank is graphite.

The gas enters the reactor from above and is removed from below through 12 tubes 300 mm and 500 mm in diameter.

Gas from the pressure chamber of the reactor (first loop), in amounts up to 18 tons/h, is pumped under the surface of the heavy water. Next the gas enters the apparatus for burning the explosive mixture with a palladium catalyst, after which it returns to the first loop. The heavy-water losses accompanying the leakage of carbon dioxide gas from the first loop, which result from the combination of this loop with the heavy-water loop, are kept within bounds by condensers set up beyond the devices used for burning the explosive mixture; the latter are cooled by water at a temperature of up to 23°C.

During the initial period of operation the carbon dioxide gas losses were reduced from 300 kg/h to 70-100 kg/h, and after seven months of operation of the station (including the period of the physical start-up, the filling of the system with heavy water, open-circuit running, etc), the heavy-water losses totaled about 500 kg.

The gas-pressure drop between the gas inlet into the fuel channel and the gas outlet from the channel (9.5 atm) acts upon the tank baseplate through the bottom of the Avial tank. The high-pressure portion of the shell is separated from the low-pressure portion by ring packing operating on the "dry friction" principle. The caisson tubes are at external pressure, which prevents the possibility of any dangerous effects resulting from underwater tube failure.

Fuel Elements and Assemblies

The construction of a fuel-element assembly is illustrated in Fig. 8. A bundle of thin rods (fuel elements) made of natural metallic uranium is arranged in a circularly symmetric pattern; the coolant cross section passing through between the elements is profiled to match the variation in energy output with the radius of the assembly [14]. The diameter of the uranium core is 6.3 mm, and the active length is 3.9 m.

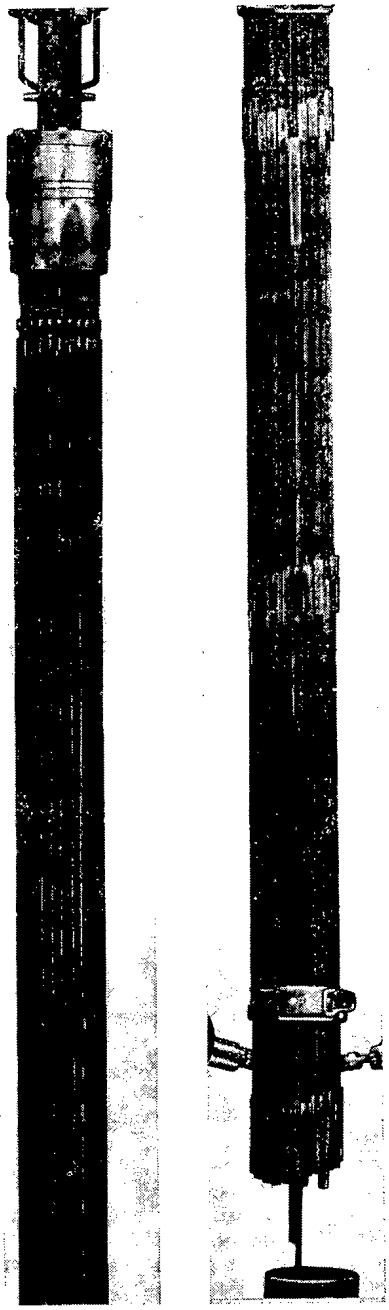

Fig. 11. Fuel-element assembly irradiated in channel M-12 of the reactor. (The top part of the assembly is shown at the left, the bottom part at the right.)

The protective covering, made of magnesium–beryllium alloy 0.45 mm thick, with 12 longitudinal fins 0.7 mm high and with titanium tips, is firmly attached to the core. The beryllium content of the covering is 2%. The bundle of rods is arranged in a tube made of a zirconium alloy with admixtures of copper and molybdenum. The rods are suspended from a plane steel grid, guaranteeing free passage of the coolant into the assembly.

The spacing of the rods is arranged by means of special sleeves made of the same zirconium alloy. The sleeves are stamped out of sheet metal 0.3-0.4 mm thick and then are welded into compartments with a trapezoidal cross section. The sleeves are attached to each rod by means of cylindrical brackets, and spaces are left in the fins for this purpose.

Six sets of sleeves, separated by distances of 650 mm between the sets, are arranged along the height of the assembly. The height of the sleeves from the top set to the bottom set increases from 30 mm to 80 mm, owing to the variations in the differential growth of the rods when they are irradiated in the reactor. A trap grid is attached to the lower part of the shield tube.

This construction of the assembly makes it possible for the rods to move freely and independently along the assembly during elongation or contraction due to radiation and heat. Each sleeve can slide freely along the adjacent sleeves. "Swelling" of the rods under irradiation takes place within the sleeves, and for this reason their attachment clamps are mounted in the spaces on the fins of the rods with appropriate gaps. This construction also protects the rods from distortion.

Designing and constructing the fuel elements and assemblies proved to be one of the most difficult problems. For this purpose, extensive technological investigations and experimental studies with full-scale assemblies were carried out on the KS-60 loop and on test stands in the USSR. The result was that investigators made practical tests of the design, carried out gas-dynamics and vibration tests, as well as heat-transfer and corrosion investigations, and, most importantly, examined problems involving the stability of the assemblies under operating conditions.

The KS-60 loop, with two full-scale channels operating at a pressure of 65 abs. atm, is a model of a gas-cooled reactor. It was used for studying problems involved in the operation of the first gas loop of the reactor, the sealing of the gas blowers, and the removal of dust, oil, and other impurities from the gas, which was very helpful in the startup of the atomic power station.

Figure 9 shows the original design of the assembly, with a rod core diameter of 4 mm and a smooth covering 0.45 mm thick; the spacing grids were rigidly connected to the shield tube and placed at a distance of 500 mm from one another, after testing for 466 h at a carbon dioxide gas temperature of 450°C and a dynamic head of 6000 kg/m^2 (1964). The assembly failed because of the rigid attachment of the spacing grids to the shield tube; the failure was further aggravated by the fact that water had accidentally gotten into the test stand.

The design finally adopted for the project, with larger-diameter rods, a finned covering, and spacing sleeves, considerably reduced the production cost of the rods and eliminated the defects mentioned above.

The KS-60 loop was used for conducting a long series of tests on full-scale assemblies with various arrangements for the spacing of the rods (grids, sleeves of various designs, fins, etc.), at various temperature

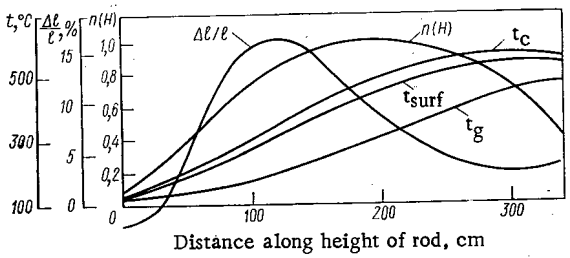

Fig. 12. Variation of the elongation, $\Delta l/l$, of rod-type fuel elements and variation of core temperature as functions of height at a maximum energy stress of 52 kW/kg.

and gas-dynamics conditions and with various thermal loads of the uranium. The temperature of the bars in the investigation reached 520°C, the temperature of the cores reached 600°C, the dynamic head of the coolant reached 12,000 kg/m^2, and the energy stress of the uranium reached 80 kW/kg.

The main result of these studies and investigations may be said to be the experimentally demonstrated possibility of achieving an average burnup value of up to 10,000-15,000 MW·day/ton in rod-type fuel elements of metallic uranium with a magnesium–beryllium covering at covering temperatures of up to 500°C, dynamic heads of up to 10,000 kg/m^2, and energy stress values of up to 80 kW/kg of uranium.

However, attaining such burnup values apparently requires increasing the thickness of the jackets and strengthening the cores in order to reduce their growth under irradiation.

The fuel elements, the shield tubes, the material for the spacing sleeves, the thin shafts, and the thermocouples for the fuel elements are supplied to the Czechoslovakian Socialist Republic from the Soviet Union. The heads, sleeves, and protective and closing plugs of the fuel channels are manufactured in Czechoslovakia.

A special shop has been established at the A-1 station for putting together the fuel-element assemblies (Fig. 10).

The heat-generating assemblies, inserted into the reactor in October, 1972, were subjected to open-circuit running and a physical startup. From December, 1972, to July, 1973, the average burnup value in the assemblies was 1500 MW·days/ton, and the maximum value was 2700 MW·days/ton. One assembly, whose JLM system readings exceeded the norm by a factor of 3, was removed from the reactor.* A total of 10,000 rods were inserted into the reactor, and only one of them was found to be out of order after testing which lasted more than one-third of a reactor run. This may be regarded as a very encouraging result.

Figure 11 shows an experimental assembly irradiated in the reactor; it had been tested in order to assess the possibility of using uranium rods with very negative "growth indices" (from −6 to −10) in the reactor. An average burnup value of 900 MW·days/ton and a maximum of 1750 MW·days/ton were attained with this assembly at core temperatures of 100-400°C. After testing, all the bars were found to be shorter, on the average, by 0.5%. The appearance of the assembly was entirely satisfactory.

The first charges of the fuel elements are considered experimental. Their testing is being carried out according to a special joint program prepared by Soviet and Czechoslovakian experts.

The bulk of the rods in the first charges had growth index values of −3 to −6. Repeated tests of such fuel elements on the KS-60 loop, under standard conditions but with temperature cycles once a day, indicated that the rods increased in length at burnup values of more than 1000 MW·days/ton.

The relative elongation ($\Delta l/l$) of the operating rods depends on the core temperature; the characteristic curve, obtained on the loop at an average burnup value of 2400 MW·days/ton, is shown in Fig. 12. The maximum elongation values are found in the region of ~350°C core temperature. At average burnup values of 3000-4000 MW·days/ton the elongation of the rods in the loop assemblies was 5-7%; this was taken as the design allowance for elongation in the standard assemblies of the reactor.

Principal Equipment of the Atomic Power Station

The station includes one reactor and three steam-generator-and-turbine units each capable of producing 50 MW of electrical power.

The steam generators, of the "tube-in-tube" type, were designed and manufactured in the Czechoslovakian Socialist Republic. The steam generator has a single-pass scheme on the gas side. The gas moves from the top toward the bottom, while the water moves from the bottom toward the top. On the steam-and-water side the steam generator consists of the following elements (listed in the direction of

* Examination revealed a corrosion spot about 5 mm in diameter on one of the rods.

water motion): common condensate heater, evaporator, and steam reheater for low pressure; economizer, evaporator, and steam reheater for medium pressure. The low-pressure and medium-pressure parts have their own separator drums. Circulation of the steam–water mixture in the evaporators of the steam generator is maintained by forced-circulation pumps (LaMont scheme). The heating surfaces of the steam generator are constructed in the form of U-shaped elements consisting of bundles of 19 tubes, each 22 mm in diameter with walls 2.5 mm thick, arranged within a tube 159 mm in diameter and with a wall thickness of 7 mm. The steam–water mixture flows through each tube, and carbon dioxide gas flows in the intertube space. The heating surfaces of the steam generator are made of carbon steel; the part of the steam generator which is adjacent to the zone of the hot carbon dioxide gas inlet is made of low-alloy carbon steel.

The capacity of each of the three units of the steam generators is: medium-pressure, 172 tons/h of steam at a pressure of 31.5 abs. atm and a reheating temperature of 410°C; low-pressure, 73.4 tons/h at 2.2 abs. atm and 185°C.

Circulation of the coolant in the first loop is maintained by six turbocompressors with gas–oil packing. Each turbocompressor is driven by a synchronous electric motor with a power of 5000 kW and a speed of 3000 rpm, installed outside the walls of the biological shielding. When the turbocompressors were manufactured at the CKD factory (Prague), there were difficulties involving vibrations of the rotor and the design of the oil packing, which were successfully overcome.

Mechanical impurities and oil are removed from the coolant at the nominal pressure of 65 abs. atm by condensing part of the gas (12 tons/h) in distillation units. At gas pressures below the nominal value, special filtration units are turned on.

Heavy water is circulated through the reactor by two leak-proof operating pumps (with a third pump in reserve); each has a capacity of 470 m^3/h. The cooling of the heavy water is carried out in special stainless-steel heat exchangers.

The KS-150 reactor has certain operational features which require special reliability for its emergency shutdown cooling system. The large heat absorber (60 tons of heavy water) is separated from the fuel elements by a gas gap and a shield, and it is difficult to transfer the heat to it. Consequently, even short-term interruptions of coolant circulation under these conditions (despite activation of the emergency protection system) may lead to rapid melting of the fuel-element jackets.

Because of the low thermal capacity of the active zone, when there is an emergency shutdown of the reactor, there will also be a "thermal shock" in the unshielded part of the hot tubes of the first loop. The stresses at the tube elbows reach 30 kg/mm^2. The number of such shocks to the strength of the structure may be limited. In order to soften the "thermal shock," the installation is so set up that the operating conditions of the turbocompressors will automatically change when there is an emergency shutdown of the reactor.

The emergency shutdown cooling system, based on the Madunice hydroelectric power station's (14 MW) hydrogenerator specially designed for this purpose, situated 10 km from the station and connected with the A-1 by a single overhead electric power transmission line, was inadequate for the high reliability requirements. Consequently, in early 1972 Soviet and Czechoslovakian experts decided to install an emergency diesel generator station with diesel engines that can go into operation within 15 sec and to equip the turbocompressors with additional motors operating at low speed (600 rpm) and power (110/55 kW each), directly connected electrically to the diesels. However, it was impossible to complete this system by the scheduled date for the startup of the station. In accordance with a proposal made by the Skoda Works and the Plzen Polytechnic Institute, the startup of the station was carried out according to the proposed time schedule for two operating units, each consisting of a steam generator, a turbine, and two turbocompressors, while the third unit was held in reserve. The motor of one of the operating turbocompressors was kept operating continuously by the Madunice hydrogenerator. The reserve gas blowers were equipped with motors having a power of 120 kW each (600 rpm) and were kept operating continuously on power supplied by the diesel installation constructed in 1972, equipped with four diesel units of 500 kW each. This system was found to be satisfactory and is being successfully used today.

LITERATURE CITED

1. A. I. Alikhanov, V. V. Vladimirskii, P. A. Petrov, and P. I. Khristenko, "A gas-cooled heavy-water power reactor," At. Énerg., 1, 5 (1956).

2. B. L. Ioffe and L. B. Okun', "Fuel burnup in nuclear reactors," At. Énerg., 4, 80 (1956).
3. P. I. Khristenko, P. A. Petrov, V. A. Mitropolevskii, K. D. Sinel'nikov, V. E. Ivanov, and V. F. Zelenskii, "Assembly of a bar-type heat-generating element for a gas-cooled heavy-water power reactor," in: Nuclear Reactors and Nuclear Power Generation [in Russian], Atomizdat, Moscow (1959), p. 172.
4. P. A. Petrov and P. I. Khristenko, A Gas-Cooled Nuclear Power Reactor (the KS-150 Reactor), Preprint ITÉF-211 (1963).
5. A. D. Galanin, Theory of Thermal Nuclear Reactors [in Russian], Atomizdat, Moscow (1957).
6. Yu. G. Abov et al., At. Énerg., 12, No. 2, 156 (1962).
7. V. F. Bel'kin and O. V. Shvedov, Jaderna Energie, 8, No. 10, 343 (1962).
8. V. F. Bel'kin, O. V. Shvedov, and B. P. Kochurov, At. Énerg., 14, 3, 281 (1963).
9. N. A. Bugrov, B. A. Medzhibovskii, V. F. Bel'kin, V. N. Popov, V. I. Ryazhskii, V. V. Boiko, I. Paulička, Š. Kačmary, Š. Rohar, and J. Kmošená, Determination of the Critical Level of Heavy Water in the KS-150 Reactor. ÉBO Report, 1972, Elektrarnia, Bohunice, Czechoslovakian Socialist Republic.
10. B. L. Ioffe and B. I. Il'ichev, A Critical Experiment in the Physical Startup of the KS-150 Reactor [in Russian], ÉBO Report, 1972, Elektrarnia, Bohunice, Czechoslovakian Socialist Republic.
11. B. L. Ioffe, Calculation of the Effectiveness of Single Shutdown Rods in the KS-150 Reactor [in Russian], ÉBO Report, 1972, Elektrarnia, Bohunice, Czechoslovakian Socialist Republic.
12. B. L. Ioffe, Calculation of the Negative Reactivity of the KS-150 Reactor with a Fully Loaded Lattice of Shutdown Rods and Regulating Rods [in Russian], ÉBO Report, 1972, Elektrarnia, Bohunice, Czechoslovakian Socialist Republic.
13. A. D. Amaev and N. F. Pravdyuk, in: Investigation of Stresses and Strength of a Reactor Vessel [in Russian], Atomizdat, Moscow (1968), pp. 241-255.
14. P. I. Khristenko, At. Énerg., 11, 6, 506 (1961).

COMPOSITE LATTICE IN THE P_3-APPROXIMATION

A. D. Galanin and B. Z. Torlin

UDC 539.125.52:621.039.51.12

It is quite accurate to replace a cell of a uniform reactor lattice by an equivalent cylindrical cell. If the lattice is nonuniform, containing for example control rods or fuel slugs with different uranium contents, such a replacement cannot be made. The problem of determining the neutron field in a cell which lacks cylindrical symmetry is appreciably more complicated, and a sufficiently accurate solution of it, even for the one-velocity equation, is beset with formidable calculational difficulties [1, 2]. It can be solved in the diffusion approximation [3], but the introduction of nondiffusion corrections is not quite unique.

The present article extends heterogeneous reactor theory [3] to the P_3-approximation of the spherical harmonics method.

We consider a composite lattice for which

$$\rho^2/a^2 \ll 1, \tag{1}$$

where a is the distance between slugs and ρ is the radius of a slug. When (1) is satisfied the neutron field can be taken as axially symmetric on and within the surface of a slug.

Some P_3-Approximation Formulas

In the spherical harmonics method the neutron field is expanded in spherical harmonics. In the notation used in [4] the coefficients $f_{k,m}(r)$ in this expansion are zero if k + m is odd, and as a consequence of the condition* $f(r, \vartheta, \varphi) = f(r, \vartheta, -\varphi)$, they reduce to the following six quantities:

$$\left.\begin{aligned} &\psi_0 = f_{0,0};\ \psi_1 = f_{1,1} - f_{1,-1};\ \psi_2 = f_{2,2} + f_{2,-2};\\ &\psi_3 = f_{2,0};\ \psi_4 = f_{3,3} - f_{3,-3};\ \psi_5 = f_{3,1} - f_{3,-1}. \end{aligned}\right\} \tag{2}$$

The following relation holds between the subscript m of the function $f_{k,m}$ and the subscript n of the function ψ_n:

n	m
0	0
1	1
2	2
3	0
4	3
5	1

(3)

If the neutron sources are isotropic and uniformly distributed in space the solution of the transport equation in the P_3-approximation can be written in the form of a six-component vector $\psi(r)$ with components $\psi_n(r)$:

$$\psi(r) = C + \hat{M}(r)\,A, \tag{4}$$

where

$$C_n = \delta_{0,n}\, q/\varepsilon, \tag{5}$$

* As in [4] $f(r, \vartheta, \varphi)$ is the collision density, and not the neutron density.

Translated from Atomnaya Énergiya, Vol. 36, No. 2, pp. 125-129, February, 1974. Original article submitted February 22, 1973.

in which q is the source strength and

$$\varepsilon=\frac{\sigma_a}{\sigma_a+\sigma_s}=\frac{l}{l_a}. \tag{6}$$

The components of the vector **A** are found from the boundary conditions: on the boundary between slug zones i and i + 1 the relation

$$l_i\psi_i=l_{i+1}\psi_{i+1} \tag{7}$$

must hold. The elements of the matrix $\hat{M}$ can be written as

$$M_{n,\nu}(r)=\begin{cases} c_{n,\nu}(\alpha_\nu)\, I_m\left(\frac{\alpha_\nu r}{l}\right) & \text{for } \nu=0,1,2; \\ c_{n,\nu-3}(-\alpha_{\nu-3})\, K_m\left(\frac{\alpha_{\nu-3} r}{l}\right) & \text{for } \nu=3,4,5, \end{cases} \tag{8}$$

where

$$\alpha_\nu=\frac{35}{18}\left[1+\varepsilon\left(\frac{11}{7}-\frac{27}{35}\mu\right)\right]\left[1\mp\sqrt{1-\frac{108}{35}\cdot\frac{(1-\mu)\varepsilon}{\left[1+\varepsilon\left(\frac{11}{7}-\frac{27}{35}\mu\right)\right]^2}}\right],\ \nu=0,1;$$
$$\alpha_\nu=\sqrt{7},\ \nu=2; \tag{9}$$

μ is the average cosine of the scattering angle. It is assumed that the remaining moments of the scattering function are zero.

The coefficients $c_{n,\nu}$ for $\nu \le 1$ are:

$$c_{0,\nu}=1;\quad c_{1,\nu}=-\frac{\varepsilon\sqrt{6}}{\alpha_\nu};\quad c_{2,\nu}=\frac{\varepsilon\sqrt{6/5}}{1-9\alpha_\nu^2/35};$$
$$c_{3,\nu}=-\frac{\varepsilon}{\sqrt{5}\,(1-9\alpha_\nu^2/35)};$$
$$c_{4,\nu}=-\frac{3\varepsilon\alpha_\nu}{\sqrt{35}\,(1-9\alpha_\nu^2/35)}; \tag{10}$$
$$c_{5,\nu}=\frac{3\sqrt{3}\,\varepsilon\alpha_\nu}{5\sqrt{7}\,(1-9\alpha_\nu^2/35)},$$

and for $\nu = 2$:

$$c_{0,2}=c_{1,2}=0;\quad c_{2,2}=1;\quad c_{3,2}=\frac{\sqrt{6}}{2};$$
$$c_{4,2}=-\alpha_2\sqrt{\frac{3}{14}};\quad c_{5,2}=-\alpha_2\sqrt{\frac{5}{14}}.$$

From the requirement that the solution be finite it follows that in the central zone, including the point r = 0, the coefficients A_3, A_4, and A_5 are zero, and in the last zone, including the point $r \to \infty$, $A_0 = A_1 = A_2 = 0$. Therefore the square matrix $\hat{M}$ becomes rectangular in the central and peripheral zones, containing respectively the first three or the last three columns of the square matrix.

Solution in a Zone with Weak Absorption

If $\varepsilon \to 0$, C in Eq. (4) tends to infinity, which must be balanced by the second term in (4). Such a compensation of large numbers is undesirable in machine calculations, and therefore the case $\varepsilon = 0$ is treated separately.

We write the first component of the vector **A** in the form

$$A_0=-\frac{q}{\varepsilon}+A_3\ln\frac{2\alpha_0}{\gamma}+A_0'. \tag{11}$$

The result of multiplying the first term in Eq. (11) by $\hat{M}$ is combined with the vector **C**, and the second with the result of multiplying A_3 by $\hat{M}$. Now we go to the limit $\varepsilon \to 0$. This does not change the form of (4), and the vector **C** and the matrix $\hat{M}$ take the form:

$$C_0=-\frac{3}{4}q\frac{1-\mu}{l^2}r^2;\quad C_1=\sqrt{\frac{3}{2}}\cdot\frac{qr}{l};$$
$$C_3=\frac{q}{\sqrt{5}};\quad C_2=C_4=C_5=0; \tag{12}$$

$$\hat{M}(r)=\begin{pmatrix} 1 & I_{0,1} & 0 & \ln\frac{r}{l} & K_{0,1} & 0 \\ 0 & 0 & 0 & \sqrt{\frac{2}{3}}\frac{l}{r(1-\mu)} & 0 & 0 \\ 0 & -\frac{\sqrt{30}}{4}I_{2,1} & I_{2,2} & \frac{2\sqrt{2}}{\sqrt{15}(1-\mu)}\left(\frac{l}{r}\right)^2 & -\frac{\sqrt{30}}{4}K_{2,1} & K_{2,2} \\ 0 & \frac{\sqrt{5}}{4}I_{0,1} & \frac{\sqrt{6}}{2}I_{0,2} & 0 & \frac{\sqrt{5}}{4}K_{0,1} & \frac{\sqrt{6}}{2}K_{0,2} \\ 0 & \frac{5}{4}I_{3,1} & -\sqrt{\frac{3}{2}}I_{3,2} & \frac{8}{\sqrt{35}(1-\mu)}\left(\frac{l}{r}\right)^3 & -\frac{5}{4}K_{3,1} & \sqrt{\frac{3}{2}}K_{3,2} \\ 0 & -\frac{\sqrt{15}}{4}I_{1,1} & -\sqrt{\frac{5}{2}}I_{1,2} & 0 & \frac{\sqrt{15}}{4}K_{1,1} & \sqrt{\frac{5}{2}}K_{1,2} \end{pmatrix}, \tag{13}$$

where

$$\left.\begin{matrix} I_{m,h}=I_m(x_h) \\ K_{m,h}=K_m(x_h) \end{matrix}\right\} x_1=\frac{\sqrt{5}}{3}x_2; \quad x_2=\sqrt{7}\,\frac{r}{l}.$$

Heterogeneous reactor theory [3] does not consider an isolated cell but an infinite lattice. Therefore it is necessary to take account of the fact that in the medium outside a slug the distance r in the argument of K_m can become arbitrarily large. Thus in considering an external moderator with small absorption ε can be taken zero everywhere except in the argument of $\alpha_0 r/l$. For weak absorption

$$\alpha_0^2=3\varepsilon(1-\mu)=(l/L)^2,$$

where L is the neutron diffusion length in the external moderator.

Therefore for an isolated slug the matrix $\hat{M}$ becomes

$$M(r)=\begin{pmatrix} K_0\left(\frac{r}{L}\right) & K_{0,1} & 0 \\ \frac{\sqrt{2}}{\sqrt{3}(1-\mu)}\frac{l}{L}K_1\left(\frac{r}{L}\right) & 0 & 0 \\ \frac{\sqrt{2}}{\sqrt{15}(1-\mu)}\left(\frac{l}{L}\right)^2 K_0\left(\frac{r}{L}\right) & -\frac{\sqrt{30}}{4}K_{2,1} & K_{2,2} \\ 0 & \frac{\sqrt{5}}{4}K_{0,1} & \sqrt{\frac{3}{2}}K_{0,2} \\ \frac{1}{\sqrt{35}(1-\mu)}\left(\frac{l}{L}\right)^3 K_3\left(\frac{r}{L}\right) & -\frac{5}{4}K_{3,1} & \sqrt{\frac{3}{2}}K_{3,2} \\ 0 & \frac{\sqrt{15}}{4}K_{1,1} & \sqrt{\frac{5}{2}}K_{1,2} \end{pmatrix}. \tag{14}$$

Solutions Outside the Slugs

Since the transport equation is linear the neutron field at an arbitrary point outside the slugs can be written as the superposition of the self-fields of all the slugs of the lattice. Expanding each term in spherical harmonics we obtain

$$f(r,\vartheta,\varphi)=\sum_{j'}\sum_{k,m} f_{k,m}^{(j')}(|\mathbf{r}-\mathbf{r}_{j'}|)\frac{P_{k,m}(\vartheta)}{\sqrt{2\pi}}e^{im\varphi_{j'}}, \tag{15}$$

where $\mathbf{r}_{j'}$ is the radius vector to the center of slug j', and $\varphi_{j'}$ is the angle between the direction of the velocity of a neutron and the vector $\mathbf{r}-\mathbf{r}_{j'}$. A particular solution has the form

$$f_{k,m}^{(j')}(|\mathbf{r}-\mathbf{r}_{j'}|)=A_{k,m}^{(\nu,j')}K_m\left(\alpha_\nu\frac{|\mathbf{r}-\mathbf{r}_{j'}|}{l}\right).$$

Using the addition theorem for spherical harmonics and the assumption of axial symmetry of the neutron self-field of a slug we find the field of the lattice close to slug j at a distance r from its axis:

$$\sum_{k,m}\frac{P_{k,m}(\vartheta)}{\sqrt{2\pi}}e^{im\varphi_j}\sum_{j'}A_{k,m}^{(\nu,j')}F_{m,\nu}^{(j,j')}(r), \tag{16}$$

where

$$F_{m,\nu}^{(j,j')}(r)=\delta_{j,j'}K_m\left(\alpha_\nu\frac{r}{l}\right)+(-1)^m I_m\left(\alpha_\nu\frac{r}{l}\right)K_0\left(\alpha_\nu\frac{r_{j,j'}}{l}\right). \tag{17}$$

Equation (16) does not take account of the fact that the lattice may contain equivalent slugs, i.e., identical slugs under the same conditions at different points of the composite cell. In considering a composite lattice the subscript j must be replaced by two subscripts j and p, where p refers to the number of the cell and j to the slug within cell p. We consider the neutron field in a cell which we arbitrarily call the zeroth cell. Then instead of (17) we obtain

$$F_{m,\nu}^{(j,j')}(r)=\delta_{j,j'}K_m\left(\frac{\alpha_\nu r}{l}\right)+(-1)^m I_m\left(\frac{\alpha_\nu r}{l}\right)\sum_p{}' K_0\left(\frac{\alpha_\nu r_{j,pj'}}{l}\right), \tag{18}$$

where $r_{j,pj'}$ is the distance from slug j of cell zero to slug j' of cell p.

Hence it follows that the vector $\psi^{(j)}(\rho)$ describing the neutron field on the surface of slug j is

$$\Psi^{(j)}=C+\sum_{j'}\hat{M}^{(j,j')}A^{(j')}, \tag{19}$$

where the $\hat{M}^{(j,j')}$ are matrices of the form (14) (since we are considering a moderator with weak absorption) in which the functions $K_m(\alpha_\nu r/l)$ are replaced by $F_{m,\nu}^{(j,j')}(\rho_j)$, and ρ_j is the radius of slug j.

To determine the elements of the matrices $\hat{M}^{(j,j')}$ it is necessary to find the sums appearing in $F_{m,\nu}^{(j,j')}$ of (18). Calculation of these sums for ν equal to 1 and 2 presents no difficulty. Ordinarily the distance between slugs is larger than l, and therefore even for the slugs nearest the one under consideration the argument of K_0 in (18) is of the order of unity or larger. Consequently only the first few terms in the sum (18) need be calculated.

For $\nu = 0$, when $\alpha_0 = l/L \ll 1$, the sum converges slowly, and it is expedient to use the results of analytic summation [3]. Taking account of the leading term and the corrections to it of order a^2/L^2 or ρ^2/L^2 we obtain

$$\begin{gathered}F_{0,0}^{(j,j')}=\frac{2\pi L^2}{S_{j'}}\left[1+\frac{\rho_j^2}{4L^2}+\frac{S_{j'}\zeta_{j,j'}}{4\pi L^2}\right];\\ F_{1,0}^{(j,j')}=\frac{L}{\rho_j}\left[\delta_{j,j'}-\frac{\pi\rho_j^2}{S_{j'}}-\frac{\rho_j^2}{4L^2}(\zeta_{j,j'}+\delta_{j,j'})\right];\\ F_{2,0}^{(j,j')}=2\left(\frac{L}{\rho_j}\right)^2\left[\delta_{j,j'}+\frac{\rho_j^2}{4L^2}\cdot\frac{\pi\rho_j^2}{S_{j'}}\right];\quad F_{3,0}^{(j,j')}=8\left(\frac{L}{\rho_j}\right)^3\delta_{j,j'};\quad S_j=\frac{S}{N_j},\end{gathered} \tag{20}$$

where S is the area of the composite cell, N_j is the number of slugs of type j in the composite cell, and the $\zeta_{j,j'}$ are quantities depending on the radius of a slug and the geometry of the cell. The values of $\zeta_{j,j'}$ for a number of lattices are given in [3].

Substitution of the expressions for $F_{m,\nu}^{(j,j')}$ into the matrix elements $M_{n,\nu}^{(j,j')}$ shows that $M_{0,0}^{(j,j')}$ is proportional to L^2. According to [3] C_0 is also proportional to L^2.

Since the result (e.g., the disadvantage factor) is finite as $L^2 \to \infty$ the calculations involve the compensation of large terms, which is always undesirable in a numerical calculation. Therefore we make some matrix transformations. We write $A_0^{(j')}$ in the form

$$A_0^{(j')}=\frac{S_{j'}}{2\pi L^2}\left[-\frac{q}{\varepsilon}\beta_{j'}+A_0'^{(j')}\right], \tag{21}$$

where

$$\sum_j\beta_j=1. \tag{22}$$

After multiplying the $A_0^{(j')}$ by the appropriate matrices and performing all the cancellations we can go to the limit $L^2 \to \infty$. If now we return to the notation $\sum_j A_0'^{(j)} \to A_0^{(1)}$ and $\beta_j \to A_0^{(j)}$ for $j > 1$, Eq. (19) is preserved and vector C takes the form

$$C_j=\begin{pmatrix}-\frac{3}{4}q\frac{1-\mu}{l^2}\left(\rho_j^2+\frac{S_1\zeta_{j,1}}{\pi}\right)\\ \sqrt{\frac{3}{2}}q(\rho_j/l-\delta_{j,1}S_1/\pi l\rho_j)\\ -\sqrt{\frac{6}{5}}\delta_{j,1}qS_1/\pi\rho_j^2\\ 0\\ -\frac{12}{\sqrt{35}}qlS_1\delta_{j,1}/\pi\rho_j^3\\ 0\end{pmatrix}, \tag{23}$$

and in the matrices $\hat{M}^{(j,j')}$ only the first columns are changed, so that $M^{(j,1)}_{m,0} = \delta_{m,0}$. For $j' > 1$ we obtain

$$\begin{aligned}
M^{(j,j')}_{0,0} &= -\frac{3}{4}\cdot\frac{(1-\mu)\,q}{\pi l^2}(S_{j'}\zeta_{j,j'} - S_1\zeta_{j,1});\\
M^{(j,j')}_{1,0} &= -\frac{\sqrt{3}\,q}{\sqrt{2}\,\pi\rho_j l} D_{j,j'};\\
M^{(j,j')}_{2,0} &= -\frac{\sqrt{5}\,q}{\sqrt{6}\,\pi\rho_j^2} D_{j,j'};\\
M^{(j,j')}_{4,0} &= -\frac{12ql}{\sqrt{35}\,\pi\rho_j^3} D_{j,j'};\\
M^{(j,j')}_{3,0} &= M^{(j,j')}_{5,0} = 0;\quad D_{j,j'} = S_{j'}\delta_{j,j'} - S_i\delta_{j,1}.
\end{aligned} \tag{24}$$

The physical meaning of the quantities β_j in (21) is easily determined from the expression for $\psi_1^{(j)}$ as the neutron current into the slug from the outside:

$$\psi_1^{(j)} = -\frac{\sqrt{6}}{l}\,q\,\frac{S_j\beta_j - \pi\rho_j^2}{2\pi\rho_j}. \tag{25}$$

It follows from (25) that the quantity $S_j\beta_j$ is equal to the area of the effective cell of a slug of type j in the composite lattice. The neutron current is zero on the boundary of this effective cell.

Using boundary conditions (7) to join solution (4) for zones inside the slugs to the solution in the form (19) for the outside surfaces we obtain a complete set of equations for all the vectors A. However the order of this system turns out to be six times the sum of the total number of zones in all the nonequivalent slugs of the composite cell. By applying the usual procedure of matrix contraction to all the multilayer slugs the order of the system is easily reduced to six times the number of nonequivalent slugs in the composite cell. In this system the unknowns are the three-component vectors describing the solutions at the center of each slug and outside it. By eliminating from the system the vectors connected with the solution in the central zones of the slugs we obtain a system whose order is only triple the number of nonequivalent slugs.

Calculation of the Average Neutron Field in Slug Zones and Moderator

To determine the values of the neutron flux ψ_0 averaged over the zones we use a relation which is easily obtained by integrating the transport equation over ϑ and φ

$$\varepsilon\psi_0 + \frac{l}{\sqrt{6}}\cdot\frac{d}{r\,dr}(r\psi_1) = q. \tag{26}$$

Hence for the i-th layer of a slug we have

$$\varepsilon_i\bar{\psi}_{0,i} = q_i - \sqrt{\frac{2}{3}}\,l_i\,[r_i\psi_1(r_i) - r_{i-1}\psi_1(r_{i-1})]\,(r_i^2 - r_{i-1}^2)^{-1}, \tag{27}$$

and for the moderator outside the slugs

$$\varepsilon\bar{\psi}_0 = q - \sqrt{\frac{2}{3}}\,\pi l\left[1 - \pi\sum_j(\rho_j^2/S_j)\right]^{-1}\sum_j\frac{\rho_j\psi_1(\rho_j)}{S_j}. \tag{28}$$

It is obvious that Eqs. (27) and (28) cannot be used to determine $\bar{\psi}_0$ in regions where the neutron absorption is rather weak. In these zones ψ_1 can be written in the form $\psi_1 = \psi_{10} + \varepsilon\delta\psi_1$. Hence for the moderator outside the slugs we obtain

$$\bar{\psi}_0 = -\sqrt{\frac{2}{3}}\,\pi l\left[1 - \pi\sum_j(\rho_j^2/S_j)\right]^{-1}\sum_j\frac{\rho_j\delta\psi_1(\rho_j)}{S_j}, \tag{29}$$

where

$$\delta\psi_1(\rho_j) = \Big[\sum_{j'}\delta\hat{M}^{(j,j')}A^{(j')}\Big]_1 + \Big[\sum_{j'}\hat{M}_0^{(j,j')}\delta A^{(j')}\Big]_1. \tag{30}$$

Here the elements of the matrix $\delta\hat{M}$ are the coefficients of ε in the expansion $\hat{M} = \hat{M}_0 + \varepsilon\delta\hat{M}$. The series expansion of $A_0^{(j)}$ is given in Eq. (21); the other A_n's do not appear in $\delta\psi_1$ because of the structure of $\hat{M}_0^{(j,j')}$.

By carrying out the indicated procedure we obtain for the moderator outside the slugs

$$\bar{\psi}_0 = A_0 + \left[1 - \pi\sum_j\rho_j^2/S_j\right]^{-1}\left[\frac{3}{4}\cdot\frac{(1-\mu)\,q}{l^2}\sum_{j,j'}\rho_j^2(\zeta_{j,j'} + \delta_{j,j'})\frac{S_{j'}}{S_j}\beta_{j'} + \frac{6\pi l}{\sqrt{35}}\sum_{j,j'}\frac{\rho_j}{S_j}F_{0,1}^{(j,j')}A_1^{(j')}\right].$$

For a nonabsorbing i-th layer $\overline{\psi}_0$ can be obtained explicitly by integrating $\psi_0(r)$ over this layer of the slug.

CONCLUSION

A program for carrying out the procedure described was written in ALGOL. The processing of one variant of a double lattice with two-zone slugs required about 10 sec of machine time on an M-220 computer, including the time for typing input and output.

A comparison of the results calculated with this program and those obtained by using the program described in [5] showed that the assumption of axial symmetry of the self-field of each slug does not lead to appreciable errors.

More detailed results of the comparison will be reported in a special letter to the editor.

LITERATURE CITED

1. V. V. Smelov and G. A. Ilyasova, in: Computational Methods in Transport Theory [in Russian], G. I. Marchuk (editor), Atomizdat, Moscow (1969), p. 173.
2. I. Aviram and Y. Yeivin, J. Nucl. Energy, 24, 289 (1970).
3. A. D. Galanin, Heterogeneous Reactor Theory [in Russian], Atomizdat, Moscow (1971).
4. A. D. Galanin, The Theory of Thermal Neutron Reactors [in Russian], Atomizdat, Moscow (1959).
5. V. V. Smelov, Atomnaya Énergiya, 33, 915 (1972).

ACOUSTIC METHOD OF MEASURING SMALL DISPLACEMENTS IN HIGH-TEMPERATURE AND RADIATION FIELDS

A. V. Zelenchuk and K. V. Naboichenko

UDC 534.6:624.058.2

Carrying out strength tests under conditions of high temperatures and irradiation is one of the current problems in modern materials research. The most important problem is the measurement of deformations.

Measurement methods based on the use of electrical transducers [1] depend considerably on the radiation flux; therefore, a gas-flow transducer was used to measure small deformations in the reactor channel [2, 3]; however, it is very cumbersome and can operate only under stationary conditions. With gas pumping, radioactive elements are transported from the core, and thus it is necessary to have additional equipment to purify the gas and shield personnel from radiation.

Acoustic measurement methods for deformations in a nuclear-reactor channel were first proposed and developed at the Moscow Engineering Physics Institute (MIFI). Readings of acoustic transducers are independent of the radiation. According to the accuracy these transducers are no worse than the measurement methods indicated above. They have the advantages of the absence of electrical elements in the core and simplicity of instrumentation; moreover, they completely eliminate the transport of radioactive elements from the reactor channel.

To measure deformations during high-temperature strength testing of materials in a small-diameter reactor channel it is most advisable to use the acoustic measurement method, based on the change in acoustic impedance of an aperture. The basic advantages of this method consist in the possibility of measuring the deformation directly on the sample being investigated (Fig. 1).

Two coaxial cylindrical waveguides filled with a gas, are separated on one side by a valve-transducer; on the other side an external waveguide has a source of sound oscillations, and the internal waveguide has a receiver of sound oscillations. The source of sound oscillations excites a plane sound wave in the external waveguide, which moves to the valve-transducer. The valve, directly connected to the source of displacements, transforms them into a variation of aperture dimensions, and hence, also into a variation in the acoustic impedence of the aperture. For a definite structure of the valve-transducer, the aperture can have the shape of a slit or a circular aperture, as well as more complex forms.

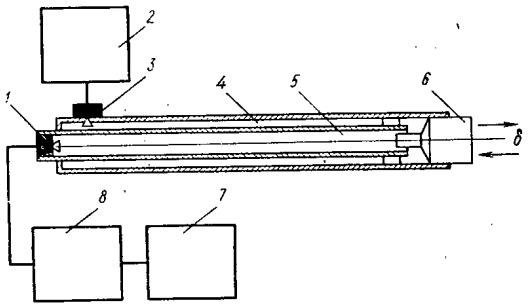

Fig. 1. Block diagram of model of acoustic transducer of small displacements: 1) receiver of oscillations; 2) sound generator; 3) oscillation source; 4) external waveguide; 5) internal waveguide; 6) valve-transducer; 7) recorder; 8) amplifier.

Sound oscillations passing through the aperture reach the internal waveguide and after reaching the sound-oscillation receiver, they induce in it a variable electrical signal, which is then amplified and recorded.

The oscillations of the gas in the transducer occur with a frequency such that only plane sound waves propagate in the waveguide [4]. The aperture formed by the valve-transducer can be considered as an element for constricting the waveguides. The acoustic power passing through the aperture [4] is described by the expression

$$N \approx \frac{4p_i^2 R_s \sigma_{ap}^2}{|Z_n|^2}, \quad (1)$$

Translated from Atomnaya Énergiya, Vol. 36, No. 2, pp. 130-132, February, 1974. Original article submitted November 27, 1972.

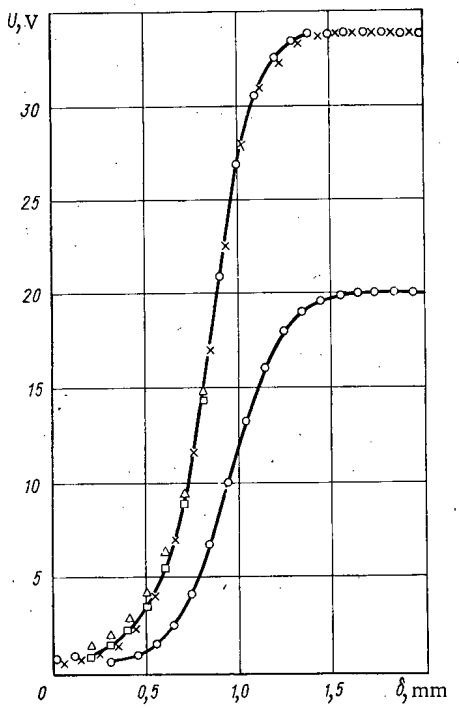

Fig. 2

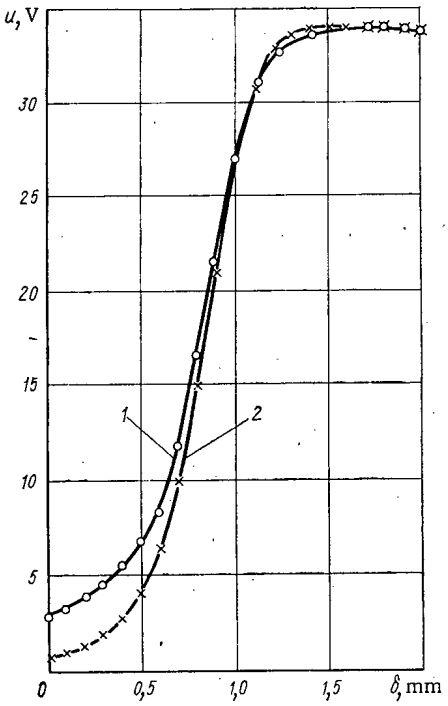

Fig. 3

Fig. 2. Dependence of operating characteristics of acoustic transducer on temperature, pressure, and composition of gas at oscillation frequency 2150 Hz: □) air, t = 20°C, p = 1 abs. atm, U_0 = 1.75 V; Δ) helium, t = 20°C; p_1 = 1 abs. atm, p_2 = 1.2 abs. atm, U_0 = 1.8 V; ○) agreement of results for air and helium, presented above; points on the lower curve) helium, t = 465°C, p = 1 abs. atm, U_0 = 1.8 V up to temperature compensation; ×) helium, t = 465°C, p = 1 abs. atm, U_0 = 3.6 V after temperature compensation.

Fig. 3. Comparison of calculated (1) and experimental (2) characteristics for oscillation frequency 2150 Hz and temperature 20°C with a helium-filled transducer.

where p_1 is the amplitude of oscillations in front of the aperture; R_S is the resistance of radiation of the aperture; σ_{ap} is the area of the aperture; Z_n is the total acoustic impedance of an aperture of arbitrary shape. The aperture radiating in the internal waveguide can be considered as a secondary source of sound oscillations.

For frequencies lower than the lowest of the natural transverse oscillations [5, 6], we can assume that

$$N_1 \approx N_2, \tag{2}$$

where $N_2 = (p_2^2\sigma_2/\rho c)$ is the acoustic power of a plane sound wave withdrawn from the aperture into the internal waveguide; p_2 is the amplitude of the pressure of a plane sound wave; σ_2 is the cross section of the internal waveguide; ρ is the gas density; and c is the velocity of sound.

Since the aperture dimensions are small compared with the wavelength, the acoustic impedance [4] can be determined from the expression

$$Z_n \approx \frac{\rho\sigma_{ap}^2}{G_{ap}}, \tag{3}$$

where Gap is the acoustic conductivity of an aperture of arbitrary shape, which is a function of the geometrical parameters of the aperture. The amplitude of a plane sound wave in the internal waveguide is found from expression (2), by equating the power averaged over time:

$$p_2 = \frac{2p_1 G_{ap}}{\sqrt{\sigma_2 \Omega}}, \tag{4}$$

where Ω is the solid angle of the radiation.

If the source excites oscillations having amplitude U_0, then when they reach the valve-transducer, they are decreased by a factor $\exp(-\beta_1 l)$. Along the second waveguide on the path from the aperture to the receiver of oscillations the amplitude decreases by the factor $\exp(-\beta_2 l)$. Further oscillations in the receiver are converted into electrical oscillations and are amplified by a factor K_{amp}. Thus, the transformed amplitude of sound oscillations recorded by the device has the form

$$U = K \exp[-(\beta_1 + \beta_2) l] U_0 G_{ap} \quad (5)$$

where β_1 and β_2 are the damping coefficients in the external and internal waveguides, respectively; $K = (2K_S K_r K_{amp}/\sqrt{\sigma_2 \Omega})$ is a constant coefficient; l is the length of the waveguide; K_S and K_r are the coefficients of transformation of acoustic oscillations into electrical oscillations of the source and the receiver; U_0 is the amplitude of the electrical oscillations of the source.

The multiplier $\exp[-(\beta_1 + \beta_2)l]$ is affected by the temperature, composition, and pressure of the gas; however, this effect can easily be eliminated if we change the amplitude U_0, i.e., we can compensate the temperature error of the transducer readings.

We present results of tests of an acoustic transducer for linear displacements, 1500 mm long, 6 mm in diameter, and having a measurement range of 0-0.5 mm.

For displacements of the valve transducer, the width, thickness, and hence also the acoustic impedance of the circular slit through which the sound oscillations pass from the external waveguide to the internal waveguide are varied.

For operating frequency $\nu = 2150$ Hz we obtained characteristics for a transducer filled with air and helium at gas pressure 1-1.2 abs. atm and temperature 20-465°C. The operating characteristics are shown in Fig. 2.

The signal at the receiver for the open position of the valve attains its maximum value and remains constant with further opening. This situation is convenient for use in introducing a correction to the temperature, which understates the value of the signal of the "plateau" due to an increase in the damping of the oscillation amplitude in the waveguides. A correction is introduced because of the increase in oscillation amplitude of the source as long as the signal of the "plateau" agrees with the signal corresponding to 20°C. All the remaining points of the operating characteristics agree with the points of the characteristics plotted for 20°C.

The temperature error can also be compensated by using a movable screen, which is periodically opened by the direct access of sound oscillations from the external waveguide to the internal waveguide in immediate proximity to the valve-transducer. In the case of such compensation the aperture of the valve-transducer does not change, which is a necessary condition for the displacement measurements. With introduction of amplitude compensation the operating characteristics also are independent of the state and pressure of the gas inside the transducer and agree well with the calculated characteristics (Fig. 3). The deviation of the experimental curve (in the lower part) from the calculated curve can be explained by the "idealization" of the valve surface, since in the calculation we did not take into account possible irregularities which for given position of the valve $\delta = 0.5$ mm are comparable with the width of the slit and cause an additional resistance to gas motion.

For the working range of the transducer we take the steepest linear section of the characteristics.

For an analysis of the measurement accuracy we obtained an error of no more than 0.45% with accuracy $\alpha = 0.9$ for threshold sensitivity $S_{th} = 2\ \mu$ over the working range 0.5 mm. From the theory of the method it follows that the measurement range is given by the dimensions and shape of the valve. To confirm this we obtained a range of measurements from 0-0.1 to 0-10 mm.

The advantages of the acoustic transducer (the independence of the readings from radiation, the simplicity of the geometry, the small radial dimensions, the possibility of amplitude compensation) allow us to use it to measure displacements in high-temperature and radiation fields, especially if these measurements must be carried out in locations that are almost inaccessible.

LITERATURE CITED

1. D. Brucklacher and W. Dienst. J. Nucl. Materials, 36, No. 2, 244 (1970).
2. A. P. Vysotskii et al., Pneumatic Measurements of Linear Dimensions [in Russian], Mashgiz, Moscow (1967).

3. Fidlers et al., Reactor Creep Machines. Symp. on In-Pile Irradiation Equipment and Technologies at AERE, Harwell, England (1966).
4. E. Skuchik, Fundamentals of Acoustics [in Russian], Mir, Moscow (1969), Vols. I and II.
5. P. M. Morse, Vibration and Sound, 2nd Ed., McGraw–Hill (1948).
6. Lord Rayleigh, The Theory of Sound, Dover (1945).

THE MAXIMUM OF NEUTRON FLUX IN A REFLECTOR WHEN MODERATED NEUTRON ABSORPTION IS TAKEN INTO ACCOUNT

V. P. Glushakov

UDC 621.039.512.45:
621.039.573:621.039.55

The L. S. Pontryagin maximum principle is used to solve for the radial distribution of nuclear fuel in a reactor which maximizes the ratio

$$J=\frac{N_{\max}}{W},$$

where N_{max} is the maximum density of thermal neutrons in the reflector, and W is the reactor power. The problem is solved in the two-group approximation, taking into account the absorption of moderated neutrons, with the fuel concentration subject to the constraint

$$0 \leqslant U(r) \leqslant U_{\max}$$

and the heat engineering

$$p=U(r)(N+an)-D \leqslant 0.$$

Here the functions N(r) and n(r) describe the distribution of thermal and moderated neutrons in the reactor zone; a and D are constants. It is shown that for weak absorption of moderated neutrons the optimum arrangements consist of zones with $U(r) = U_{max}$ and $p(r) = 0$, with the maximum in J occurring in a single-zone reactor with $U(r) = U_{max}$. Similar results have been obtained for this problem when the absorption of moderated neutrons is neglected [1]. However, when there is intense absorption of moderated neutrons, a zone appears in the central part of the optimum reactor for which $U_0(r) < U_{max}$. This is the zone of the classical variational calculus, which could not be realized if the moderated neutron capture were neglected. The value of J_{max} is an increasing function of the fuel concentration, so that the case of greatest interest is that of strong absorption, for which a two-group model which neglects absorption of moderated neutrons gives an incorrect result for the character of the optimum arrangements.

The functions $J(N_{max})$ or J(W) are determined in the article for the case of the optimum reactor; this enables one to choose a variant for which the reactor components [2] of the cost are minimum.

LITERATURE CITED

1. T. S. Zaritskaya et al., At. Énerg., 32, No. 6, 480 (1972).
2. A. N. Erykalov and Yu. V. Petrov, At. Énerg., 25, No. 1, 52 (1968).

Translated from Atomnaya Énergiya, Vol. 36, No. 2, pp. 133-137, February, 1974. Original article submitted June 28, 1972.

CALCULATION OF DOSES FROM FAST-REACTOR RADIATION LOOPS

V. A. Rudoi, E. M. Vetrov, A. Kh. Breger, N. I. Polyanskii, and V. P. Tikhonov

UDC 621.039.553

One of the most important problems of radiochemical equipment construction [1] is the development and production of radiation loops to provide intense economical γ sources for large-scale radiochemical processes.

The use of fast power reactors for the simultaneous generation of electrical power and for chemical production raises the problem of calculating dose distributions from sodium radiation loops containing plane surface radiators.

We propose a simple formula for the absorbed dose rate at a point above a plane rectangular surface radiator

$$P = P_\gamma \psi \bar{\sigma}_s G(m, n, \mu d) B_{\text{dis}}, \tag{1}$$

where P_γ is the γ ionization constant in $(R/h)/(\mu Ci/cm^2)$, Ψ is the conversion factor from Roentgens to rads, $\bar{\sigma}_S$ is the average surface activity of the radiator in $\mu Ci/cm^2$, G(m, n, μd) is the γ attenuation function, and B_{dis} is the distributed source dose buildup factor in integral form.

The average surface activity $\bar{\sigma}_S$ can be written as

$$\bar{\sigma}_s = \frac{2\pi}{\mu_s} \cdot \frac{A_r}{V_r + V_p + V_{rad}} (1 - e^{-\frac{3}{2}\mu_s t}). \tag{2}$$

Here A_r is the total activity of the coolant in the primary reactor loop; V_r, V_p, and V_{rad} are respectively the volumes in cm^3 of the coolant in the reactor, the piping, and the radiator, μ_S is the γ attenuation coefficient of the radiator material in cm^{-1}, and t is the thickness of the radiator in cm.

We calculate the attenuation function by the relation

$$G(m, n, \mu d) = \frac{\pi}{2} E_1(\mu d) - \operatorname{arctg} n E_1\left(\mu d \sqrt{1 + \frac{m^2 n}{\operatorname{arctg} n}}\right) - \operatorname{arctg} \frac{1}{n} E_1\left(\mu d \sqrt{1 + \frac{m^2 n}{\operatorname{arctg} 1/n}}\right), \tag{3}$$

where μd is the thickness of the absorbing layer in mean free paths, n and m are the relative dimensions of the radiator–irradiated object system, H and L are the source dimensions, and b is the distance from the source to the detector point.

The accuracy of the expression for G (m, n, μd) was determined by comparison with computer calculated data in [2]. The comparison showed that the values of G(m, n, μd) given by (3) do not differ from the data in [2] by more than ~3%.

The value of B_{dis} is given by

$$B_{\text{dis}} = B_p + A(\mu d)\, e^{-\frac{K(z) D(n)}{\sqrt[3]{m}}}, \tag{4}$$

which is obtained from an analysis of the values of B_{dis} calculated for ^{24}Na energies (E_1 = 1.38 MeV, E_2 = 2.76 MeV) and water, aluminum, and iron thicknesses up to 5 mfp.

The values of B_p, the dose buildup factor for a point source, were taken from [3, 4] for small penetrations, and K(z), D(n), and A(μd) are coefficients. The values of these quantities are tabulated. Equation (2) is accurate to ±10%.

An experimental test of the proposed relations using a ^{24}Na radiation source showed good agreement between the measured and calculated results, within the limits of experimental error. Calculations performed by the proposed method for conditions described in [5] showed satisfactory agreement with the results in that paper.

Original article submitted November 27, 1972.

LITERATURE CITED

1. A. Kh. Breger et al., Fundamentals of Radiochemical Apparatus Construction [in Russian], Atomizdat, Moscow (1967).
2. N. G. Gusev et al., Shielding Against Distributed Sources [in Russian], Gosatomizdat, Moscow (1961).
3. V. Holland, Data of an International Conference on the Peaceful Uses of Atomic Energy [Russian translation], Vol. 13, Inostr. Lit., Moscow (1958), p. 339.
4. V. E. Drozdov et al., Radiobiologiya, 7, 165 (1967).
5. V. Manowitz et al., Large Radiation Sources in Industry, Vol. 1, IAEA, Vienna (1960), p. 65.

CERTAIN CHARACTERISTICS OF VARIABLE-PHASE FOCUSING IN PROTON LINEAR ACCELERATORS

A. D. Vlasov

UDC 621.384.64.01

Variable-phase focusing (VPF) is attractive because of the possibility of doing without complicated and expensive magnetic lenses and their supply systems. In 1966 V. V. Kushin [1] discovered a means of significantly increasing the efficiency of VPF by introducing a constant component in the law of the periodic variation in the equilibrium phase and also (with Mokhov [2]) by simultaneously introducing a periodic change in the amplitude of the accelerating wave;

$$\varphi_p = \pm\varphi_1 - \varphi_2, \quad E_M = E_0 \pm \Delta E = E_0(1 \pm \varepsilon). \tag{1}$$

It is known that in the case of VPF the usual autophasing is replaced by alternating phasing. It is shown in the present article that the expression for the amplitude of the oscillations of particle energy differs from the corresponding autophasing expression only by the replacement of the factor $\sqrt{\sin\varphi_p}$ by $\sqrt{\nu_f^2/2B}$. Here ν_f is the so called amplitude coefficient, and B is the VPF parameter [1]. For the typical values of these parameters $\nu_f = 1/3$, B = 10, $\varphi_p = 37°$, we obtain $\sqrt{\nu_f^2/2B} = 0.075$, and $\sqrt{\sin\varphi_p} = 0.77$.

The capture in energy for VPF is thus at least a factor of ten smaller than in the case of autophasing. This should not be a significant effect when VPF is used immediately following the ion gun or the high-voltage accelerator, where the resulting beam has a small spread in energy. A small capture in energy can, however, cause a loss of at least 90% of the particles, if VPF is used after a preliminary acceleration of the protons in a linear accelerator with autophasing. A preliminary grouping with VPF can also cause a considerable loss in particles for the same reason.

The article gives a comparison of thermal losses in an accelerator with VPF with those of an "etalon" accelerator with autophasing. Assuming the average rate of acceleration of the particles to be equal, the following expression was obtained for the ratio of the powers of these losses:

$$\frac{P_f}{P_e} = \frac{\cos^2\varphi_{p.e}}{\cos^2\varphi_1\cos^2\varphi_2}\cdot\frac{1+\varepsilon^2}{(1+\varepsilon\,\mathrm{tg}\,\varphi_1\,\mathrm{tg}\,\varphi_2)^2}\cdot\frac{R_{sh.e}}{R_{sh}}\cdot\frac{1+\delta}{1+\delta_e}. \tag{2}$$

Here R_{sh} and δ are the shunt resistance and the ratio of the length of the intersection interval to the length of the section of the accelerator, $R_{sh.e}$ and δ_e are the same for the etalon accelerator, and $\varphi_{p.e}$ is its equilibrium phase.

The first factor on the right-hand side of Eq. (2) depends only on the angles φ_1, φ_2, and $\varphi_{p.e}$; one can take $\varphi_{p.e} = 37°$. This factor is less than one for small values of φ_1 and φ_2. As a result, VPF does not in principle require special losses in power. Rather large values of φ_1 and φ_2 are, however, required for the effectiveness of VPF, which causes an increase in the thermal losses. Thus, for $\varphi_2 \leq 20$ and $\varphi_1 = 45°$, the first factor is between 1.3 and 1.4; for $\varphi_1 = 55°$, it is approximately two. The second factor, which depends on the coefficient of modulation of the amplitude ε, does not exceed unity for $\mathrm{tg}\,\varphi_1$, $\mathrm{tg}\,\varphi_2 \geq 0.41$.

Original article submitted March 15, 1973.

For proton energies of up to 100-150 MeV, when the Alvarez accelerating system is used, the third factor is less than unity. Inasmuch as lenses are unnecessary in VPF, the drift tube diameters are less, and $R_{sh} > R_{sh.e}$. For energies above 100-150 MeV, the lenses can only be placed between the sections, $R_{sh} = R_{sh.e}$, and the third factor is equal to one.

The fourth factor, on the other hand, is equal to one in the case of an Alvarez system, and is less than unity at higher proton energies, where $\delta e > \delta$ as a result of the placement of the lenses between the sections. The product of the third and the fourth factors in Eq. (2) is therefore always less than unity, which causes a decrease in the thermal losses.

Equation (2) was obtained with the help of V. V. Kushin. The author is indebted to him for a discussion of this and other aspects of the work.

LITERATURE CITED

1. V. V. Kushin, At. Énerg., 29, No. 2, 123 (1970).
2. V. M. Mokhov and V. V. Kushin, At. Énerg., 34, No. 3, 209 (1973).

ANGULAR AND SPECTRAL DISTRIBUTIONS OF THE INTENSITY OF SCATTERED GAMMA-RADIATION IN THE 20 keV AND 6 MeV RANGE OF INITIAL ENERGIES

S. N. Sidneva and A. S. Strelkov

UDC 539.166.3

The angular and spectral distributions of the intensity of scattered γ-radiation from a point isotropic source in an infinite medium consisting of air are calculated by making use of a statistical sampling method. The initial quantum energy E_0 was varied from 20 keV to 6 MeV. The distributions were obtained at distances of 1, 2, 3, 4, 6, and 8 mean free paths from the original radiation. The characteristics of the field of the scattered radiation which were found are the values of intensity, averaged over the chosen interval of the variable (solid angle or energy), and adjusted to unit interval of the variable and to a unit quantum emergent from the source.

The results of the calculation of the angular distributions are given in the form of the dependence of the fraction of the intensity of the scattered radiation arriving at a distance $\mu_0 R$ within a given solid angle $\Delta\Omega$, as compared to the total intensity of the scattered radiation at this distance. The transition to absolute values of average intensity is made through the build-up coefficient of the energy flux [1]. The angular distributions obtained for the intensity of the scattered radiation are approximated by expressions of the form

$$\frac{dI(\theta)}{d\Omega} = \frac{Ce^{-\theta/\theta_0}}{\sin\theta} \quad (1)$$

and

$$4\pi R^2 e^{\mu_0 R} \frac{dI(\theta)}{d\Omega} = A_1 e^{-\theta/\theta_1} + A_2 e^{-\theta/\theta_2}. \quad (2)$$

Tables are given showing the dependence of θ_0, θ_1, θ_2, A_1, and A_2, on the distance $\mu_0 R$ and the initial energy E_0. The limits of applicability and the accuracy of the approximation equations (1) and (2) are discussed.

The spectral distributions of the intensity of the scattered radiation are listed for energies E_0 from 20 to 100 keV at 10 keV intervals, since at higher initial energies they are to within the accuracy of the calculation the same as the distributions in an infinite aqueous medium produced by a point isotropic source [2].

Original article submitted April 21, 1973.

The form of the spectral distribution is transformed in proportion to the decrease in the initial energy from the known form for $E_0 > 250$ keV to a distribution having one maximum (the initial energy ~100-50 keV). As the initial energy decreases further, it becomes a decaying spectrum with a maximum value of intensity at an energy equal to the initial energy. Also noteworthy is the approximate equality of the form of the spectral distribution at distances greater than $4\mu_0 R$, which was noted earlier in the case of higher initial energies.

The spectral distributions are approximated by the expression

$$4\pi R^2 e^{\mu_0 R} \frac{dI(E_0, \mu_0 R, E)}{dE} = \exp(a + bx + cx^2 + dx^3), \quad (3)$$

where $x = (E-15)/(E_0-15)$ (E_0 and E, keV).

An analysis of the accuracy of the description of the spectral distributions given by Eq. (3) is carried out. The coefficients of the approximation formulas are listed in tabular form.

LITERATURE CITED

1. M. N. Vrubel', S. N. Sidneva, and A. S. Strelkov, At. Énerg., 34, No. 1, 47 (1973).
2. G. Goldstein and D. Wilkins, in: The Shielding of Transport Equipment From Nuclear Engines [Russian translation], (V. V. Orlov and S. G. Tsypin, editors), Izd-vo Inostr. Lit., Moscow (1961), p. 212.

REFINEMENT OF NEUTRON-PHYSICS PARAMETERS FOR AQUEOUS SOLUTIONS OF HIGHLY ENRICHED URANYL FLUORIDE AND URANYL NITRATE SALTS CONSISTENT WITH THE DATA OF CRITICAL EXPERIMENTS

Yu. Yu. Vasil'ev, V. N. Gurin, and B. G. Ryazanov

UDC 621.039.519.4

A wide variety of Laplace transform techniques have been developed for estimating the critical dimensions of reactors which are geometrically simple in shape [1]. The accuracy of the derivation of the critical dimensions by this method is determined by the errors in the values of the material parameter, the extrapolation distance, and the reflector savings. These quantities are usually determined either by calculation or by experiment. In this paper, the material parameter and the extrapolation distance are calculated from a system of three-group, macroscopic constants, fitted by the method of least squares, which best describes the results of one-region critical experiments for a given reactor composition. The application of this method to the interpretation of the work of Rowlands and MacDougall [2] allows one to estimate the errors in predicting the material parameter and the extrapolation distance as a function of the accuracy of the original constants and the critical experiments.

Aqueous solutions of uranyl fluoride UO_2F_2 and uranyl nitrate $UO_2(NO_3)_2$ (the uranium enrichment is 93.5 and 90%, respectively) are investigated. Critical experiments in assemblies in the form of a sphere, cylinder, and parallelepiped are analyzed. The calculation is conducted in the three-group diffusion approximation. The more accurate values of the material parameter, the extrapolation distance, the multiplication constant for neutrons in an infinite medium, and the migration area, together with the errors in their prediction, are presented in the form of curves as a function of the uranium concentration in the solution.

The authors are grateful to B. G. Dubovskii for his interest in the work and for his helpful comments.

Original article submitted May 21, 1973.

LITERATURE CITED

1. B. G. Dubovskii et al., Critical Parameters of Systems with Fissionable Materials and Nuclear Safety, Handbook [in Russian], Atomizdat, Moscow (1966), p. 95.
2. J. Rowlands and J. MacDougall, Physics of Fast Reactor Operation and Design, BNES, London (1969).

INVESTIGATION OF THERMAL CONDUCTIVITY AND ELECTRICAL CONDUCTIVITY OF DISPERSED MATERIALS MADE OF URANIUM AND MOLYBDENUM DIOXIDES

L. E. Kakushadze and R. B. Kotel'nikov

UDC 621.039.544.57

Shortcomings of uranium dioxide, which is the fuel in atomic-reactor fuel elements, are its low thermal conductivity and its brittleness. Therefore there is interest in cermets based on uranium dioxide with the addition of an appropriate metal. We investigate the thermal conductivity and electrical conductivity of cermets made of particles of uranium dioxide (Fig. 1) coated with molybdenum (1), and those made of mixtures of similar particles with molybdenum powder (2). To prepare the samples we used a grit made from uranium-dioxide particles of the pebble type, obtained by sintering, scattered over the fractions −315 + 200; −600 + 400; −840 + 700; −1190 + 1000 μ with lattice parameter 5.468 Å and corresponding formula $UO_{2.00}$ (composition: 87.47 wt. % uranium, 11.76 wt. % oxygen). A molybdenum coating was applied to the particles by vaporization in vacuum. The mean particle dimensions of molybdenum powder was 2.5 μ. The samples were made by hot pressing in vacuum, and were as follows: diameter 10 mm, length 15-20 mm, density 95% of theoretical, mean grain dimension in UO_2 particles 19 μ, and molybdenum concentration 5, 10, 15, and 20 vol. %. The continuity of the molybdenum matrix is characterized by a matrix coefficient (in percent), equal to the ratio of the specific surface of the boundaries between UO_2 particles occupied by molybdenum to the specific surface of all the boundaries. If the particle dimensions are −315 + 200 μ, the matrix coefficient for 5, 10, 15, and 20 vol. % molybdenum in cermet 1 was 92, 97, 99, and 100%, and in cermet 2 it was 68, 78, 84, and 90%, respectively. It increased with increasing particle diameter. As a result of tests for cermet 1 in a vacuum of $6 \cdot 10^{-5}$ mm Hg at 2390 and 2270°K for 10 and 120 h, respectively, the matrix coefficient did not decrease.

The thermal conductivity was measured by the method of the radial thermal flux in samples with uniform volume heat release for a steady-state thermal regime in the temperature range 1300-2200°K. The samples were heated by direct passage of an electric current of industrial frequency in a vacuum $\sim 1 \cdot 10^{-4}$ mm Hg. The temperature was measured with an optical pyrometer. In addition to the thermal conductivity, we also measured the electrical conductivity. The calculation error for a single measurement of the coefficient of thermal conductivity was ±21%; for the electrical conductivity it was ±4.6%. Experimental values were converted to zero porosity. It was determined that for cermets with particle diameter − 315 + 200 μ the thermal-conductivity coefficient λ and the electrical conductivity σ are described by the following equations:

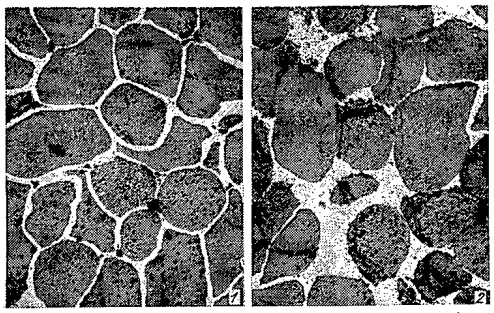

Fig. 1. Cermets with 15 vol. % molybdenum and uranium-dioxide particle diameter −315 + 200 μ: 1) cermet of coated particles; 2) cermet of the mixture.

for the cermet 1

$$\lambda = \lambda_{Mo}\left(1+\frac{v_{UO_2}}{\frac{1-v_{UO_2}}{3}+\frac{\lambda_{Mo}}{\lambda_{UO_2}-\lambda_{Mo}}}\right)$$

(the equation of V. N. Odelevskii);

Original article submitted July 12, 1973.

$$\sigma^{0.65} = v_{Mo}\sigma_{Mo}^{0.65};$$

for cermet 2

$$\lambda^{0.50} = v_{Mo}\lambda_{Mo}^{0.50} + v_{UO_2}\lambda_{UO_2}^{0.50};$$
$$\sigma^{0.52} = v_{Mo}\sigma_{Mo}^{0.52},$$

where v is the fractional volume concentration.

The conductivity increases with decreasing dimension of UO_2 particles. At 2200°K the thermal conductivity of cermet 1 with particles −315 + 200 μ is 30%, and the electrical conductivity is 40%, greater than for the cermet with particles −1190 + 1000 μ. This is presumably explained by the presence in the surface layer of UO_2 particles of the interaction products with molybdenum. The relation between thermal conductivity, electrical conductivity, and temperature is optimally described by the equation $\lambda = 5.20 + 3.44 \cdot 10^{-8} \sigma T$ (here λ is in W/(m·deg), σ is in $\Omega^{-1} \cdot m^{-1}$, and T is in °K). Independently of the composition, the dimensions of particles of uranium dioxide, and the type of cermet, with the calculation made according to this formula with probability 91% error, the determinations of λ according to this value of σ does not exceed ±21%. The known literature values are in agreement in this region.

TRANSMISSION OF GAMMA-RADIATION THROUGH TWO-SECTION CHANNELS WITH RECTANGULAR CROSS SECTION IN A CONCRETE SHIELDING

S. A. Erin and A. V. Larichev

UDC 539.122:621.039.538

A well known method of calculating the transmission of γ radiation through two-section channels in a shielding made of concrete is based upon the differential albedo concept. However, in the transition to multi-section channels, certain difficulties are encountered when this method is used.

Another approach to the solution of the problem is based upon the well-known empirical formula

$$P(L_2)/P(L_2 = 0) = CL_2^{-k}, \quad (1)$$

where $P(L_2)$ and $P(L_2 = 0)$ denote the γ-radiation dose on the axis of the second channel section and at the crossover point of the axes of the two sections, respectively; $L_2 = l_2/W_2$ is a parameter which characterizes the axial coordinates of the detector situated in the second section at a distance l_2 from the intersection point of the axes; W_2 denotes the width of the second section of the channel; and C and k denote empirical constants which depend upon the dimensions of the channel and the energy (E_γ) of the γ quanta of the source.

The transmission of γ radiation from pointlike isotropic ^{198}Au, ^{137}Cs, and ^{60}Co sources has been studied on a model of a two-section channel bent at a right angle and situated in a concrete shield.

It is convenient to split the total characteristic of the radiation field into two components at the point under consideration:

$$P(L_2) = P^{refl}(L_2) + P^{angl}(L_2), \quad (2)$$

where $P^{refl}(L_2)$ and $P^{angl}(L_2)$ denote the doses in the second section due to reflection of radiation which entered into the channel and is reflected from the walls and due to radiation passing through the angular projection, respectively. It was observed that the $P^{refl}(L_2)$ component obeys Eq. (1); the experimental data were used to determine for this component the C and k values for which simple empirical relationships were assumed. It was observed that k is practically independent of the energy of the γ quanta and is given by the ratio of the width of the first channel section to its height:

Original article submitted July 30, 1973.

$$k = 2 + 0.43 \frac{W_1}{H} \quad \text{for} \quad 0.17 \leqslant \frac{W_1}{H} \leqslant 1.70. \tag{3}$$

In the case of channels with quadratic cross section, C depends only upon E_γ and L_1 ($L_1 = l_1/W_1$ is a parameter which characterizes the axial coordinates of the source); we obtained for $C(E_\gamma, L_1)$ within a limited variability range

$$C(E_\gamma, L_1) = 10^{-2}(5.8 - 0.45 L_1) E_\gamma^{-(0.74 - 0.4 \lg L_1)} \tag{4}$$

for $0.2 \leq E_\gamma \leq 3.0$ MeV and $1.5 \leq L_1 \leq 6.0$.

A relationship of the form

$$P^{\text{refl}}(L_2)/P^{\text{angl}}(L_2) = B(bL_1 + X) - a, \tag{5}$$

was established for the components $P^{\text{refl}}(L_2)$ and $P^{\text{angl}}(L_2)$. Empirical formulas, which are valid within a wide variability range of E_γ and the dimensions of the channel were used for the coefficients. The proposed method of determining C, k, and $P^{\text{angl}}(L_2)$ can be extended to channels in other shielding materials and to multi-section channels, because it follows from an analysis of the published data that Eq. (1) holds for a large number of cross sections.

LETTERS TO THE EDITOR

RADIOACTIVITY OF DEPOSITS IN LOOP OF VK-50 REACTOR POWER STATION MEASURED WITHOUT SAMPLING

V. D. Kizin, V. I. Polyakov, and Yu. V. Chechetkin

UDC 621.039.524.4-97: 621.039.553

Mass transfer of radioactive isotopes through loops of reactor facilities is of practical interest from the vantage point of radiation safety in the operation of nuclear power stations. Experimental investigations of the activity in deposits on process piping and equipment, with the object of verifying different models and methods for activity calculations, are restricted by difficulties in sampling the deposits. Earlier investigations [1] on results of measurements of smears, scrapings, and coupons taken from equipment that had been disassembled or opened up still could not yield a complete picture of the radioactivity distribution over the entire loop.

We made use of scintillation γ-ray spectrometers with collimators extending 15 cm and 25 cm in length and 10 mm and 20 mm in diameter within a lead shielding arrangement that could be disassembled, in our measurements of specific radioactivity in deposits on piping throughout the loop (piping dimensions ϕ 194 $\times$ 15 mm; ϕ 219 $\times$ 12 mm; ϕ 426 $\times$ 13 mm, etc.). The spectrometric sensors in the shielding were placed right up against the piping or at a distance of 5 meters away, and the pulse height analyzer was positioned at a distance of 70 meters away from the sensor. The absolute radioactivity per unit piping or equipment surface area was determined on the basis of approximate formulas derived elsewhere [2].

Comparison of investigative techniques was carried out on the piping of the drainage system serving the high-pressure separator. Coupons were cut from piping and sample smears were taken for the comparison, following sampling-free analysis of the activity of the deposits on the piping. Results of radioactivity measurements taken on the coupons were found to be in close agreement with the sampling-free measurements at the same points (the greatest discrepancy found was 23%). At the same time, results obtained from analysis of smears taken from the piping ran a little too low. The smear ratio in these experiments ranged from 0.5 to 0.96. It was pointed out that the specific activity in the deposits varied 26-fold (isotope ^{65}Zn) over a small section of piping extending about one meter in length, or 16-fold in the case of isotopes ^{60}Co and ^{59}Fe. Consequently, the results can turn out either too high or too low, in analysis based on the standard procedure of measurements adopted in cases of the sort, with sample smears taken at the same point, with the results obtained extended to a larger stretch of piping.

The measurements performed showed that the amount of specific activity of the isotopes in surface deposits on different portions of the loop differed anywhere from 10^2-fold to 10^4-fold. The radioactivity of the isotope ^{65}Zn was decisive over all portions of the loop. The specific activity of this isotope in the deposits on steam lines upstream of the high-pressure and low-pressure separators, the turbine, and the feedwater pump, were respectively: $1.8 \cdot 10^{-2}$, $2.3 \cdot 10^{-3}$, $1.4 \cdot 10^{-4}$, $0.6 \cdot 10^{-5}$ Ci/m^2. The radioactivity of ^{59}Fe, ^{60}Co, and ^{54}Mn in the deposits was anywhere from 1/50 to 1/3 the level of ^{65}Zn radioactivity, while the radioactivity of isotopes originating in fission fragments was 10^2 to 10^3 times smaller.

The results of a sampleless analysis supplemented the overall distribution pattern of the radioactivity in the deposits [1]. These results can be used to check on the several computational procedures, and they are also useful in estimating the total amount of radioactivity in the deposits on the surfaces of the nuclear power station process loop. For example, despite the small fraction of surface area (~5% of the loop surface area), over 90% of all of the radioactivity at a VK-50 reactor nuclear power station is concentrated on the area extending from the reactor to the throttle check valve (and including the high-pressure separator): ~6.6 Ci ^{65}Zn; 0.22 Ci ^{59}Fe, ^{60}Co, and ^{54}Mn; and 0.07 Ci ^{144}Ce, ^{137}Cs, and ^{140}Ba.

Translated from Atomnaya Énergiya, Vol. 36, No. 2, p. 138, February, 1974. Original article submitted January 3, 1973.

We find concentrated in the condenser of the turbine (accounting for ~66% of the loop surface area) 0.33 Ci ^{65}Zn, 0.06 Ci of other corrosion elements, and less than 0.01 Ci fission products. The contribution of radioactivity in the deposits found on all of the remainder of the loop, with the exception of the reactor itself, is ~3%.

Consequently, when investigating the distribution, transport, and buildup of radioactivity in the loops of reactor installations, the sampleless γ-ray spectrometric analysis method can serve as an important back-up research tool which aids greatly in many instances in enhancing the accuracy, representativeness, and updatability of the analysis. Hence, the method can be used to estimate, with accuracy sufficient for practical purposes, the amount of radioactivity in deposits on different portions of the loop, to study the behavior of the radioisotopes under varying sets of process conditions, and to ascertain the radioactivity of short-lived isotopes present.

One clear disadvantage of the method is difficulty in interpreting the complicated γ-ray spectra (e.g., the fact that the activity of ^{60}Co and ^{59}Fe cannot be determined separately in this method). But this disadvantage can be gotten around if we use a Ge(Li)-detector in shielding with a collimator when taking our sampleless measurements.

LITERATURE CITED

1. L. N. Rozhdestvenskaya et al., At. Énerg., 30, 122 (1971).
2. V. I. Polyakov and Yu. V. Chechetkin, At. Énerg., 31, 139 (1971).

DEPENDENCE OF RATE OF SPUTTERING BY FISSION FRAGMENTS ON SPUTTERED-LAYER THICKNESS

B. M. Aleksandrov, N. V. Babadzhanyants,
I. A. Baranov, A. S. Krivokhatskii,
L. M. Krizhanskii, and G. A. Tutin

UDC 546.799

One can prepare thin, fine-grained spectrometric sources from ^{252}Cf [1, 2] and other transuranic elements [3] by sputtering matter using fission fragments. It is important to know the optimal sputtered-layer thickness at which the rate of sputtering by fission fragments is maximal. Thus, this dependence of sputtering rate on layer thickness was studied. Moreover, the role of α decay in self-sputtering of layers containing α-emitting isotopes was clarified. Obtaining such data and comparing them with energy losses by heavy charged particles in matter can aid in explaining the sputtering mechanism.

The layers studied were prepared by electrolysis, the most economical and common method for preparing primary layers. Either ^{241}Am or ^{238}Pu in hydroxide form was deposited on thick titanium backings, with subsequent air drying. The active-spot diameter was 9 mm. Four groups of primary layers were prepared with 10-12 sources per group. There was one group of ^{241}Am sources with mean thickness of each layer with respect to Am from 0.5 to 160 $\mu g/cm^2$ and three groups of ^{238}Pu with mean thickness with respect to Pu from 0.2 to 20-30 $\mu g/cm^2$. Americium- or plutonium-layer sputtering was produced by fission fragments from a thin ^{252}Cf source passing through a collimator so that the fragments were normally incident on the sputtered surface [2]; the air pressure was 10^{-5} torr. Collectors made of transparent nickel films (film thickness ~ 90 $\mu g/cm^2$) were placed between the fragment source and the sputtered layer, at a distance of 1 mm from the latter. Between the collector and source there was another thin nickel film for shielding. The sputtered-layer thicknesses, and also the quantity of Am or Pu atoms transferred to the collectors, were determined from their α activity in an α gun or 4π gaseous counter. Spectral purity was monitored on a semiconductor α spectrometer.

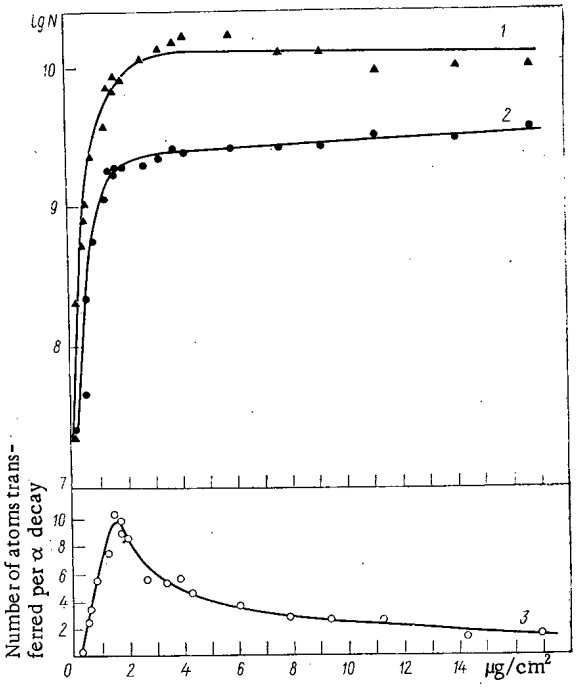

Fig. 1. Dependence of quantity of ^{238}Pu atoms collected during sputtering on the layer thickness: 1) 10-min sputtering by fission fragments; 2) 10-min self-sputtering; 3) calculated for one α decay of layer.

Before sputtering the prepared surfaces using fission fragments, we determined experimentally the quantity of atoms sputtered in vacuum from each layer's surface as a result of Am or Pu α decay, i.e., due to their own α particles ($E \approx 5.5$ MeV) and recoil nuclei ($E \approx 90$ keV). Measurement data for one plutonium group are shown in Fig. 1 (curves 2 and 3). Data for other Am and Pu groups are similar. We found that as the layer thickness and, consequently, the number of α decays in it, increases, the layer-sputtering rate (curve 2) and the quantity of atoms sputtered due to one α decay in the layer (curve 3) increase rapidly up to

Translated from Atomnaya Énergiya, Vol. 36, No. 2, pp. 139-140, February, 1974. Original article submitted March 6, 1973; revision submitted September 6, 1973.

thickness 1.5-2 $\mu g/cm^2$, reaching 10 atoms per α decay. Subsequently, the sputtering rate increases very slowly and the quantity of atoms sputtered per α decay decreases. To clarify the role of α particles and recoil nuclei in self-sputtering of matter, we irradiated three Pu layers having thickness 0.8, 1.3, and 5.6 $\mu g/cm^2$ ($1.0 \cdot 10^7$, $1.6 \cdot 10^7$, and $7.0 \cdot 10^7$ α decays per min) with only α particles from the same external ^{238}Pu source. The number of α particles incident on each layer from the external source was $1.5 \cdot 10^8$ per min. Recoil nuclei from this source were stopped by the nickel shielding film and did not reach the sputtered layer. The dispersed atoms were collected at another nickel film located between the sputtered layer and the shielding film. We found that irradiating the layers with a flux of α particles up to 15 times more intense than the intrinsic α-particle flux intersecting the surface does not increase the number of atoms collected. Consequently, the fundamental role in self-sputtering of thin layers in which α decay occurs is played not by α particles, but by recoil nuclei; their sputtering ratio is significantly greater than that for α particles. However, the mean free path in matter for heavy recoil nuclei having energies ~ 90 keV is several orders smaller than that for α particles having energies 5.5 MeV. Therefore, as layer thicknesses are increased, recoil nuclei at greater depths in the layers will not participate in sputtering of matter from the surface. This can explain the falloff in curve 3 (Fig. 1) at layer thicknesses greater than 2 $\mu g/cm^2$.

On irradiating Am and Pu layers with fission fragments from an external source, we subtracted from the overall number of atoms collected at the collector those atoms transferred by α decay in the layers. The results of sputtering layers only by fission fragments, converted to a 10-min collection, are shown by curve 1. The fragment flux to each layer over 10 min was $1.7 \cdot 10^7$. The average sputtering ratio with layer thicknesses 2-4 $\mu g/cm^2$ and greater is 500 and 750 atoms per fragment for Am and Pu, respectively. Here, the average deviation from the mean value in this region is 30%, while individual values differ from the mean by a factor of 2 in both directions.

DISCUSSION

The data on self-sputtering of thin ^{241}Am and ^{238}Pu layers are evidence that the fundamental role in sputtering matter is played by those ^{237}Np and ^{234}U recoil nuclei formed as a result of α decay in these layers at depths no greater than a few $\mu g/cm^2$ from the surface.

The small and approximately equal values of the average layer thicknesses at which the rates of sputtering by recoil nuclei and fission fragments reach saturation, show that sputtering of matter proceeds from the surface in both cases, while the data spread is apparently related to the surface structure of these layers, particularly to their granularity. However, we must note that the sputtering ratios for the same layers differ significantly (~ 10 atoms per recoil nucleus and $\sim 10^3$ atoms per fragment), which probably indicates that the mechanisms of sputtering by these particles are different. Actually, heavy recoil nuclei have energy ~ 90 keV and sputter matter due to a mechanism based on elastic collisions with the atoms of the substance [4]. Fission fragments have kinetic energy 90 MeV and at the start of their path (the case we are examining) they expend on elastic collisions tenths of a percent of the energy which goes to ionizing the atoms of the substance. Calculations made in accordance with [5, 6] show that in a Pu layer 2 $\mu g/cm^2$ thick a recoil nucleus will lose several keV to elastic collisions; a fission fragment will lose less than 1 keV, while sputtering 100 times more atoms than the recoil nucleus. We should note that to sputter 1000 atoms, one must expend no less than several keV energy to overcome these atoms' binding force alone; this is significantly more energy than fission fragments expend on elastic collisions in a Pu layer 2 $\mu g/cm^2$ thick. The assumption remains that this energy is transferred to the atoms of the substance from fission fragments to a smaller degree through elastic collisions and to a larger degree through ionization of the substance's atoms; the losses to this for fission fragments in such a layer are several tens of keV. It has previously been remarked [2] that the basic mechanism, related to ionization losses, for sputtering of matter by fission fragments could be either an ion burst or a thermal electron "peak," at least for the first third of the path. In the latter case, possibly, it would be sufficient to take into account only δ electrons arising with low energies, but with large cross section. We should note that the primary-source layer thickness (2-4 $\mu g/cm^2$) is optimal when the secondary sources are produced through sputtering the substance by fission fragments, since the sputtering ratio does not increase with further increase in the layer thickness. One cannot, using the method surveyed, prepare layers thicker than 1.5-2 $\mu g/cm^2$ (if the fragment flux is incident on the layer and the collector) due to reverse sputtering of the substance by fission fragments from the collector and equilization of the direct and reverse sputtering rates.

In conclusion, the authors thank V. A. Yakovlev, V. A. Knyazev, V. E. Ulanov, V. V. Obnorskii, and G. V. Solov'ev for their assistance.

LITERATURE CITED

1. S. Pauker and N. Steiger-Sfafrir, Nucl. Instr. and Meth., 91, No. 4, 557 (1971).
2. B. M. Aleksandrov et al., At. Énerg., 33, No. 4, 821 (1972).
3. B. M. Aleksandrov et al., Theses of the XXII Conference on Nuclear Spectroscopy and Nuclear Structure [in Russian], Nauka, Leningrad (1972), p. 278.
4. M. Thompson, Defects and Radiation Damage in Metals [Russian translation], Mir, Moscow (1971).
5. N. Bohr, Passage of Atomic Particles Through Matter [Russian translation], IL, Moscow (1950).
6. J. Lindhard, Mat.-Fys. Medd. Kgl. Danske. Vid. Selskab, 33, No. 14, 1-40 (1963).

SOME CHARACTERISTICS OF OPTIMAL TRANSIENT PROCESSES WITH A CONSTRAINT ON THE RATE OF VARIATION OF REACTOR POWER

T. S. Zaritskaya and A. P. Rudik

UDC 621.039.514:621.039.516.232

The theory of the optimization of xenon and samarium transient processes in nuclear reactors has been investigated in detail in many works [1, 2]. A significant simplification in all these works was the assumption that it is possible for the reactor power to vary in a jump. We have investigated xenon and samarium transient processes taking account of constraints on the rate of variation of reactor power by the method of the Pontryagin maximum principle [3]. The following results were obtained.

Nature of the Variation of Control. The typical form of an optimal control in problems without a constraint on the rate of variation of power, when by a control we mean the reactor power W itself, is characterized by the following three stages: the first stage $0 \le t \le t_1$, $W(t) = 0$; the second stage $t_1 \le t \le t_2$, $W(t) = W_m(t)$, where $W_m(t)$ is a given function of time that ensures maximum permissible concentration of the isotope that strongly absorbs neutrons; the third stage $t_2 \le t \le T$, $W(t) = W_{max}$, where W_{max} is the maximum permissible reactor power, T is the end of the optimization period, which is not given. As can be seen, in these problems there are four jumps in power: at $t = 0$ [from $W_{sta}(t < 0)$ to $W(t > 0) = 0$], $t = t_1$ and $t = t_2$, and also at $t = T$, when the reactor is converted from $W_{max}(t < T)$ to $W_{max}(t > T) = \text{const}$.

It is shown that in similarly formulated optimization problems with constraints on dW/dt the nature of the optimal control is varied in the following way: instead of a three-stage control, a seven-stage control is optimal – at each point of the discontinuity in W(t) a section with maximum permissible dW/dt of the necessary sign is introduced.

Figure 1 shows the simplest example of an optimal transient samarium process, when there are no constraints on the samarium concentration. The phase plane of the promethium–samarium concentration is shown*; it is required that the reactor be shifted, after minimum time, from point a to point $\tilde{a}$, and then at point a a stationary power corresponding to it must be established. The trajectory $ab\tilde{a}$ corresponds to the case without constraints on dW/dt: first stage ab–$W(t) = 0$; second stage $b\tilde{a}$–$W(t) = W_{max}$. The trajectory $a1234\tilde{a}$ corresponds to the case with a constraint on dW/dt: first stage $a1$–$\max(-dW/dt)$; second stage 12–$W(t) = 0$; third stage 23–$\max(dW/dt)$; fourth stage 34–$W(t) = W_{max}$; fifth stage $4\tilde{a}$–$\max(dW/dt)$.

Although the trajectory $a1234\tilde{a}$ is within $ab\tilde{a}$, the time for conversion of the reactor is greater along the first trajectory than along the second one.

Nature of Approach to Point $\tilde{a}$. In problems without constraints on dW/dt the trajectory on the promethium–samarium phase plane always approaches the equilibrium point $\tilde{a}$ from above. In similar problems with a constraint on dW/dt the approach to point $\tilde{a}$ depends on the magnitude of $\max(-dW/dt)$ and the value of $W(t > T)$. Figure 2 shows the trajectory on the section $4\tilde{a}$ for the same value of $\max(-dW/dt)$, but for different values of $W(t > T)$.

* The promethium–samarium concentration is normalized to the ratio σ/γ, where σ is the neutron absorption cross section in samarium; γ is the yield of promethium for a single fission.

Translated from Atomnaya Énergiya, Vol. 36, No. 2, pp. 140-141, February, 1974. Original article submitted April 11, 1973.

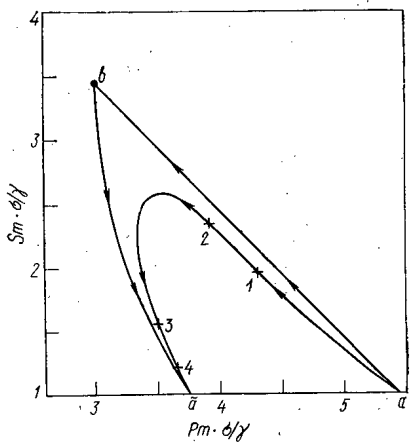

Fig. 1

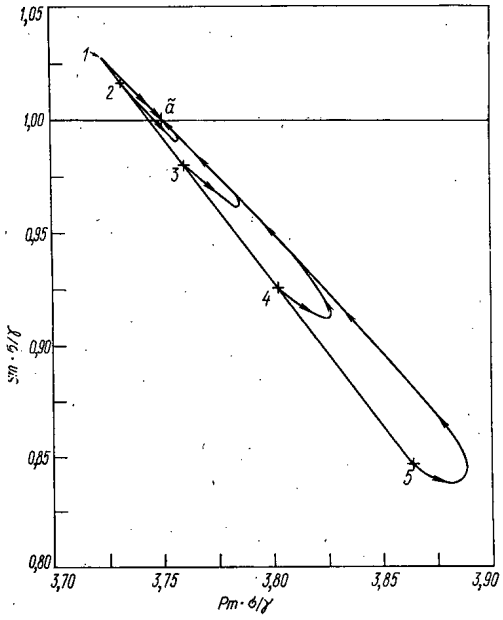

Fig. 2

Fig. 1. Comparison of optimal trajectories: $ab\tilde{a}$) without constraints on dW/dt; $a1234\tilde{a}$) with constraints on dW/dt.

Fig. 2. Approach of optimal trajectories to point $\tilde{a}$. Trajectories $1\tilde{a}$, $2\tilde{a}$, . . . , $5\tilde{a}$ correspond to powers $W_{sta}(\tilde{a})$, 0.75 $W_{sta}(\tilde{a})$, 0.5 $W_{sta}(\tilde{a})$, 0.25 $W_{sta}(\tilde{a})$, and W = 0, respectively.

In conclusion we should note that the existence of constraints on dW/dt for certain cases can lead to additional complications in the optimal-control process, in particular, when the transition time T is given.

LITERATURE CITED

1. M. Ash, Optimal Shutdown Control of Nuclear Reactors, Academic Press, New York (1966).
2. A. P. Rudik, Nuclear Reactors and the Pontryagin Maximum Principle [in Russian], Atomizdat, Moscow (1971).
3. L. S. Pontryagin et al., The Mathematical Theory of Optimal Processes, John Wiley (1962).

REALITY OF THE EIGENVALUES OF REACTOR BOUNDARY VALUE PROBLEMS IN THE MULTIGROUP DIFFUSION APPROXIMATION

B. D. Abramov

UDC 621.039.51.134

In [1, 2] there is posed the problem of calculating several eigenvalues α and several eigenfunctions Ψ of reactor boundary value problems in the multigroup diffusion approximation of the nonstationary neutron transport equation, i.e., boundary value problems for the differential equation

$$\alpha V^{-1}\Psi - \operatorname{div} D \operatorname{grad} \Psi + (\Sigma - \Sigma_s)\Psi = \chi(\nu\Sigma_f)\Psi, \tag{1}$$

where V, D, and Σ are diagonal matrices of the average group velocities, the diffusion coefficients, and the total cross sections respectively; Σ_S is a matrix describing transitions due to scattering processes; χ is a column vector, i.e., the normalized fission spectrum, $\nu\Sigma_f$ is a row vector whose components are the fission cross sections [3]. All the matrices are real and piecewise-constant with respect to coordinates. Solutions of Eq. (1) are sought in the class of functions satisfying certain continuity conditions in G (where G is the bounded region of m-dimensional ($m \leq 3$) Euclidean space occupied by the reactor) and a boundary condition on the outer surface of the reactor of the form [1, 3, 4]

$$\Psi + 2D\frac{\partial\Psi}{\partial n}\Big|_S = 0. \tag{2}$$

Eigenvalues and eigenfunctions are sometimes [2] calculated numerically by algorithms based on the assumption that the eigenvalues being calculated are simple and real. We show that such an assumption is not always valid, so that a further development of algorithms for calculating further complex conjugate and multiple eigenvalues becomes necessary. We present an example of a special kind of boundary value problem, some of whose eigenvalues can be complex and multiple.

We consider a boundary value problem for a homogeneous reactor [1, 2]. We assume that G is a uniform region so that the cross sections do not depend on the coordinates, and the boundary condition on the piecewise-continuous surface S of volume G is taken in the form

$$\Psi + \beta\frac{\partial\Psi}{\partial n}\Big|_S = 0, \tag{3}$$

where $\beta \geq 0$ is a number and not a matrix as in Eq. (2). Each component $\Psi^{(j)}(x)$ (where $j = 1, 2, \ldots, n$; n is the number of energy groups and $x = \{x_1, x_2, \ldots, x_m\}$) of the vector function $\Psi(x)$ can be expanded in a Fourier series regularly convergent in G [1, 4] in terms of the orthonormal set of eigenfunctions $u_k(x)$ of the Laplacian operator ∇^2, complete in $L^2(G)$, with the boundary condition (3), such that

$$-\nabla^2 u_k = \mu_k u_k, \quad \mu_k > 0, \quad k = 1, 2, \ldots, \tag{4}$$

i.e., we can write

$$\Psi(x) = \sum_{k=1}^{\infty} f_k u_k(x). \tag{5}$$

The vectors f_k, the expansion coefficients in (5), are determined from the equations

$$\alpha f_k = (B_k + XY) f_k, \quad k = 1, 2, \ldots, \tag{6}$$

Translated from Atomnaya Énergiya, Vol. 36, No. 2, p. 142, February, 1974. Original article submitted May 10, 1973.

where

$$B_k = -V(\mu_k D + \Sigma - \Sigma_s),\ X = V\chi,\ Y = \nu\Sigma_f. \tag{7}$$

Thus the eigenvalues of the boundary value problem for a given k are the eigenvalues of the matrix XY + B_k. We present a sufficient condition for the reality of all the eigenvalues α.

THEOREM. Suppose the eigenvalues of the matrix B_k are simple and real and for each $\varepsilon \in (0, 1]$ the roots $\alpha(\varepsilon)$ of the equation $\{1-\varepsilon[Y, (\alpha-B_k)^{-1}X]\}\det(\alpha-B_k) = 0$ are simple, i.e., $[Y, (\alpha-B_k)^{-2}X] \neq 0$. Then the eigenvalues of the matrix XY + B_k are real. Here $(a, b) = \sum_{i=1}^{n} a_i b_i$.

We cite an example with complex eigenvalues. Let n = 3 and (cf. Eqs. (6) and (7))

$$B_k = \begin{pmatrix} -b_k & 0 & 0 \\ b_{21} & -b_k & 0 \\ 0 & b_{32} & -b_k \end{pmatrix};\quad XY = \begin{pmatrix} 0 & 0 & c \\ 0 & 0 & 0 \\ 0 & 0 & 0 \end{pmatrix}. \tag{8}$$

The matrix $B_k - XY$ has one real and two complex conjugate values of α.

Therefore special types of boundary value problems can have complex eigenvalues.

LITERATURE CITED

1. G. J. Habetler and M. A. Martino, in: Nuclear Reactor Theory, (G. Birkhoff and E. Wigner, editors), Am. Math. Soc., Providence (1961).
2. B. I. Kolosov, in: Theoretical and Experimental Problems of Nonstationary Neutron Transport [in Russian], (V. V. Orlov and É. A. Stumbur, editors), Atomizdat, Moscow (1972), p. 166.
3. G. I. Marchuk, Methods of Calculating Nuclear Reactors [in Russian], Gosatomizdat, Moscow (1961).
4. V. S. Vladimirov, Equations of Mathematical Physics [in Russian], Nauka, Moscow (1971).

MOMENTS OF THE MODERATION FUNCTION AND ITS FEW-GROUP MODELS FOR WATER – METAL MIXTURES

E. A. Garusov and Yu. V. Petrov

UDC 621.039.51.13

The applicability of the diffusion approximation to the description of slowing-down of neutrons in water–aluminum reactor cores has been discussed in earlier articles [1, 2]. In the case of pure ordinary water, the diffusion approximation leads to serious errors in calculations of neutron leakage from small zones. As the aluminum fraction is increased, reliance on the diffusion approximation becomes feasible, and the number of energy groups into which the moderation interval can be broken down increases concomitantly. This article discusses application of these results to other water–metal mixtures.

In order for the optimum small-group computational model to yield the correct value of neutron leakage from the reactor core, it would have to do a good job of reproducing the moderation function in response to fairly modest changes in the sources of fast neutrons. This would require, at least, that the model

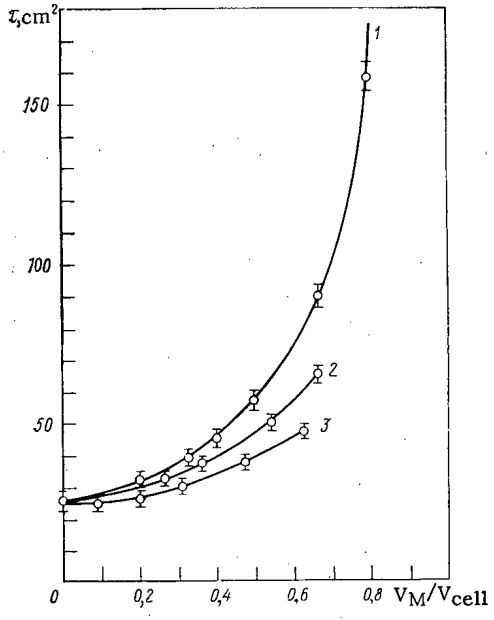

Fig. 1

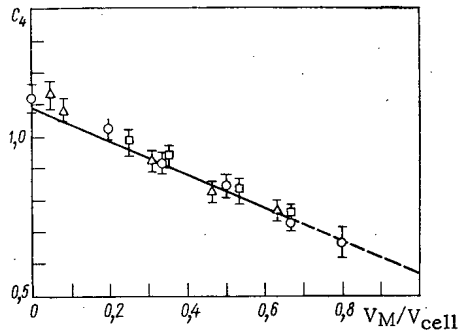

Fig. 2

Fig. 1. Dependence of age τ of fission neutrons slowed down to 1.44 eV on volume fraction of metal in mixtures of H_2O and aluminum (1), zirconium (2), and iron (3).

Fig. 2. Dependence of the coefficient C_4 on the volume fraction of the metal in the mixtures of H_2O and aluminum (○), iron (Δ), and zirconium (□). The data points indicate the weighted-average "experimental values," the continuous line is drawn through those points using the method of least squares, and the dashed line applies to extrapolated values; the top (leftmost) point applies to pure water.

Translated from Atomnaya Énergiya, Vol. 36, No. 2, pp. 143-144, February, 1974. Original article submitted June 11, 1973.

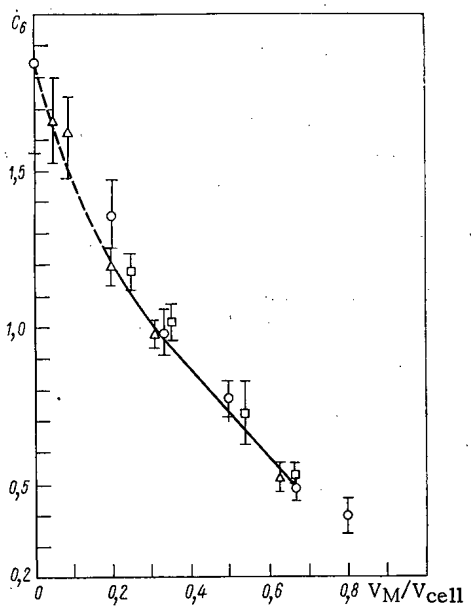

Fig. 3. Dependence of the coefficient C_6 on the volume fraction of metal in the mixture of H_2O with aluminum, iron, and water (explanations and notation as in Fig. 2).

yield the value of the Fourier transform of the moderation function at not very large $B^2\tau$ values, where B^2 is the geometrical shape factor; τ is the neutron age. When $B^2\tau \leq 1$, the Fourier transform can be expanded in a series in powers of $(-B^2\tau)$, and the dimensionless coefficients of the expansion

$$C_{2m} \equiv \frac{\langle r^{2m} \rangle}{(2m+1)!\,\tau^m}$$

are expressible in terms of the moments $\langle r^{2m} \rangle$ of the moderation function; these moments are determined experimentally.

Figures 1-3 present experimental values of τ, C_4, and C_6 as functions of the volume fraction of the metal (aluminum, iron, zirconium) in a mixture with H_2O. These values were obtained by processing the experimental results on slowing down of ^{235}U fission neutrons to the energy of the indium resonance (1.44 eV) in an infinite medium. The iron data and zirconium data include some slight heterogeneous effects due to anisotropy and resulting from the finite thickness of the metallic plates. The aluminum data are reduced to zero plate thickness. The $\langle r^{2m} \rangle$ values were first normalized to τ proper when the mean values of C_4 and C_6 in different experiments were calculated, and were then averaged with weight corresponding to experimental error. In the case of iron and zirconium, we used experimental data reported in [3, 4], as well as results of Monte Carlo calculations [5, 6]. Aluminum data are also reported in [2], where the reader will also find the averaging procedure detailed.

It is clear from Fig. 2 and Fig. 3 that the dimensionless coefficients C_4 and C_6 depend solely on the volume fraction of water in the cell, and are independent of the type of metal in question within the limits of experimental error. Nevertheless, the dimensionless constant τ depends substantially on the properties of the metal (see Fig. 1). The coefficient C_4 is a linear function with the same degree of exactness, of the fraction of metal in the cell: V_M/V_{cell}. The dependence of C_6 on the ratio V_M/V_{cell} is not explicitly nonlinear in nature, however, although it can be linearized in the range $1/3 \leq V_M/V_{cell} \leq 2/3$.

Any theoretical model designed for calculations of critical masses in reactor cores of comparatively modest dimensions must reproduce the values of τ, C_4, and C_6. The expression for C_{2m} in the diffusion approximation is cited in [2], as a function of the number of groups, the width of the energy interval, and the spectrum of the source. It is clear from Fig. 2 and Fig. 3 that when the ratio $V_M/V_{cell} < C_6/3 > C_4 > C_2 = 1$ (for pure ordinary water $C_4 = 1.13 \pm 0.03$; $C_6 = 1.85 \pm 0.26$; $C_8 \approx 3$), i.e., the C_{2m} values increase with increasing m, which contradicts the applicability conditions for the diffusion approximation [2]. In the neighborhood of the point $V_M/V_{cell} \approx 1/3$, we can resort to the one-group diffusion model of slowing-down ($C_4, C_6 \approx 1$). In the interval $1/3 < V_M/V_{cell} \leq 2/3$, which is typical of most research reactors with a highly developed heat-transfer surface (e.g., the VVR-M and SM-2 reactors), the C_4 and C_6 values are less than unity and occur in the ranges $0.75 \leqslant C_4 \leqslant 1$; $0.5 \leqslant C_6 \leqslant 1$. It is clear from an earlier article [2] that these values can be reproduced by the few-group models (e.g., the two-group model). Nondiffusion corrections have to be taken into account in this interval in the conversion to many energy groups. When the ratio $V_M/V_{cell} > 2/3$, C_4 and C_6 lie below that range, which is set by the two-group diffusion model, and the number of groups cannot be less than three.

In the case of pure metals ($V_M/V_{cell} = 1$), linear extrapolation of the straight lines in Fig. 2 and Fig. 3 yield close values of C_4 and C_6, but values somewhat larger than those obtained from Fermi age theory ($C_4 = 0.5$; $C_6 = 1/6$). This difference seems to stem from the nonmonoenergicity of the sources, the contribution of direct-incidence neutrons, and inelastic slowing-down. Data on other moderators yield similar results, in particular in processing of experimental data on slowing down of neutrons in graphite we obtain [7]: $\tau = (308 \pm 2)$ cm^2; $C_4 = 0.58 \pm 0.01$; $C_6 = 0.26 \pm 0.02$.

Some of the most commonly used computational programs fail to reproduce adequately the lower-order moments of the Fourier transform of the slowing-down function. For example, the three-group model of slowing-down for the MUFT-IV four-group diffusion program [8] yields C_4 and C_6 values which

differ markedly from the experimental values, particularly in the range of low concentrations of metal where the predicted values are well below unity. The τ values are computed quite accurately. Even though terms with the coefficients C_4 and C_6 occur with different signs in the power expansion of the Fourier transform, and errors are partially compensated, just the same the error in the critical mass due to the error in the approximations of the slowing-down function may amount to several percent in the case of real reactor cores.

The Fourier transform of the slowing-down function directly describes neutron leakage solely from bare reactors within the framework of the second Weinberg–Wigner theorem, which itself is approximate [1]. In order to calculate leakage from zones with real reflectors, we have to assign a major role not only to the successful choice of moderation model, but also to the statement of correct boundary conditions. Even though the effect of the reflector on the selection of moderation model in the core has not been given detailed study to date, design calculations of water–aluminum reactors with ordinary-water reflectors have shown that the few-group model reproducing experimental values of τ, C_4, and C_6 can be used in calculating critical mass to within 0.5% [2].

LITERATURE CITED

1. E. A. Garusov and Yu. V. Petrov, At. Énerg., 17, 375 (1964).
2. E. A. Garusov and Yu. V. Petrov, At. Énerg., 32, 225 (1972).
3. R. Paschall, Reactor Sci. and Tech., Parts A/B, 20, 25 (1966).
4. R. Paschall, Nucl. Sci. and Engng., 23, 256 (1965).
5. H. Alter, Reactor Sci. and Tech., Parts A/B, 20, 37 (1966).
6. H. Alter, Nucl. Sci. and Engng., 23, 264 (1965).
7. R. Campbell et al., Nucl. Sci. and Engng., 20, 445 (1964).
8. Reactor Physics Constants, ANL-5800, 2nd Edit. (1963).

INVESTIGATION OF THE RADIOACTIVITY OF THE ATMOSPHERIC LAYER CLOSE TO THE WATER IN THE ATLANTIC (JANUARY-APRIL, 1973)

A. S. Vinogradov, M. M. Domanov, P. N. Kodochigov, B. A. Nelepo, and A. G. Trusov

UDC 551.46:539.16

Up to the present time, global radioactive fallout is the most powerful, steady source of artificial radioactivity in our environment. After signing the Moscow Agreement on Partial Suspension of Nuclear Arms Testing, the radioactive contamination of the atmosphere was maintained by the activities of the countries which had not joined the agreement (People's Republic of China, France). The intensity of the source of atmospheric radioactivity is therefore nowadays still at the level of the end of the fifties. Maxima

TABLE 1. Concentrations of the Radioisotopes in the Atmospheric Layer Near the Water (January-April, 1973).

Date	Coordinates		Concentration of the radioisotopes (nCi/m³)·10⁻²			Date	Coordinates		Concentration of the radioisotopes (nCi/m³)·10⁻²		
	latitude	longitude	^{7}Be	^{137}Cs	^{144}Ce		latitude	longitude	^{7}Be	^{137}Cs	^{144}Ce
18/I	53°50′ N	06°30′ E	3,5	0,01	—	10/III	11°00′ N	75°40′ W	2,0	0,01	0,10
19/I	50°04′ "	01°42′ W	3,6	0,01	0,10	12/III	16°52′ "	79°30′ "	2,9	0,005	—
20/I	45°40′ "	07°40′ "	2,3	0,05	0,13	13/III	19°34′ "	80°27′ "	2,6	0,01	0,20
21/I	38°59′ "	11°11′ "	2,0	0,01	—	14/III	19°16′ "	80°25′ "	4,9	0,014	—
22/I	33°32′ "	13°04′ "	1,4	—	0,50	15/III	18°59′ "	80°16′ "	5,1	0,05	0,30
23/I	28°02′ "	15°21′ "	6,0	0,005	0,03	16/III	18°40′ "	80°20′ "	5,5	0,08	0,40
24/I	23°26′ "	20°28′ "	3,5	0,01	0,10	17/III	18°39′ "	80°28′ "	5,7	0,08	0,40
25/I	22°55′ "	27°57′ "	7,0	0,03	0,35	18/III	18°27′ "	80°27′ "	5,2	0,03	0,30
26/I	22°21′ "	34°50′ "	4,5	0,005	0,13	19/III	19°16′ "	80°40′ "	8,2	0,05	0,20
27/I	22°43′ "	42°14′ "	5,5	0,01	0,13	20/III	18°59′ "	80°29′ "	8,8	0,002	—
28/I	21°12′ "	49°27′ "	9,8	0,05	—	21/III	19°10′ "	80°27′ "	7,7	0,02	0,34
29/I	21°14′ "	56°46′ "	7,3	0,02	—	22/III	19°04′ "	80°29′ "	7,8	0,04	0,28
30/I	20°23′ "	62°55′ "	5,2	0,01	0,25	23/III	19°37′ "	76°50′ "	7,0	0,066	0,26
31/I	19°37′ "	67°29′ "	1,9	—	0,05	25/III	19°31′ "	76°40′ "	8,7	0,03	0,20
1/II	20°05′ "	68°22′ "	3,2	0,02	0,10	27/III	21°30′ "	81°29′ "	10,3	0,06	0,58
2/II	19°38′ "	67°39′ "	3,5	0,04	0,10	28/III	20°08′ "	84°30′ "	8,5	0,05	0,50
4/II	19°38′ "	67°39′ "	5,5	0,07	0,10	29/III	22°03′ "	87°56′ "	6,4	0,05	0,51
5/II	19°40′ "	67°42′ "	6,0	0,06	0,25	30/III	20°49′ "	92°00′ "	8,8	0,02	0,47
6/II	19°26′ "	67°51′ "	5,8	0,01	0,25	4/IV	23°22′ "	91°40′ "	10,0	0,06	0,35
7/II	19°16′ "	68°05′ "	5,3	—	0,22	5/IV	23°37′ "	92°25′ "	10,0	0,06	0,28
8/II	19°32′ "	68°27′ "	10,4	0,052	0,40	6/IV	23°05′ "	91°11′ "	10,7	0,06	0,29
9/II	19°35′ "	68°07′ "	8,1	0,04	0,50	7/IV	22°40′ "	89°30′ "	9,2	0,04	0,3
10/II	19°40′ "	68°10′ "	14,5	0,09	—	8/IV	22°50′ "	84°00′ "	17,0	0,15	0,94
11/II	17°11′ "	67°05′ "	9,7	0,07	0,40	9/IV	23°40′ "	82°05′ "	19,0	0,12	0,78
12/II	11°09′ "	65°20′ "	3,2	0,005	0,10	10/IV	23°40′ "	82°05′ "	15,0	0,10	0,60
18/II	13°06′ "	62°05′ "	5,6	0,03	0,41	11/IV	25°20′ "	75°00′ "	18,7	0,14	0,78
19/II	13°18′ "	61°59′ "	7,8	0,04	0,41	12/IV	25°55′ "	68°34′ "	28,7	0,19	1,20
20/II	13°04′ "	63°06′ "	8,9	0,04	0,47	13/IV	26°13′ "	61°09′ "	8,6	0,06	0,36
21/II	13°56′ "	65°25′ "	9,0	0,05	0,45	14/IV	26°23′ "	53°10′ "	5,8	0,03	—
22/II	14°12′ "	66°44′ "	5,0	0,02	—	15/IV	26°46′ "	46°14′ "	10,0	0,08	0,60
24/II	14°12′ "	66°44′ "	8,2	0,10	0,80	16/IV	26°59′ "	38°52′ "	11,9	0,08	0,36
25/II	11°49′ "	69°00′ "	2,2	0,02	0,08	17/IV	27°11′ "	31°47′ "	3,0	0,02	0,13
2/III	14°52′ "	73°49′ "	5,2	0,03	—	18/IV	27°30′ "	24°06′ "	9,5	0,09	0,42
3/III	14°59′ "	74°00′ "	5,9	0,02	0,13	19/IV	30°05′ "	19°07′ "	11,3	0,08	0,50
4/III	14°73′ "	73°32′ "	2,1	0,01	0,25	20/IV	32°57′ "	14°07′ "	13,8	0,05	0,50
5/III	14°73′ "	73°32′ "	1,8	0,005	—	21/IV	38°57′ "	12°17′ "	9,7	0,05	0,34
6/III	12°26′ "	81°43′ "	1,6	0,005	—	22/IV	44°05′ "	10°30′ "	9,8	0,04	—
7/III	12°15′ "	81°21′ "	1,9	0,01	0,13	23/IV	49°20′ "	9°03′ "	4,0	0,04	0,25
8/III	10°41′ "	76°25′ "	1,6	—	0,10	24/IV	53°24′ "	3°52′ E	3,5	0,03	0,27

Translated from Atomnaya Énergiya, Vol. 36, No. 2, pp. 145-147, February, 1974. Original article submitted October 3, 1973.

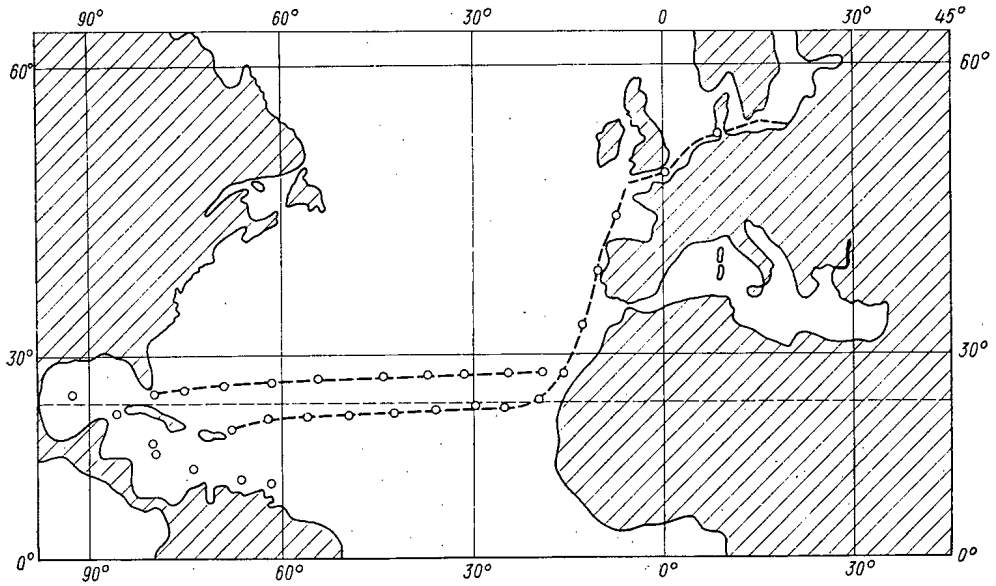

Fig. 1. Route of the 14th voyage of the scientific-research vessel "Akademik Kurchatov."

of radioactivity, which are related to tropospheric fallout after individual explosions set off by the nonmember countries to the agreement, are periodically produced and recorded. The radiation conditions in the Northern hemisphere are also influenced by the activities on the nuclear testing site of the People's Republic of China, whereas the test site of France on the Mururoa Atoll in the Pacific is the main source determining the radioactivity of the Southern hemisphere.

The present article describes the results of measurements of the radioactivity in the atmospheric layer close to the water; the measurements were made during the 14th voyage of the scientific-research vessel "Akademik Kurchatov" in the spring of 1973 (see Fig. 1).

Samples of atmospheric air were taken with an aspiration technique. A small air-blast of the ship with an air throughput of $31.5 \cdot 10^3$ m^3/day was employed. An FPP-15 filter was placed at the inlet of the air-blast. The exposure lasted for several days.

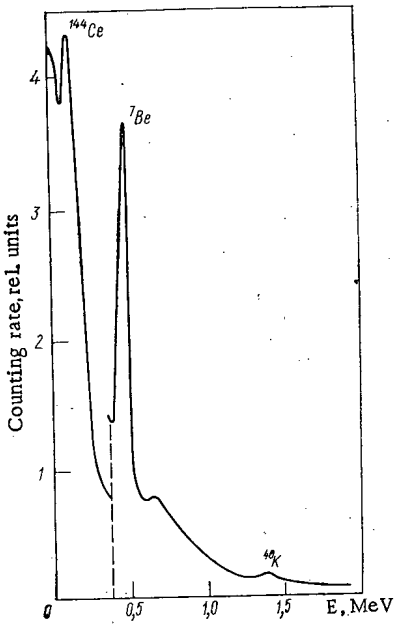

Fig. 2. Gamma-spectrum of atmospheric samples.

After exposure, the filters were burnt to ashes and weighed. The total radioactivity was determined with a low-background SBT-13 ring counter provided with a 3 cm thick lead shield. A PS-16 unit with a BTS-4 input block was used as the counter. The total background of the setup was 10 pulses/min.

The duration of the measurement on a sample depended upon the mean-square error (3%) and was determined with the formula

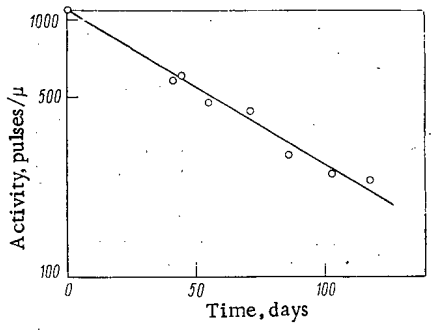

Fig. 3. Time dependence of the activity of the isotope with the energy ~0.5 MeV.

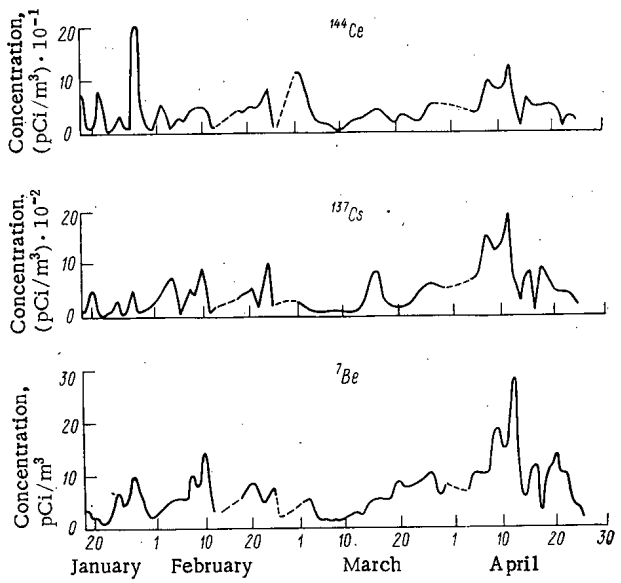

Fig. 4. Concentration of the ^{7}Be, ^{137}Cs, and ^{144}Ce isotopes in the atmospheric layer close to the water.

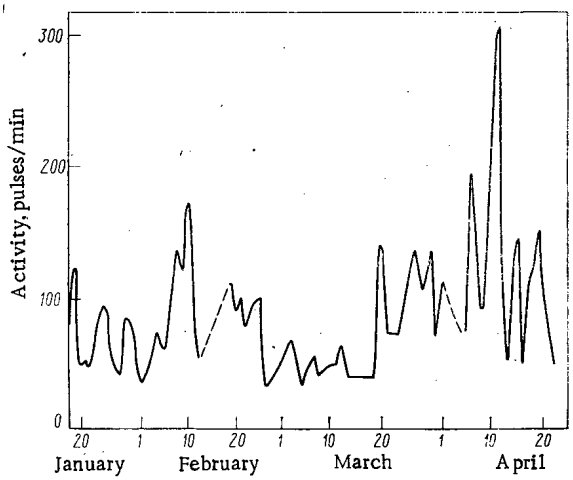

Fig. 5. Total β activity of the samples.

$$t = \frac{N_{A+B} + N_B}{0.03^2 (N_{A+B} - N_B)},$$

where t denotes the time (min); N_{A+B} denotes the number of pulses which were produced by the combination of sample and background and were counted; and N_B denotes the background.

A γ-spectroscopical analysis of the radioactive samples was made on board the ship with the aid of a standard multi-channel AI-128 γ-spectrometer. The detector of the "Vorya" set with an NaI crystal activated by thallium was used as the sensing element; the crystal had a size of 60 × 60. The sensing element was shielded from external irradiation by the lead shield of a low-background UMF-1500 unit (wall thickness of the shield 5 cm). The total counting efficiency of the unit was about 7%. Final information in the form of the spectral distribution of the number of pulses over the channels was derived from the analyzer with the aid of BZ-15m number-printing unit.

A low-background laboratory unit with a 10 cm thick lead shield and a sensing element consisting of a 63 × 63 NaI crystal was used to determine the half-line period of ^{7}Be. The counting efficiency of this unit was 7.2%.

A γ-spectrum of an atmospheric sample is shown in Fig. 2. This spectrum can be compared with the spectrum which is typical for atmospheric fallout of the moratorium period, in which the basic peak is the ^{7}Be peak (E_γ = 0.48 MeV).

The relative activity of ^{137}Cs and ^{144}Ce was insignificant and varied for, say, cesium, between 10^{-15} and 10^{-13} Ci/m^3, which agrees with the available literature data. The ^{40}K peak which is usually found in the atmospheric layer close to the water due to the removal of potassium salts from the surface of the ocean can be qualitatively recognized on the spectrogram.

Figure 3 depicts in logarithmic coordinates the time dependence of the radiation intensity of the isotope having the radiation energy ~0.5 MeV. The half-life which was determined for the isotope from this dependence was 52 days, which is an additional confirmation of the presence of the ^{7}Be isotope.

The results of the measurements are summarized in Table 1.

Figure 4 is used to list the measured concentrations of the radioactive ^{7}Be, ^{137}Cs, and ^{144}Ce isotopes in the atmospheric layer near the water over the Atlantic and the Caribbean.

The correlation between the time-dependent variations in the concentration of the three isotopes, as well as the total β activity of the samples (Fig. 5), indicate that the ratio between the isotopes is stable in

the atmosphere on the entire route on which measurements were made from the vessel. A strong fractionation of the isotopes during their precipitation is obviously not observed. A noticeable variation in the radioisotope ratio can be possibly related to the precipitation of radioactive nuclides of greatly different ages.

Based on the data which were obtained, a substantial increase in the total radioactivity of the atmosphere can in some cases be explained by an increase in the intensity of the exchange between the stratosphere and the atmospheric layer close to the water. The concentration of the radioisotopes increased particularly in the time between April 8 and April 12 and between the points with the coordinates 22°50' N, 84°00' W and 25°55' N, 68°34' W. The total concentration of the radioisotopes in the atmosphere increased 2.5 times in those days, but the ratio of the isotopes was constant. The observed maximum of the fallout is apparently related to the passage of a strong cyclone whose center was at that time situated over North America.

CHRONICLES

THE SECOND FAST-REACTOR SYMPOSIUM OF THE CMEA COUNTRIES

V. B. Lytkin

The Symposium was held at Obninsk from October 1 to October 5, 1973. A total of 96 reports was presented. Specialists from Bulgaria, Czechoslovakia, the German Democratic Republic, Poland, Romania, and the USSR took part in the Symposium.

The reports covered the following topics:

1. Prospects for the development of nuclear power in the member countries of the Council for Mutual Economic Assistance (CMEA) and the place of fast reactors in nuclear power. Analysis of the fuel balance and economic efficiency of nuclear power generation using fast reactors. Various types of fast reactors as compared with sodium-cooled reactors.
2. Experience in the design, construction, and operation of fast reactors. Development and testing of basic technological equipment. Problems involved in the production of fuel elements and absorbing elements for fast reactors. Heat exchange and hydrodynamics of the active zone.
3. Technology of sodium coolants, specific problems in thermophysics, study of materials, and radiation stability.
4. Physics and safety of fast reactors. Investigation of neutron-physics characteristics.

All of the reports devoted to prospects for the development of fast reactors and their economic indicators were characterized by a systems approach. The basic properties of various types of atomic power stations can be most completely and objectively reflected by systems criteria.

The problem of more efficiently using the natural reserves of uranium is of great significance for the solution of the principal problem of nuclear power generation, namely, substantially increasing the available fuel base. For that reason, uranium consumption is one of the most important systems criteria in the selection of a strategy for the development of nuclear power generation and the optimization of reactor characteristics. In the Soviet reports (V. B. Lytkin et al., S. M. Feinberg*) and in the reports of R. Rockstroh and D. Hermann (German Democratic Republic) and S. Novak and T. Reitzi (Czechoslovakia) it was shown that the inclusion of fast reactors in the development program for nuclear power generation leads to a considerable reduction in the consumption of natural uranium. This means that fast reactors have a considerable economic advantage over thermal reactors and can remain competitive with them even when the fast reactors require higher unit investment costs. According to the data given in a report by V. N. Bobolovich et al. (USSR), fast reactors can be incorporated into the optimum structure of nuclear power generation even in cases in which the unit investment cost for fast reactors is 1.5-1.6 times the unit investments cost for thermal reactors.

A number of interesting conclusions were also presented in the reports of P. Wentzel (German Democratic Republic) and O. D. Kazachkovskii, S. V. Bryunin et al., and E. V. Kirillov (USSR), devoted to the technical and economic aspects of nuclear power generation.

The characteristic doubling time of fast-reactor power plays an important role in improving the efficiency of utilization of natural uranium resources and improving the economic efficiency of fast reactors.

* Deceased.

Translated from Atomnaya Énergiya, Vol. 36, No. 2, pp. 148-150, February, 1974.

For the conditions prevailing in the Soviet Union, it is desirable to keep this doubling time no greater than 6-8 years. The BN-600 reactor, now under construction, would have a doubling time of 11-12 years (assuming a time of one year for the external fuel cycle). A report by V. V. Orlov et al. discussed the possible ways of reducing the doubling time to as little as 4-5 years by using oxide fuel and sodium coolant, the techniques for which have by now been fairly well mastered. Efforts are also being made to attain short doubling times for those types of fast reactors which can serve as alternatives to sodium-cooled reactors. As an example of such an alternative, experts have proposed the construction of gas-cooled fast reactors using helium at a pressure of 300-500 abs. atm (S. M. Feinberg,* USSR) or nitrogen tetroxide (A. K. Krasin, V. B. Nesterenko, USSR) at a pressure of 150-170 abs. atm. For gas-cooled fast reactors there is also the potential use of the gas-turbine cycle, which makes it possible to reduce the unit investment cost. However, reactors of this type are still in the initial stage of development.

A great deal of interest was aroused by reports on the startup and adjustment operations on the BN-350 reactor, the energy startup of which took place on July 16, 1973. The results of these operations, described mainly in the reports of A. I. Leipunskii* et al., V. V. Orlov et al., and D. S. Yurchenko et al†., indicate that all the calculated physical characteristics of the reactor were in satisfactory agreement with the actual values obtained by carrying out a program of physical measurements on the reactor.

An important place was given to the discussion of problems related to the design and construction of reliable steam generators for sodium-cooled fast reactors. In a report by V. F. Titov et al., it was noted that in present-day development of sodium–water steam generators, two lines of design are being followed: single-vessel design, with unit power corresponding to the power of the circulation loop, and modular design, with different power values for the different modules. Single-vessel steam generators are more compact and use less metal but require more complex manufacturing technology than modular steam generators. Furthermore, in single-vessel generators it is more difficult to find and repair defective (leaking) tubes. Modular steam generators are larger and require more metal but are more reliable in operation because it is possible to localize failures within an individual module. It is thought that the first generation of sodium-cooled steam generators will have to be of the sectional modular type.

The reliability and long operating life of sodium–water steam generators depend primarily on the correct choice of structural materials. Three different trends are observable today in the use of structural materials for sodium-type steam generators: low-alloy, unstabilized, and stabilized steels of such types as 1Kh2M and 1Kh2MFB; chrome steels containing 9-12% chromium; and austenitic steels based on Kh18N9 or Kh20N30.

Of great importance in the choice of structural materials will be the practical experience to be obtained in the operation of the first large fast reactors, the BN-350 and the BN-600.

A report by O. D. Kazachkovskii et al. stated that the once-through steam generator of the BOR-60 reactor has been operated for more than 10,000 hours without any failure. To check the condition of the heat-exchange tubes, after 4,000 hours and 8,000 hours of operation of the steam generator, the vessel had been opened and tube specimens had been cut out of the zone of the evaporator that had been found to have poorer heat exchange than initially. Metallographic analysis showed that the tube surfaces were in good condition both on the sodium side and on the water side.

Three reports presented by Czechoslovakia (F. Dubšek et al., F. Strmiská et al.) were devoted to problems involving the design and manufacture of sodium–water steam generators at the First Brno Machine Construction Plant. In collaboration with NIIAR of Dimitrovgrad, USSR, workers at the First Brno Machine Construction Plant researched, designed, and constructed a 30-MW experimental steam generator for the BOR-60 reactor. Designs are being worked out for modular steam generators to be used in larger fast reactors.

Problems connected with the production of operationally reliable fuel elements which are capable of withstanding high loading and burnup values were discussed in reports by I. S. Golovnin, N. P. Agapova et al., A. S. Zaimovskii et al., A. Ya. Ladygin et al., and Yu. I. Likhachev et al. (USSR).

Oxide fuel is the kind that has been most thoroughly tested in experimentation and operation up to now. No massive failure of oxide fuel elements has been observed at burnup values of less than 10-11%;

* Deceased.

† See pp. 113, 119, and 132 of this issue.

however, individual fuel elements have failed. The interaction of the oxide with the stainless-steel jacket that has been observed in a number of cases is due to the presence of fission fragments, oxygen, and relatively high temperatures. In order to reduce the corrosion caused by the fission fragments, it is desirable to use fuel whose composition is below the stoichiometric value and also to use oxygen-absorbing getters. In addition, it is important to know how the properties of the stainless steel in the jacket will change under the influence of high integral fluxes of neutrons and high temperatures. In the design of the fuel elements it is necessary to take account of changes in the long-term strength and long-term plasticity, of high-temperature embrittlement, and of neutron creep and swelling.

In the above-mentioned report of Yu. I. Likhachev et al., as well as in the report of V. I. Subbotin et al., it was noted that the durability of fuel elements is significantly affected by nonuniformities in temperature around the jacket, which may be particularly severe in the case of corner or wall fuel elements and may reach 30-100°C, causing not only thermal stresses but also additional stresses resulting from the nonuniform swelling of the jacket material. Because of this, the material of fuel element jackets must meet strict standards of strength, compatibility with the fuel and the sodium, and radiation-swelling value.

For a number of years, specialists in the Soviet Union have been systematically working on the comprehensive evaluation of stainless steels of various compositions with a view to selecting materials to be used in fuel-element jackets for fast reactors. A report by N. P. Agapova et al. gave information on a number of properties (heat-resistance, structure, susceptibility to radiation damage, resistance to sodium corrosion, etc.) of 0Kh16N15M3B steel, developed as a material for the fuel-element jackets used in the BR-5, BOR-60, and BN-350 reactors.

A. S. Zaimovskii et al. (USSR) presented the results of investigations on how irradiation in the active zone of the BR-5 reactor affected the mechanical properties, structure, and swelling values of 1Kh18N10T and 0Kh16N15M3B steels with various types of initial treatment.

A number of reports were devoted to the conditions of operation for fuel elements in the active zone from the viewpoint of hydrodynamics and temperature distribution.

The participants also heard a number of reports on how the corrosive action of sodium is affected by the amount of oxygen it contains and on methods for monitoring oxygen and hydrogen values. In this connection, mention should be made of a report by H. Ullmann et al. (German Democratic Republic) and a joint report by the USSR (F. A. Kozlov et al.) and the German Democratic Republic (H. Ullmann et al.), which described the principles involved in the measurement of oxygen and hydrogen concentrations in the sodium loop by means of galvanic cells containing a solid electrolyte and presented the results obtained when instruments developed at the Central Institute of Nuclear Research (Rossendorf) were tested at the Physics and Energy Institute (Obninsk).

A large number of reports were devoted to problems of reactor physics and methods of physical calculations. The main trends of such work in the Soviet Union were considered in reports by V. V. Orlov et al., Yu. A. Kazanskii et al., V. A. Dulin et al., A. M. Kuz'min et al., and O. D. Bakumenko et al. In the main, there are four traditional trends: basing reactor calculations on nuclear data, improving the methods of reactor calculations, macroscopic investigations on critical assemblies, and investigations using models of power reactors.

The need for various constants has sharply increased in connection with the design and construction of atomic power stations.

In order to automate the calculation of group constants, workers at the Physics and Energy Institute are working out a system for providing constants for atomic-reactor calculations (known by its Russian initials as SOKRATOR). It includes a library of evaluated and recommended data, a set of programs for servicing the library, a set of programs for converting nuclear data of various types into reactor constants, and a set of programs for calculating microconstants. Work on the establishment of a library of evaluated data is now in progress.

Fast-reactor calculations frequently make use of one-dimensional multi-group models, chiefly in a diffusion approximation. This is because the programs are simple and convenient, requiring little calculation time. Other calculation methods are also used. In particular, a variational-iterative method has been used for preparing programs for the two-dimensional design of reactors, to be used in large-scale calculations for the optimization of reactors.

The immediate purpose of macroscopic investigations using critical assemblies with simple structure and geometry is to explain the reasons for divergences between the measured and calculated characteristics.

Investigations have shown that the most important corrections that must be taken into account in calculations or experiments are corrections relating to the dimensions of specimens used in measuring reactivity coefficients and corrections connected with the heterogeneous structure of critical assemblies.

The purpose of modeling projected fast reactors on critical assemblies is to verify the accuracy of the predicted physical design characteristics. At the present stage of development of calculation methods and systems of group constants, this is a necessary procedure. The report of V. V. Orlov et al. described the results of a study of a model of the BN-600 reactor on the BFS-2 test stand. Measurements made on fast-thermal critical assemblies were discussed in reports by K. Fermann and G. Huttel (German Democratic Republic) and L. Adamski and K. Bukowski* (Poland). The first report described an insertion lattice inthe ring reactor at Rossendorf, and the second described the P-ANNA-1 two-zone critical assembly and the experiments carried out on it.

The results of investigations of neutron-count statistics on the BFS-24-1 fast neutron critical assembly at the Physics and Energy Institute were presented in a joint report prepared by Soviet and Polish scientists (A. M. Abramov et al.).

A report by É. A. Stumbur et al. discussed the use of pulsed neutron methods for studying the physical characteristics of fast reactors; experiments had been carried out on a series of critical assemblies of the BFS-1 and BFS-2 types.

Calculation methods for fast reactors were also presented in reports from Czechoslovakia, the German Democratic Republic, and Romania.

A number of reports [L. Adamski, Z. Rusynowski (Poland), D. Albert et al. (German Democratic Republic), L. Moisin (Romania), and D. Jozefowics (Poland)] were devoted to the construction of various kinds of measuring equipment. A Soviet report by V. G. Dubovskii et al.† described a highly sensitive startup apparatus which had been used for monitoring the BN-350 reactor during the process of assembling the critical mass and carrying out a program of physical experiments. Problems involving the nuclear safety of fast reactors were discussed in a report by I. Suchomel and V. Adamik (Czechoslovakia).

The Second Fast-Reactor Symposium of the CMEA Countries showed that during the six years since the first Symposium great advances had been made in the development and construction of reactors of this type. Extensive research on fast reactors is now in progress in the CMEA member countries. The exchange of information that has been set up among them will help to bring about further progress in this field.

* Deceased.

† See p. 128 of this issue.

XXV SESSION OF COMECON PERMANENT COMMISSION ON PEACEFUL USES OF ATOMIC ENERGY

V. A. Kiselev

The XXV session of the COMECON Permanent Commission on the peaceful uses of atomic energy was held in Moscow, November 20-23, 1973.

Participating in the deliberations of the Commission were delegations from Bulgaria, Hungary, the GDR, the Republic of Cuba, Poland, Rumania, the Soviet Union, Czechoslovakia. Present in response to invitations were representatives of the Interatominstrument international economic association on nuclear instrumentation, and representatives of the Joint Institute for Nuclear Research.

Topics concerned with implementation of the decisions of the XXVII session of the COMECON, the Executive Committee of the Council, and measures elaborated in the Comprehensive Program of further deepening and improvement of collaboration and development of socialist economic integration of COMECON member-nations were on the agenda at this session.

The course of development of forecasts into the fuel and energy (including nuclear power) needs of the COMECON member-nations, extrapolated to 1990, and proposals on further activities of the Commission in this area, were discussed.

The Commission approved the program of scientific and technical collaboration between COMECON member-nations in the field of fast reactors, a draft program of scientific and technical collaboration covering the period to 1980, and basic trends to 1990 in the field of conservation and improvement of the environment as far as radiation safety is concerned, and also went into topics associated with the preparation of a draft plan for scientific and technical collaboration between COMECON member-nations for the 1976-1980 period.

Information on the work done by the Provisional International Scientific Research Team for carrying out reactor physics research on the VVÉR type critical assembly built at the Central Physics Research Institute (in Budapest) was discussed, and the importance, fruitfulness, and great promise, of this work was duly noted.

The Commission confirmed recommendation on specialization of production of isotope wares, and also prepared for signing an Agreement on multilateral international specialization and cooperation in the production of isotope wares.

The Commission's 1974-1975 work plan was confirmed, and the work plan for 1974 in the field of standardization likewise.

Appropriate recommendations and resolutions were adopted on all of the topics on the agenda.

Translated from Atomnaya Énergiya, Vol. 36, No. 2, p. 150, February, 1974.

COLLABORATION DAYBOOK

A conference of COMECON member-nation specialists on the distribution between the various involved countries of the production of stable isotopes and labeled compounds incorporating stable isotopes was held in Tbilisi, August 14-17, 1973, in line with the 1973 work plan of the COMECON Permanent Commission on the peaceful uses of atomic energy [PKIAÉ SÉV]. Specialists from the GDR, Rumania, the USSR, and the COMECON Secretariat took part in the deliberations. Reports were heard from leaders of the delegations on the proposed development, in the several countries, of the production of stable isotopes, proposals by those nations on specialization of production and coordination in the field of developing labeled compounds. A preliminary exchange of opinions was followed by detailed discussions of proposals bearing on specialization in the production of stable isotopes and compounds labeled by stable isotopes. The discussion resulted in the preparation of the following proposals for further discussion by the Commission on specialization of production: 145 such compounds in the GDR, including some deuterated compounds, and ^{15}N-labeled compounds; compounds tagged by the isotopes ^{10}B and ^{11}B in the USSR, plus some deuterated compounds (a total of 340 in the listing); six compounds tagged with deuterium and ^{15}N in Rumania.

The conference deemed it convenient to continue its work on further specialization of production of stable isotopes and compounds labeled by stable isotopes, including coordination of work in COMECON member-nations on development of listings of isotope compounds.

* * *

The 26th session of the PKIAÉ SÉV workteam on nuclear instrumentation was held September 11-14, 1973, in Liberec (Czechoslovakia).

Participating in this session were specialists from Bulgaria, Hungary, the GDR, Poland, Rumania, USSR, Czechoslovakia, the COMECON Secretariat, and also representatives of the Interatominstrument agency.

Further development of collaboration in the field of nuclear instrumentation was discussed, and a work plan for 1974-1975 was drawn up for the workteam.

The workteam agreed on proposals dealing with further problems facing the Commission in the field of nuclear instrumentation in connection with the setting up of Interatominstrument, and decided upon the sequence and terms of development of unitized designs of a system for control, protection, and monitoring of power reactors, and prepared agreed-upon decisions on various other topics.

The session also discussed standardization in the field of nuclear instrumentation, and elaborated a draft work plan in the field of standardization.

* * *

A conference of specialists of the COMECON member-nations on radiation-protection and radiation techniques was held in Mamaia (Rumania) on September 11-15, 1973.

Participating in this conference were specialists from Poland, Rumania, the USSR, Czechoslovakia, the COMECON Secretariat, and a representative of the Interatominstrument agency.

The conference discussed an analysis of national standards in effect in COMECON member-nations that was prepared by the COMECON Secretariat, and which applies to radiation-protection products, the identity of these standards with COMECON recommendations on standardization with regard to the basic indices and regulations, and information on production of these products in the COMECON member-nations.

Translated from Atomnaya Énergiya, Vol. 36, No. 2, pp. 150-152, February, 1974.

Draft recommendations on the standardization of aerosol filters, viewing windows, γ-ray nondestructive testing devices, protective lead blocks, reports with technical estimates on revision of recommendations on standardization adopted earlier (standardization of laboratory furniture and of laboratories designed to facilitate handling of radioactive materials), were agreed upon.

Appropriate resolutions were adopted on all of these topics. The conference agreed upon a work plan in the field of standardization of radiation-protection and radiation products for the 1974-1975 period.

* * *

A conference of specialists on analysis of radiopharmaceutical preparations was held September 25-28, 1973, in Leningrad. Taking part were specialists from Hungary, the GDR, Poland, Rumania, the USSR, the COMECON Secretariat, and Czechoslovakia.

Summaries of work on the coordination plan for scientific and technical investigations, "Correlation of methods for monitoring the characteristics of unitized radioactive medical preparations," were discussed and deliberated. Reports were heard on the outlook for carrying out scientific research work in the COMECON member-nations based on multilateral and bilateral collaboration and agreed on proposals dealing with joint work in analysis of radiopharmaceutical preparations over the 1975-1980 period.

Proposals on the content and implementation of work during 1974 were agreed upon.

* * *

The second session of the KNTS [Coordination scientific technical council] on research reactors of PKIAÉ SÉV was held in Predeal (Rumania) on September 25-28, 1973.

Specialists from Bulgaria, Hungary, Poland, Rumania, the USSR, and Czechoslovakia participated in the session, along with a staffmember of the COMECON Secretariat.

Reports from delegations of specialists on progress of research in the field of techniques of in-pile measurements and monitoring and control of nuclear research reactors were heard and discussed. Draft work plans for realization of collaboration programs on the topics: "Improvements in existing research reactors, expansion of experimental capabilities and coordination of their utilization for different directions in research," and "Development of new research reactors with improved neutron physics characteristics" were agreed upon.

The participants at this session also discussed and agreed upon draft programs and scheduling of a symposium on "Experience in the operation and use of research reactors," to be held in Rumania September 30 through October 4, 1974.

Several topics relating to enhancing the role of coordination scientific technical councils and improving the implementation of their decisions in action were discussed at the session.

* * *

The second session of the KNTS on radiation safety was held in Dresden, September 25-28, 1973. Participating in the work of the council were specialists from Bulgaria, Hungary, the GDR, Poland, Rumania, the USSR, Czechoslovakia, and the COMECON Secretariat. A draft program of scientific and technical collaboration between COMECON member-nations for the period extending to 1980, and relating to basic trends in work in this area for the 1981-1990 period as well, extending into the field of environmental conservation and environmental improvements as far as pertains to radiation safety, was discussed. The council discussed the status of the work done in line with the existing plans in 1973, and approved the 1974 work plan.

* * *

The third session of the KNTS on water management, water treatment, and leakproofing of nuclear power station fuel elements was held in Novaya Voronezh', October 9-12, 1973. Participating in the work of the session were specialists from Bulgaria, Hungary, the GDR, Poland, Rumania, the USSR, Czechoslovakia, and a staff member of the COMECON Secretariat.

A report on results of work done on the second, third, and fourth power generating units of the Novaya Voronezh' nuclear power station in the area of water management, corrosion, and water purification was discussed, as well as a report on providing nuclear power stations of COMECON member-nations

with ion exchange resins, and a report on the results of work done on deactivation of the primary loops of VVÉR reactor units, and on the outlook for further development of work on deactivation.

The participants of this session expressed their satisfaction at the results obtained in operating the Novaya Voronezh' nuclear power station, which constitutes a reliable basis for successful operation of similar nuclear power generating stations in COMECON member-nations engaged in nuclear power developmental programs.

It was pointed out that proposals put forth by the USSR delegation on supplying ion exchange resins to nuclear power generating stations in COMECON member-nations contain concrete requirements on requirements and specifications imposed on ion exchange resins serving specific functions, and on the selection of concrete brands and grades of ion exchange resins. At the present time, COMECON member-nations have at their disposal an ample range of ion exchange resins satisfying those requirements, so that the nuclear power situation in those COMECON member-nations is not hampered by any need to acquire ion exchange resins from the capitalist countries.

The participants at this session engaged in a rounded discussion of problems associated with the techniques, periodicity, and degree of deactivation of the primary loop of the VVÉR-440 and VVÉR-1000 reactors.

Routine problems faced by the KNTS over the next two years to come were discussed and agreement was reached on perspectives. The 1974-1975 work plan of the KNTS was discussed and improved.

* * *

A conference of COMECON member-nations' specialists on radiation sterilization of materials and medical wares and on the development of procedural documentation unique to specific countries in that domain was held October 9-12, 1973, at Sukhumi. Specialists from the GDR, Poland, Rumania, the USSR, Czechoslovakia, took part in the conference, along with a COMECON Secretariat staffmember.

The following procedural documents were discussed and recommended for adoption and implementation in the COMECON member-nations:

medical technical specifications for polymeric materials to undergo radiation sterilization, and from which wares to be put in contact with the blood stream or blood substituents are to be fabricated;

medical and technical specifications on polymeric materials and resins intended for the fabrication of syringes and cannulas for throwaway needles sterilized by radiation exposure;

procedures for monitoring pyrogenicity of radiation-sterilized polymeric systems intended for taking blood samples, blood transfusions, and blood substituents and throwaway injection syringes, and procedures for monitoring the toxicity of the above wares and products;

basic microbiological terms and concepts prevalent in the field of radiation sterilization.

The status of work on the preparation of new procedural documents with features unique to those countries, was discussed, and a forthcoming comprehensive plan for further development of work in this area covering the 1974-1977 period, was discussed, and agreement was reached on the agenda for the next conference scheduled to be held in the first half of 1975 somewhere in the Soviet Union.

* * *

The seventeenth session of the workteam on reactor science and reactor engineering and nuclear power was held in Moscow, October 16-19, 1973. Specialists from Bulgaria, Hungary, and GDR, Poland, Rumania, the USSR, Czechoslovakia, and COMECON Secretariat staffmembers, were in attendance.

Major problems concerning reactor science, reactor engineering, and nuclear power, came under discussion, and a proposal was launched to use the combined forces of scientists of the COMECON member-nations to develop further work in this area in the 1976-1980 period.

The further development of joint efforts in the field of fast reactors was discussed and approved, and the discussion extended to matters of an organizational nature, resulting in the adoption of pertinent resolutions.

INFORMATION

PROBLEMS OF INTERACTION OF LASER LIGHT AND RELATIVISTIC ELECTRONS WITH PLASMA

M. V. Naidenov

A session of the Working Group on the study of interaction of laser light and relativistic electrons with plasma took place August 13-30, 1973, in Trieste, Italy.

The working group was organized on the initiative of the International Atomic Energy Agency (IAEA) to discuss the feasibility of using superpowerful laser-light and relativistic-electron beams for thermonuclear research. Interest in these problems has increased recently, and some success has been obtained (megaampere relativistic-electron beams have been produced; optimistic results have been obtained for two-dimensional calculations of compression and microburst of a D–T drop under the influence of laser illumination).

The leading theoreticians in the field of plasma physics and specialists in the fields of interaction of light and electron beams with plasma, plasma turbulence, and numerical modeling gathered in Trieste. R. Z. Sagdeev, L. I. Rudakov, A. A. Galeev, and others from the USSR participated.

In the first few days, general problems were discussed at seminars and meetings at which information was exchanged. Later, the participants were divided among three subgroups: these dealt with linear theory of light-beam parametric instability (led by M. Rosenbluth, USA, and P. Kow, India); heating efficiency and reflection of laser light in a plasma corona surrounding a D–T medium (led by D. Porsluid, USA, and A. Galeev, USSR); plasma-heating by high-power relativistic-electron beams, and plasma turbulence (led by L. I. Rudakov, USSR, and R. Sudan, USA).

The conference was led by R. Z. Sagdeev.

A major portion of the subgroups' work concerned discussion and analysis of so-called numerical experiments on the interaction of light and electron beams with plasma, which have been conducted at several American computer centers and laboratories. This tendency in plasma physics has grown especially quickly in recent years. The studies consist of calculations, using modern computers, on the physical processes in model plasma. For example, in typical calculations the plasma is represented as 100,000 charged layers (50,000 plane condensers) which are driven by the light wave's electromagnetic field. The computers used in American computer centers allow one to follow the behavior of this many particles for hundreds of oscillation periods of the incident wave and obtain information on the light reflection factor, the plasma heating rate, and the turbulence characteristics of the light-excited plasma. Although such a numerical experiment cannot be compared to a concrete real experiment (since even the best modern computers do not allow calculations on an experiment corresponding to real conditions), the data obtained from such calculation are the basis for developing a theory which itself must allow such comparison. Thus, the discussions showed that the plasma turbulence characteristics in the numerical experiments are universal and independent of the means of excitation (by light or electron beam). This fact is intelligible from the theory of strong Langmuir turbulence, developed by Soviet theoreticians. The progress achieved in understanding plasma turbulence shows the fruitfulness of this approach.

The subgroup on studying the heating efficiency and laser-light reflection in a plasma corona surrounding a D–T medium surveyed the theoretical aspects of reverse parametric scattering by a plasma drop and discussed the most important methods for decreasing this scattering. Reverse parametric light

Translated from Atomnaya Énergiya, Vol. 36, No. 2, p. 153, February, 1974.

scattering by a plasma drop is one of the most important processes impeding laser-light absorption by the plasma in experiments on laser thermonuclear synthesis.

Commentaries on experiments now being conducted on the interaction of intense laser light with plasma noted that induced Brillouin scattering has not yet been observed. Also discussed were questions of plasma modeling; several easily interpretable experiments, which will make possible reliable comparisons between theoretical assumptions and experimental results, were suggested.

All participants at the conference noted the usefulness of the discussions and seminars. They expressed thanks to IAEA and to A. Salamu, the Director of the International Center on Theoretical Physics, for the conference's good organization. They also expressed the opinion that similar meetings would be useful in the future.

PROBLEMS OF RADIATION AND ENVIRONMENTAL PROTECTION

G. V. Shishkin, I. A. Bochvar,
and V. A. Krasnikov

These problems have been discussed at the Meeting of the IAEA Research Group in Budapest on September 3-7. Most participants came from countries lying on the Danube. Representatives of Great Britain, France, the German Democratic Republic, Netherlands, USA, and Canada also participated in the Meeting.

Problems of personal dosimetric monitoring in atomic power plants and nuclear laboratories, the contamination of the environment and in particular of the Danube by radioactive wastes have been discussed in twenty papers. The question of contamination of the Danube river, in particular, aroused great interest and provoked a lively discussion. The Meeting worked out recommendations which will be published by the IAEA and distributed to the member countries.

Several reports dealt with problems of personal dosimetry.

I. Boitor (Hungary) reported on a program of measuring the absorbed dose from photographic film. Application of machine dose-counting is very convenient as it ensures a uniform measuring technique. The accuracy of the method is estimated to be ±20%. L. Boros (Hungary) described a dosimeter based on thermoexoelectronic emission and having very high sensitivity. The dosimeter is still under laboratory investigation.

S. Mark (Hungary) reported on an analysis of the radiation field in the vicinity of a research reactor. In estimating the readings of activation detectors, the authors use theoretical spectra allowing for the role of scattered neutrons in the local neutron field.

The report of R. Wilson (Canada) dealt with personal dosimetry of internal and external irradiation at the Pickering Heavy-Water Reactor. The structure of a system of personal dosimetric monitoring has been described. Film dosimeters, direct-reading ionization chambers, nuclear emulsions, LiF thermoluminescence dosimeters for skin dose measurements of the hands are used: LiF and indium and sulfur foils are used for emergency dosimetry.

The present personal monitoring system is to be modified and albedo and track dosimeters will be used for neutron dosimetry. Measurement of γ-radiation dose and of $\beta - \gamma$ radiation skin dose will be based entirely on LiF thermoluminescent detectors.

Protection of the environment from radioactive wastes of industrial atomic power plants has been the topic of several papers.

M. Ruhf et al., (FRG) analyzed the discharge waters of the Hundermingen reactor and their effect on the activity of the Upper Danube. Eighteen isotopes, products of uranium fission or corrosion of activated materials, have been found in this discharge. The highest activity is due to tritium (98% in 1972); other isotopes are: ^{89}Sr, ^{90}Sr, ^{134}Cs, ^{137}Cs, ^{131}I, ^{140}Ba, ^{140}La, ^{58}Co, and ^{60}Co. The 84.6 Ci of various activation and fission products discharged into the Danube in 1972 increased the activity of its waters by 26.4 pCi/liter. The dose due to pollution of waters used by the population of the Upper Danube basin (in drinking water, in fish caught in the Danube, in cattle feeding on its banks, in irrigation water, etc.,) has been calculated. It has been shown that the total population dose does not exceed 1 mrem/year per person which amounts to 1/170 part of the maximum dose recommended by the ICRP (5 rem in 30 years). The measurements and calculations referred to the operation of one 237 MW reactor; it is foreseen that several reactors with a total power of 12,800 MW will be in operation by 1977.

Translated from Atomnaya Énergiya, Vol. 36, No. 2, p. 154, February, 1974.

Hungarian specialists (L. Sabo et al.,) reported that the pollution of the Danube waters in Hungary reached 10 pCi/liter and occasionally even 35 pCi/liter, which exceeds the maximum norms adopted by the country.

Bonar (France) described the results of monitoring the radioactive pollution of the Rhone river and its floodplain. The French workers consider that the critical nuclide is ^{137}Cs (and not ^{90}Sr). The present level of activity is quite low.

D. Miller (USA) reported on the prospects of atomic power plants in the USA. It is anticipated that by 1990 the USA will have 500 atomic power plants with a total power of 508 mill. kW. They will produce about 44% of electrical energy consumed by that time. Such a program requires close attention to problems associated with pollution of the biosphere by radioactive wastes. The USA now has 750 monitoring stations scattered over the entire country. These stations are equipped with instrumentation capable of detecting tritium in rain and discharge waters, the radioactivity of air and of river waters, and radioactive iodine in milk. The stations are now used also to monitor the wastes of atomic power plants. All information is reported to the USA Environmental Protection Agency.

After hearing and discussing the presented papers the Meeting adopted the following recommendations for protecting the Danube from radioactive pollution:

1) all Danube countries having nuclear programs should make available information on the volume and nature of use of Danube waters involved in the program and on the population using these waters including prospects of future growth;

2) the countries should provide data on liquid radioactive wastes discharged into the Danube;

3) models of ecological chains should be uncovered and analyzed and the input parameters of these models determined;

4) exposure dose limits for the population groups and maximum allowable amounts of radioactive wastes discharged into the Danube should be established;

5) the system of monitoring, i.e., simultaneous sampling in border areas, standardization and unification of sampling techniques, the sampling frequency, etc., should be the subject of agreement between the countries involved;

6) a common system of alarm signals in case of critical situations (such as for example emergency discharges) should be organized, and exchange of information and mutual warning should be ensured.

Close cooperation between the interested countries will make it possible to establish unified environment methods which is a first step to the adoption of common standards for its protection.

MODERN RESEARCH IN NUCLEAR METEOROLOGY

A. G. Trusov and M. S. Tsitskishvili

Research in nuclear meteorology attracts the attention of more and more specialists in various fields of science. The growing rate of technological progress, the rapid development of nuclear power engineering, and the pollution of the atmosphere by artificial radioisotopes, make the problem of environment protection one of the most acute.

The International Symposium on the theme "Meteorological Aspects of Radioactive Pollution of the Atmosphere," organized in October, 1973 by the Central Hydrometeorological Administration Office of the Council of Ministers of the USSR, the Institute of Experimental Meteorology, and the Transcaucasian Hydrometeorological Research Institute, provided an opportunity to review the advances in this field.

The Symposium has been attended by 70 specialists from the German Democratic Republic, Poland, Rumania, the Soviet Union, and Czechoslovakia.

Fourty-four papers read at the Symposium dealt with the following topics:

1) theoretical models of the migration of radioactive isotopes in the atmosphere and the use of these isotopes as tracers in meteorological studies;

2) natural radioactive isotopes in the atmosphere, their physicochemical properties, and purification processes;

3) the rules of global circulation in the atmosphere and fallout of artificial radioactive isotopes and their role in meteorological processes;

4) problems of radioactive pollution of the atmosphere associated with the growing peaceful uses of atomic energy.

In particular, the presented papers described:

1) several numerical models of the propagation of radioactive isotopes from instantanenous and permanent sources;

2) specific uses of radioactive tracers in the study of intertropical convergence, stratospheric –tropospheric exchange, and the distribution of fallouts in mountainous regions;

3) generalized data on the distribution of emanating isotopes over large territories;

4) calculation of the inflow of cosmogenic radioisotopes into the atmospheric boundary layer;

5) models of washout and fallout processes of radioactive aerosols from the atmosphere;

6) quantitative description of the transport of artificial radioactive impurities from the stratosphere to the troposphere;

7) the relation between the pollution of the Earth surface and of the atmospheric boundary layer and meteorological conditions;

8) methods of calculating the propagation of atmospheric impurities taking into account meteorological factors;

Translated from Atomnaya Énergiya, Vol. 36, No. 2, p. 155, February, 1974.

9) methods of standardization of the allowable discharge from smokestacks of atomic power plants; the importance of meteorological service in the protection of population in connection with the growth of nuclear power production has been stressed.

The Symposium noted the fruitful use of radioactive tracers in the analysis of atmospheric processes and approved the application of nuclear meteorology methods in the study of propagation and removal of radioactive industrial wastes from the atmosphere. The study of local sources and their global influences is of particular importance in view of the growing peaceful uses of atomic energy.

The Symposium stated that nuclear power engineering is one of the human activities in which the possible dangers can be reduced to minimum. New improved methods must be developed for processing radioactive wastes and other impurities. Particular attention should be devoted to tritium, krypton, and iodine in view of the difficulties associated with their isolation from the environment.

Research must be continued on the prevention of harmful effects of radioactive material discharged by the atomic industry into the environment, and on the behavior of biologically dangerous long-lived radioactive materials in the outer environment.

The Symposium approved methods of calculating the propagation and fallout of radioactive discharges, and methods of standardizing the allowable discharges in conjunction with atmospheric processes.

The proceedings of the Symposium are to be published.

RV-1200 RADIATION TECHNOLOGICAL FACILITY FOR VULCANIZING THERMOSTABLE ADHESIVE ELECTRICALLY INSULATING TAPE AND RUBBER – GLASS-FABRIC COMPOSITE

N. A. Pekarskii, V. B. Osipov,
I. Ya. Poddubnyi, G. N. Lebedeva,
S. V. Mamikonyan, B. M. Terent'ev,
S. V. Aver'yanov, E. D. Chistov,
V. A. Gol'din, R. R. Safin,
and G. I. Marfin

The RV-1200 full-scale radiation-chemical reactor, which has already undergone technological tests, has been put into service in the Soviet Union and has begun producing industrial wares.

Work on radiation-induced vulcanization of various grades of rubbers shed light on the perspectives open for devising and creating new materials or materials with improved properties, inasmuch as the effect of ionizing radiations on polymeric materials was discovered to result in modifications of the physical and mechanical properties of the irradiated polymers. Through radiation vulcanization, rubber grades acquire a structure contrasting with the structure of similar materials produced in conventional vulcanization by chemical means, and the new properties inherent uniquely in the radiation vulcanizates, such as adhesion to metals and autohesion, are of great interest. The radiation vulcanizates exhibit heightened stability to heat and frost, excellent resistance to attack by water, considerable mechanical strength, and resistance to wear.

Research carried out to date [1] has shown that radiation-induced vulcanization of rubber mixes with a polyheterosiloxane rubber base results in the acquisition of new insulating materials, such as highly thermostable electrically insulating adhesive tape and rubber–glass-fabric composite. The tape does

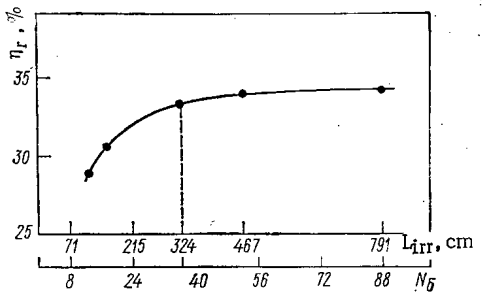

Fig. 1

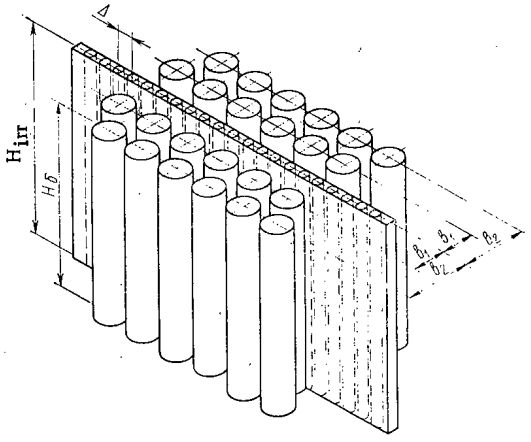

Fig. 2

Fig. 1. Dependence of η_r on irradiator length or on number of blocks (E_0 = 1.25 MeV, distance from tape blocks to irradiator b = 14.5 cm).

Fig. 2. Arrangement of tape blocks relative to irradiator plane at b_1 = 10 cm, b_2 = 23 cm, L_{irr} = 387 cm, H_{irr} = 120 cm, Δ = 9 cm.

Translated from Atomnaya Énergiya, Vol. 36, No. 2, pp. 155-159, February, 1974.

TABLE 1. Calculated Radiation Parameters for Several Variants in Arrangement of Tape Blocks Relative to Irradiator Plane

Arrangement of tape blocks	Number of tape blocks	Height of blocks, cm	η_r, %	Volume of mass of blocks needed for specified nonuniformity, %	Maximum deviation from volume average ratio ($P_\gamma/P_\gamma M$), %	Irradiator activity, kCi	Exposure time, h
In one row on each side of irradiator $\rho_b = 0.88$ g/cm^3, $d_b = 1.7$ cm	18	80	17,0	97	18	$8{,}28 \cdot 10^5$	8,6
		90	20,0	85	23,5	$7 \cdot 10^5$	10,8
		80	20,0	88	25	$7 \cdot 10^5$	10,7
	20	90	22,5	77	33	$6{,}36 \cdot 10^5$	12,0
In two rows on each side of irradiator, $\rho_b = 0.7$ g/cm^3, $d_b = 15$ cm	20	90	24,0	90	20	$6{,}36 \cdot 10^5$	10,5

good service for 300 full days at 250°C, over 100 full days at 300°C, 5 to 10 min at 410°C. It will stick to metals, operates stably in cold down to −60°C, resists attack by water, offers tensile strength to 60 kgf/cm^2, relative elongation to 500%, electrical strength to 30 kV/mm, and resistivity greater than 10^{14} Ω/cm.

The rubber–glass-fabric composite exhibits excellent thermal stability (above 250°C), resists cold and frost down to −60°C, resists attack by water, offers tensile strength greater than 400 kgf/cm^2, electrical strength to 30 kV/mm, and resistivity greater than 10^{14} Ω/cm.

The LETSAR radiation-fabricated adhesive tape* and the radiation-fabricated RETSAR rubber–glass-fabric composite* are being produced for industrial needs, in the form of coils respectively 13-15 cm and 12-25 cm in diameter, with polyethylene backing sandwiched in between the rubber layers, to prevent self-adhesion in storage. Tape 26 mm in width is being fabricated in two variants: shaped tape (in triangular form) of 0.5 mm maximum thickness and rectangular tape 0.2 mm. The rubber–glass-fabric composite is being made with rubber coating on one side or on both sides, in sheet 80 cm wide and 0.25 mm in thickness.

Radiation-induced vulcanization of rubber mixes, initiated by ^{60}Co γ-emmision, is carried out at relatively high absorbed exposure doses on the order of 13.5 Mrad, while the tape and the rubber–glass-fabric composite with optimum physicomechanical and electrical properties are obtained with a fairly high radiation dose field homogeneity of ±15%.

An irradiator featuring an activity output on the order of 500 kCi, and a large-size exposure chamber with thick biological concrete shielding, access to which can be gained only through labyrinths, are required for a full-scale process of this type, with the due attention to specific productivity and the need for uniform exposure.

Basic Parameters and Design of the RV-1200 Facility. This facility is provided with an exposure chamber 6 m in diameter and 2.2 m high, with the ^{60}Co source of radiation located at the center of the chamber. The best procedure is to irradiate the tape in the form of cylindrical blocks made up from separate coils, in order to maintain the productivity of the facility, uniformity of exposure, and a fairly high radiation efficiency (η_r).

The irradiator was selected in the form of an extended plane comprising a large array of rodlike tubular elements, given the cylindrical shape of the blocks of tape and the high absorbed exposure dose (and as a result of comparing design variants of rodlike, cylindrical, and slablike irradiators). A (computerized) method of engineering physics calculation was employed to determine the activity of the irradiator, by computing the absorbed energy distribution of γ-radiation, in particular η_r, on the basis of the superposition principle.

Figure 1 shows results of calculations of η_r as a function of the irradiator length L_{irr} (at irradiator height H_{irr} = 120 cm), or as a function of the number N_b of cylindrical tape blocks arrayed in a single row on both sides of the irradiator plane. It is clear from the diagram that η_r is maximized in practice at L_{irr} = 324 cm (and respectively $N_b \geq 36$), under the conditions stated. The best dimensions for the slab type

* The fabrication process for these electrically insulating materials is now protected by patents [2-4].

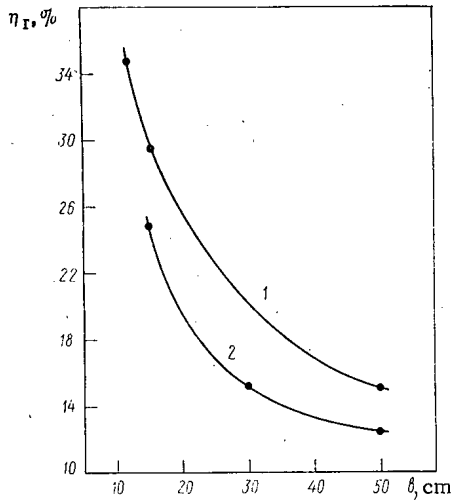

Fig. 3. Dependence of η_r on distance from tape block to irradiator at E_0 = 1.25 MeV: 1) N_b = 36, $H_b = H_{irr}$ = 120 cm, Δ = 7.755 cm, ΔL_{irr} = 57 cm; 2) N_b = 32, H_b = 100 cm, H_{irr} = 120 cm, Δ = 7 cm.

irradiator are arrived at [5] from the condition that the area of the slab plane approximately satisfy the inequality $S_{irr} \geq 4$ m^2, and the following dimensions are designed for the active part of the irradiator: H_{irr} = 120 cm; L_{irr} = 387 cm.

The calculated activity of the ^{60}Co charged into the irradiator is 764 kCi. A total of 404 sources with a 0.7 r/sec exposure dose rate are positioned at a distance of 1 m (1.95 kCi) and 212 sources of exposure dose rate $1.6 \cdot 10^{-1}$ r/sec are positioned at a distance of 1 m (0.45 kCi), distributed uniformly in 44 out of 87 tubular elements. The remaining 43 elements are intended for periodic reloading of sources (the activity of the source diminishes with time).

Figure 2 shows how the tape blocks are arrayed relative to the irradiator plane. The required dose field nonuniformity with respect to the height and length of the tape blocks is achieved by creating overlaps of the active irradiator area above the area of the object. This problem (in terms of the thickness of the tape blocks) is solved by placing the object at different distances from the irradiator. The results of the calculations are plotted in Fig. 3. But the most effective way of achieving the required dose field nonuniformity (±15%) with respect to the thickness of the tape blocks is by rotating the objects about their axes. The irradiator is treated as an assemblage of point sources when calculating the absorbed dose fields.

Results of calculations of η_r, the degree of nonuniformity of exposure, the activity of the irradiator, and the exposure time for different variants are presented here in tabular form.

The distribution of dose rates as radiation absorbed in the tape blocks and in the rubber–glass-fabric composite was also determined by chemical dosimetry, using industrial nonplasticized films of cellulose triacetate 140 ± 5 μ thick. It was found that absorbed dose rate deviations with respect to the height of the tape blocks were not in excess of the specified levels (±15%), and the figure was ±7% along the length of each row of tape blocks.

The RV-1200 facility (Fig. 4) is installed in the electrical insulating tape and rubber–glass-fabric composite production department, and forms a rectangular room with a cylindrically shaped exposure chamber (2) centered within it, an annular conveying channel (16) lined on all sides with concrete shielding walls (17) designed to form (in plan view) two mutually overlapping half-crescents. The advantages of a chamber of that configuration over rectangular-shaped chambers with zigzag channels is demonstrated in a separate article [6]. Given the same effective area, the cylindrical chamber is more compact and cheaper since the conveying channel is organically incorporated into the design of the shielding walls and shielding materials are curtailed 30% in that case. Moreover, the constant radius of curvature of the annular channel leads itself better to conveying the products, while ensuring the required number of reflections of direct radiation.

Also installed in the exposure chamber are:

1. The irradiator 6, consisting of 87 pressuretight tubular elements 5 with ^{60}Co sources sealed by shielding plugs and mounted on the crossarm 3. The irradiator is equipped with a pneumatic system for automatically dumping the tubular elements; this emergency system is actuated in any of six distinct emergency situations.

2. A storage tank 14 for the irradiator; this tank comprises a rectangular unit with 87 lead-lined channels. The lead, acting as thermal shield, makes it possible to take up as much as 10,000 kcal/h of heat released by the radiation sources (up to 70% of the entire amount of energy absorbed in the structural materials). The top of the storage tank is surrounded by cast iron shielding slabs 13, the bottom by removable concrete slabs, both for the purpose of cutting down on radiation intensity to the permissible level.

3. An irradiator displacing mechanism 7. This mechanism comprises a system of two vertical screws with nuts, on which the irradiator crossarm is mounted. The screws operate in unison and are powered by an electric power drive working through a transmission system.

4. The tape block rotation mechanism 1. This system meshes with gears, and is required to maintain the specified dose field uniformity with respect to the thickness of the object.

5. A loading device 4, which is a set of cast iron shielding slabs with 22 holes similar to the holes in the storage tank that are covered over by the shielding plugs.

The facility is provided with an assembly chamber 8 which is used in assembling the tubular elements of the irradiator, temporary storage of sources, carrying out work associated with reloading of sources and checking sources for hermetic sealage. There are also a viewing window, a master-slave manipulator 10, a storage tank 9, and a worktable.

The conveying device 15, a chain of 10 suspended four-wheel carriages on which the tape blocks are arrayed in two rows, is used to move the tape blocks into position for irradiation. Two conveying chains with the products each move into the exposure chamber through their own conveying channel and line up on both sides of the irradiator plane. The radiation vulcanization conditions are established in line with technological regulations governing the production of the electrically insulating tape and rubber–glass-fabric composite. Exposure uniformity in each row of tape blocks is achieved through transverse irradiation of the conveying chains from each side of the irradiator.

The facility features a control system, dosimetric monitoring, and interlocks, and is controlled from a control panel located in the operations rooms.

The ^{60}Co sources are loaded into the channels of the storage tank in the assembly chamber. All of the sources were distributed, depending on the activity ratings and the date of fabrication in the tubular elements of the irradiator, so as to bring about the required dose field uniformity over the irradiator plane. The sources are charged into the tubular elements in the assembly chamber, with the aid of the master-slave manipulator. The assembled tubular elements are then transferred from the assembly chamber to

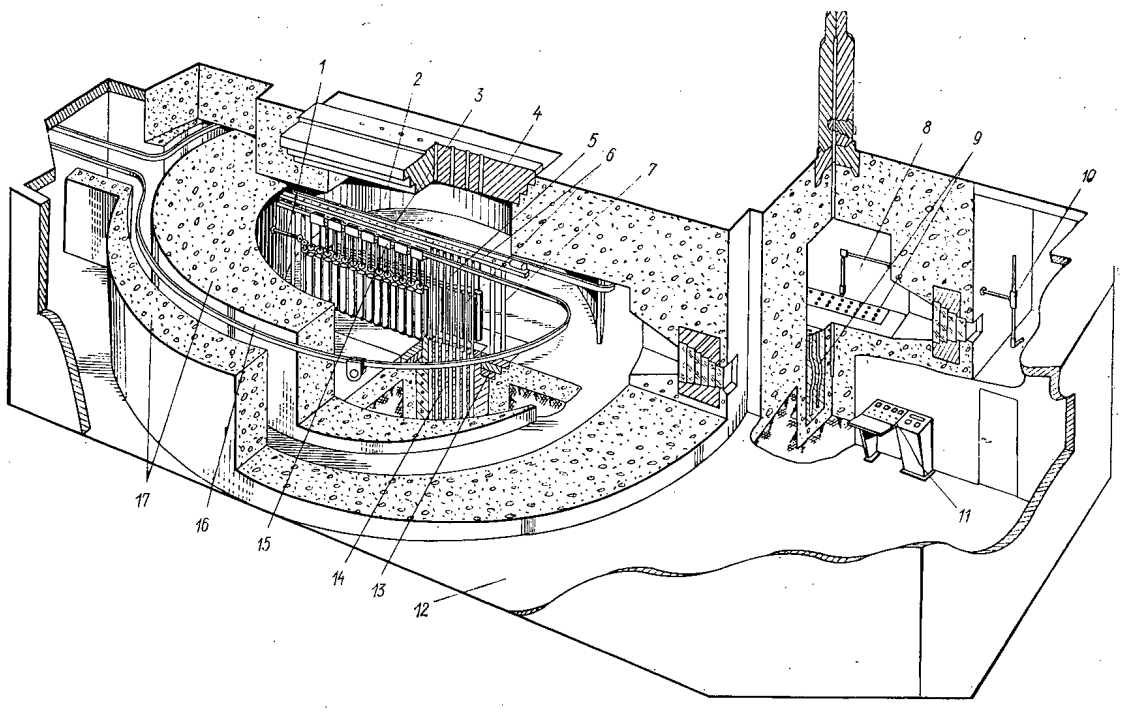

Fig. 4. General view of the RV-1200 facility.

the irradiation exposure chamber with the aid of a special reloading container, and are mounted on the crossarm of the irradiator, each in its own hole. Dosimetric checks on all components of the biological shielding with the irradiator in different positions then followed, simultaneous with the loading of the sources and the assembly of the irradiator, and that demonstrated the effective performance of all of the shielding equipment.

LITERATURE CITED

1. S. V. Aver'yanov, et al., Kauchuk i Rezina, 22, No. 8, 1 (1963).
2. I. Ya. Poddubnyi, et al., French Patent No. 2.029.871, Priority date October 12, 1970.
3. I. Ya. Poddubnyi, et al., West German Patent No. 1935963, Priority date December 17, 1970.
4. I. Ya. Poddubnyi, et al., India Patent No. 125128, Priority date December 12, 1970.
5. B. M. Terent'ev, N. A. Pekarskii, and V. A. Zhabin, Radiation Chemistry; Proceedings of the All-Union Scientific and Technical Conference on "20 years of production and use of isotopes and sources of nuclear radiation in the USSR national economy" (Minsk, 1968) [in Russian], Atomizdat, Moscow (1972), p. 468.
6. E. B. Mamin, P. P. Moiseenko, and N. A. Pekarskii, in: Proceedings of the All-Union Conference on Radioactive Isotopes and Nuclear Radiations in the USSR National Economy [in Russian], Vol. 1, Gostoptekhizdat, Riga (1961), p. 233.

FLOW CHECK DEVICE FOR LIQUID-METAL LOOPS

S. N. Ogorodnikov, R. V. Orlov,
and R. N. Khomich

Stringent requirements are placed on the flow-check devices used in plasma accelerators [1] operating under severe thermal stess and in highly corrosive environments. The major such requirements are high reliability, leaktightness, very high switching rates ($\geq 10^4$), comparatively short response times. The flow check devices [2] based on a system with a needle-on-seat mechanical seal feature suffer from short service life and impairment of the seal because of the frequent on-off switchings. The flow check device based on freezing of the working fluid in the channel through the action of a coolant has a longer opening time.

The flow check device [3] described here for liquid-metal loops (alkali metal loops), which is simple in design and reliable in service, is free from the above shortcomings.

The basic design is shown in Fig. 1. The channel is leakproofed by freezing the working fluid. The device is designed in the form of two stainless steel tubes (one coolant tube and one working tube) respectively 10 × 1 mm and 6 × 1 mm in cross section. The working tube 1 through which the working fluid flows runs through the coolant tube 3 (at an angle) and is hermetically welded to the latter, such that a cavity 2 is formed between the outer surface of the working tube and the inner surface of the coolant tube. The coolant employed is compressed air. The two tubes are heated by direct filament current which is kept constant throughout the experiment. The performance of the flow check device is monitored by a X–A thermocouple installed to measure the temperature of the outer wall of the coolant tube. $T_1 = 200°C$ is assigned as the initial temperature at which the flow check device opens, and $T_2 = 120°C$ as the closing temperature.

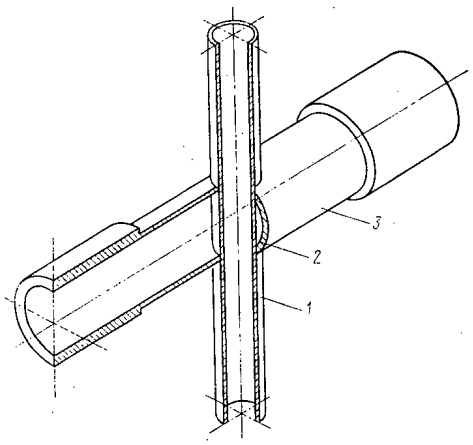

Fig. 1

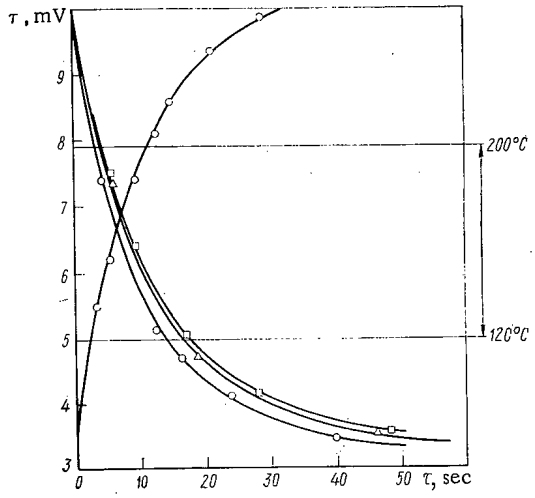

Fig. 2

Fig. 1. Basic design of flow check device: 1) working tube; 2) cavity; 3) coolant tube.

Fig. 2. Dependence of temperature of outer wall of coolant tube on time and on working fluid flowrate: ○) working fluid flowrate zero; △) working fluid flowrate 0.05 g/sec; □) working fluid flowrate 0.3 g/sec.

Translated from Atomnaya Énergiya, Vol. 36, No. 2, pp. 159-160, February, 1974.

The geometrical parameters of the flow check device and the amount of cooling air for the specified flowrate of working fluid are determined such that the specified operating response time (~10 to 15 sec) will be attained. By using the one-dimensional form of the differential thermal conduction law $\partial q/\partial \tau = a^{\partial 2} q/\partial x^2$, we obtain for the freezing rate $v = 2q/c\rho R$, where q is the specific thermal flux; c is the specific heat; ρ is the density of the working fluid; R is the working tube radius. Hence, we have $\tau = \Delta T/v$ for the freezing time.

Figure 2 shows the time dependence of the temperature of the outer wall of the coolant tube, derived experimentally, for fixed flowrates of coolant air and different flowrates of working fluid. The flowrate of coolant air for 0.3 g/sec flowrate of working fluid, with the flow check device closed, is $8.5 \cdot 10^3$ liters /h, as against $1.3 \cdot 10^3$ liter/h with the flow check device opened. It is clear from Fig. 2 that the measured response time of the flow check device is close to the calculated time, ~15 sec. A flow check device of this type that has been in service for two years (without failure) was investigated experimentally on a lithium stream in a vacuum chamber, for several hundred hours during which time it withstood $\sim 10^3$ open-close cycles. The tests showed that the device operates reliably with repeated open-close cycling over the selected range of working fluid flowrates (to 0.3 g/sec), and that the response time of the device undergoes virtually no change as the flowrate of working fluid is varied.

LITERATURE CITED

1. Collection of Articles: Plasma Accelerators, edited by L. A. Artsimovich et al. [in Russian], Mashinostroenie, Moscow (1973).
2. R. G. Perel'man, Design and Operation of Liquid-Metal Systems [in Russian], Atomizdat, Moscow (1968).
3. R. N. Khomich et al., Flow check device for liquid-metal loops, Patent No. 1662912/25-8, May 11, 1971.

breaking the language barrier

WITH COVER-TO-COVER ENGLISH TRANSLATIONS OF SOVIET JOURNALS

in physics

Title	# of Issues	Subscription Price
Astrophysics *Astrofizika*	4	$120.00
Fluid Dynamics *Izvestiya Akademii Nauk SSSR mekhanika zhidkosti i gaza*	6	$180.00
High-Energy Chemistry *Khimiya vysokikh énergii*	6	$155.00
High Temperature *Teplofizika vysokikh temperatur*	6	$150.00
Journal of Applied Mechanics and Technical Physics *Zhurnal prikladnoi mekhaniki i tekhnicheskoi fiziki*	6	$175.00
Journal of Engineering Physics *Inzhenerno-fizicheskii zhurnal*	12 (2 vols./yr., 6 issues ea.)	$175.00 ($87.50/vol.)
Magnetohydrodynamics *Magnitnaya gidrodinamika*	4	$125.00
Mathematical Notes *Matematicheskie zametki*	12 (2 vols./yr. 6 issues ea.)	$185.00
Polymer Mechanics *Mekhanika polimerov*	6	$140.00
Radiophysics and Quantum Electronics (Formerly Soviet Radiophysics) *Izvestiya VUZ. radiofizika*	12	$180.00
Solar System Research *Astronomicheskii vestnik*	4	$ 95.00
Soviet Applied Mechanics *Prikladnaya mekhanika*	12	$175.00
Soviet Atomic Energy *Atomnaya énergiya*	12 (2 vols./yr., 6 issues ea.)	$175.00 ($87.50/vol.)
Soviet Physics Journal *Izvestiya VUZ. fizika*	12	$180.00
Soviet Radiochemistry *Radiokhimiya*	6	$165.00
Theoretical and Mathematical Physics *Teoreticheskaya i matematicheskaya fizika*	12 (4 vols./yr. 3 issues ea.)	$160.00

Back volumes are available. For further information, please contact the Publishers.

SEND FOR YOUR FREE EXAMINATION COPIES

PLENUM PUBLISHING CORPORATION
227 WEST 17th STREET
NEW YORK, N. Y. 10011
Plenum Press • Consultants Bureau
• IFI/Plenum Data Corporation

In United Kingdom: 4a Lower John Street, London W1R 3PD, England